

# Improving Outcomes in NF1 Spine Fusion

**Justin Daniel Bobyn**

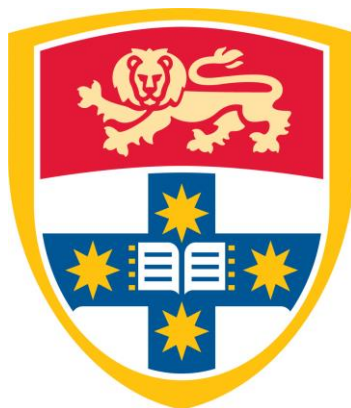
MBBS BSc

A thesis submitted in fulfilment of the requirements of the degree of  
**Doctor of Philosophy**

**Supervisor:** Prof David G Little

**Associate Supervisor:** Dr Aaron Schindeler

**2018**



**The University of Sydney  
Sydney Medical School**

## **Declaration of Contributions**

The work presented in this thesis was conducted during a combination of full time and part-time candidature to fulfil the requirements of Doctor of Philosophy through the Sydney Medical School, The University of Sydney. Unless otherwise stated, all experiments and analysis were conducted by myself at the Orthopaedic Research and Biotechnology Unit at the Children's Hospital Westmead. Animal Ethics were approved by CMRI/CHW Animal Ethics Committee. All surgeries, unless otherwise stated, were performed by myself. Anaesthetics were performed by Kathy Mikulec-Langton and Lauren Peacock. Confocal imaging methods were developed with Dr Laurence Cantrill, unless otherwise specified. Experimental conception, and manuscript and thesis editing were conducted in conjunction with my supervisors Prof David Little and A/Prof Aaron Schindeler.

In Chapters 2 and 3, the surgical approach was developed with Dr Anton Rasch. Dr Rasch also assisted in performing the surgeries.

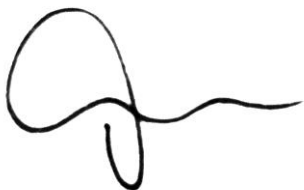
In Chapter 4, culture of AdCre virus was prepared by Dr Nikita Deo.

In Chapter 5, the ectopic bone experiments were conceived and analyzed by Dr Mille Kolind. These surgeries were performed by Kathy Mikulec-Langton and Lauren Peacock. Spine fusion surgeries were conducted at the Department of Reconstructive Sciences, School of Dental Medicine, UConn Health, Farmington, CT, USA under the supervision of Dr Ivo Kalajzic. Anaesthetics were provided by Dr Brya Matthews.

## Statement of Originality

This is to certify that to the best of my knowledge, the content of this thesis is my own work. This thesis has not been submitted for any degree or other purposes.

I certify that the intellectual content of this thesis is the product of my own work and that all the assistance received in preparing this thesis and sources have been acknowledged.



Justin D Bobyn

The content of this thesis is the sole work of Dr Justin Bobyn, unless otherwise stated.



Prof David Little

A/Prof Aaron Schindeler

## **Acknowledgements**

I would like to thank everyone who contributed to this research and guided me along the way, especially those who dragged me kicking and screaming to the finish line.

## Abstract

NF1 (neurofibromatosis type 1) is a relatively common genetic disease which may be characterized by the presence of scoliosis and altered bone metabolism, amongst its many orthopaedic manifestations. Traditionally, spine fusion procedures have been used to correct and limit the progression of this deformity. NF1 bone healing at the tibia and spine feature impaired bone anabolism, excessive catabolism, and fibrosis. Fibrotic tissue in the tibia and between the vertebrae can lead to pseudarthrosis, which can require substantive clinical intervention. In particular, complications associated with the spine can represent a significant source of morbidity in this population, often presenting with persistent deformity, pain, and hardware failure. Revision procedures, themselves a source of morbidity, are often required when a primary procedure has failed. This thesis explores systematic approaches to modelling deficient NF1 spine healing and treatment to improve outcomes in this patient population.

A murine model of posterolateral fusion using rhBMP-2 (bone morphogenetic protein-2) was developed to test a range of pharmacological interventions. This model was first applied to *Nf1* heterozygous mice and was reproducible and reliable. *Nf1*<sup>+/-</sup> mice exhibited a mild orthopaedic phenotype with increased osteoclasts on histology. Treatment with the bisphosphonate Zoledronic acid (ZA) increased the bone volume of the fusion masses in both control and *Nf1*<sup>+/-</sup> mice, though the improvement was larger in controls.

Several studies have shown that tibial pseudarthroses can be associated with a localized double inactivation of the *Nf1* gene, and we speculated that this could underlie local lesions in the spine. To recapitulate this, we utilized a model where a

Cre-expressing adenovirus induced local double inactivation in *Nf1<sup>flox/flox</sup>* mice. This was then applied to the established spine fusion model. Consistent with the clinical presentation of spinal pseudarthrosis, a limited amount of rhBMP-2 bone was formed and substantive fibrous tissue was present. Targeted treatments with pharmaceutical agents were next trialled in this model. The MEK inhibitor PD0325901 increased bone volume in all groups while ZA increased bone density. In summary, this model represents a robust platform upon which to test targeted interventions to reduce the fibroproliferative phenotype of NF1.

A second goal of this research project was to investigate the cellular contributors to spine fusion in general, which could be used to design new treatments both for NF1 and non-NF1 spine fusion. To accomplish this, a murine genetic model of lineage tracking was employed. This featured Tie2-Cre: Ai9 and  $\alpha$ SMA-creERT2: Col2.3-GFP: Ai9 reporter mice. Spine fusion operations were performed in these mice, and the distribution of lineage-labelled cells were traced using fluorescence. Notably, Tie2 lineage cells co-labelled with TRAP positive cells, suggesting a primary contribution to the osteoclasts but not osteoblasts of the fusion mass. Conversely,  $\alpha$ SMA lineage cells co-labelled with *Col2.3-GFP* expressing osteoblasts, suggesting new bone primarily arises from mesenchymal cells with negligible input from endothelial cells undergoing transdifferentiation.

In conclusion, treatment of scoliosis remains a challenge in individuals with NF1. The development of a fibroproliferative model of spine fusion in an *Nf1* deficient mouse represents a robust platform upon which to test targeted interventions to improve outcomes in NF1. Additionally, advancements in genetic modeling of human disease in animals may provide new models in which to investigate this process.

## Original publications

Over the course of this thesis, several studies have been written into articles, peer reviewed and accepted into scientific journals.

### Publications related to this thesis

**Bobyn, J.**, A. Rasch, M. Kathy, D. G. Little and A. Schindeler (2014). "Maximizing bone formation in posterior spine fusion using rhBMP-2 and zoledronic acid in wild type and NF1 deficient mice." J Orthop Res **32**(8): 1090-1094.

**Bobyn, J.**, A. Rasch, D. G. Little and A. Schindeler (2013). "Posterolateral inter-transverse lumbar fusion in a mouse model." J Orthop Surg Res **8**: 2.

**Bobyn, J. D.**, D. G. Little, R. Gray and A. Schindeler (2015). "Animal models of scoliosis." Journal of Orthopaedic Research **33**(4): 458-467.

Kolind, M., **J. D. Bobyn**, B. G. Matthews, K. Mikulec, A. Aiken, D. G. Little, I. Kalajzic and A. Schindeler (2015). "Lineage tracking of mesenchymal and endothelial progenitors in BMP-induced bone formation." Bone **81**(Supplement C): 53-59.

### Publications not related to this thesis

El-Hoss, J., K. Sullivan, T. Cheng, N. Y. Yu, **J. D. Bobyn**, L. Peacock, K. Mikulec, P. Baldock, I. E. Alexander, A. Schindeler and D. G. Little (2012). "A murine model of neurofibromatosis type 1 tibial pseudarthrosis featuring proliferative fibrous tissue and osteoclast-like cells." J Bone Miner Res **27**(1): 68-78.

Schindeler, A., R. J. Mills, **J. D. Bobyn** and D. G. Little (2017). "Preclinical Models for Orthopedic Research and Bone Tissue Engineering." Journal of Orthopaedic Research.

# Contents

Declaration of Contributions .....	2
Acknowledgements .....	4
Publications related to this thesis .....	7
Publications not related to this thesis .....	7
Table of Figures .....	11
Glossary of Abbreviations.....	17
1. Literature Review.....	<u>1719</u>
1.1.1 Skeletal anatomy.....	<u>1820</u>
1.1.2 Bone anatomy and histology .....	<u>1820</u>
Cellular composition of bone .....	<u>1924</u>
1.1.3 Embryonic development of bone.....	<u>2022</u>
(i) Endochondral ossification .....	<u>2123</u>
(ii) Intramembranous ossification.....	<u>2224</u>
1.1.4 Bone repair.....	<u>2325</u>
(i) Primary fracture healing .....	<u>2426</u>
(ii) Secondary fracture healing.....	<u>2426</u>
1.1.5 Failure of the bone repair process.....	<u>2628</u>
(i) Blood supply.....	<u>2729</u>
(ii) Mechanical stability .....	<u>2830</u>
1.1.6 Cellular contributors to bone repair .....	<u>2934</u>
(i) Clinical evidence for extraosseous cell contribution to osteogenesis .....	<u>2934</u>
(ii) Experimental evidence for extraosseous cell contribution to osteogenesis	
<u>3032</u>	
(iii) A genetic basis for HO.....	<u>3133</u>
(iv) BMP and vascular calcification.....	<u>3234</u>
1.1.7 Cellular tracking .....	<u>3234</u>
(i) The Cre-LoxP system .....	<u>3335</u>
1.2 Scoliosis .....	<u>3537</u>
1.2.1 The anatomy of the spine.....	<u>3537</u>
1.2.2 Scoliosis .....	<u>3739</u>
1.3 Spine Fusion .....	<u>3941</u>
1.3.1 Indications for spinal fusion.....	<u>3941</u>



1.3.4	Historical treatments for spinal deformity .....	<u>4042</u>
1.3.5	Early instrumentation for spinal correction .....	<u>4042</u>
	(ii) Early instrumented spinal fusion procedures.....	<u>4143</u>
1.3.6	Anabolic approaches for spinal fusion.....	<u>4345</u>
1.3.7	BMP delivery systems .....	<u>4446</u>
1.3.8	Adverse effects associated with BMP induced spine fusion .....	<u>4648</u>
1.3.9	Failure of Spine Fusion Surgery .....	<u>4749</u>
	(i) Influence of vascularity on spinal fusion success .....	<u>4749</u>
	Blood supply and the fusion bed .....	<u>4749</u>
	Osteoporosis is a condition associated with poor vascular supply and poor surgical outcome.....	<u>4850</u>
	Factors influencing bone vascularity .....	<u>4951</u>
(ii)	Mechanical stability .....	<u>5052</u>
1.4	Neurofibromatosis type 1 (NF1) .....	<u>5254</u>
1.4.1	NF1 is characterized by scoliosis .....	<u>5254</u>
1.4.2	NF1 is a RASopathy that is plagued by poor bone healing .....	<u>5658</u>
1.5	Animal Models of Scoliosis.....	<u>5759</u>
1.5.1	Biomechanical forces in scoliosis modelling.....	<u>5759</u>
1.5.2	Quadrupedal Models of Scoliosis .....	<u>5860</u>
	Mechanical models.....	<u>5860</u>
	Genetic models .....	<u>6365</u>
1.5.3	Bipedal Models of Scoliosis.....	<u>6970</u>
	Mechanical models.....	<u>6970</u>
	Neuroendocrine models .....	<u>7072</u>
1.5.4	Summary .....	<u>7375</u>
1.6	Hypothesis and Aims.....	<u>7476</u>
2.	Posterolateral intertransverse lumbar fusion in a mouse model.....	<u>7879</u>
	Abstract .....	<u>7879</u>
	Introduction.....	<u>8182</u>
	Methods .....	<u>8283</u>
	Results .....	<u>8788</u>
	Discussion .....	<u>9495</u>
3.	Maximizing bone formation in posterior spine fusion using rhBMP-2 and zoledronic acid in wild type and NF1 deficient mice .....	<u>9899</u>

	Introduction.....	<a href="#">100404</a>
	Materials and Methods .....	<a href="#">101402</a>
	Results .....	<a href="#">104406</a>
	Discussion .....	<a href="#">110444</a>
4.	Spine fusion in a murine model of double inactivation of NF1 in the spine	
	<a href="#">114415</a>	
	Abstract .....	<a href="#">114415</a>
	introduction.....	<a href="#">116447</a>
	methods .....	<a href="#">119420</a>
	results.....	<a href="#">124425</a>
	discussion.....	132
	conclusions.....	135
5.	Lineage tracking of mesenchymal and endothelial progenitors in BMP-induced bone formation .....	137
	Introduction.....	139
	Materials & Methods.....	141
	Results .....	145
	Discussion .....	153
6.	DISCUSSION.....	160
	REFERENCES.....	182

## Table of Figures

Figure 1. 1 Human skeleton with axial (pink) and appendicular (blue) divisions. ....	17
Figure 1. 2 Endochondral ossification. Hyaline cartilage model with bone collar (1) ; Cavitation within cartilage model (2) ; Internal cavity invaded by periosteal blood supply with cancellous bone formation (3) ; medullary cavity formation and appearance of secondary ossification site in epiphysis (4) ; ossification of epiphyses and remainder of cartilage at physeal plates and articular surfaces. ....	22
Figure 1. 3 Intramembranous ossification. (1) Ossification centre appears within connective tissue membrane. (2) Osteoblasts secrete osteoid which mineralizes to form bone. Trapped osteoblasts become osteocytes (3) Random laying down of osteoid results in a poorly organized trabecular network of bone. Vascularized mesenchyme is laid down on the surface of the bone. (4) Dense mesenchyme becomes the periosteum and the bone deep to this thickens forming a cuff of mature lamellar bone. ....	23
Figure 1. 4 Secondary fracture healing. (1) Normal bone. (2) Fracture with disruption of blood vessels and haematoma formation. (3) Cartilaginous callus. (4) Replacement of cartilaginous callus by bony callus. (5) Remodelled bone. ....	26
Figure 1. 5 Anatomy of the spine and morphology of a typical lumbar vertebra. ....	36
Figure 1. 6 A) Normal spine (i) compared with thoracic (ii) and lumbar (iii) scoliotic deformity. B) Congenital deformity of spine secondary to partial unilateral failure of formation (i) complete unilateral failure of formation (ii), unilateral failure of segmentation (iii), and bilateral failure of segmentation (iv).....	38
Figure 1. 7 Instrumented spine fusion permits correction of scoliotic deformity with fixation of bilateral rods via pedicle screws extending into vertebral body. ....	42
Figure 1. 8 Illustration from Aldovandri's 'Monstrorum Historia' depicting of an individual with what is now been thought to be NF1. [1].....	54
Figure 1. 9 Mechanical asymmetry along the spine of a quadruped can be created via A) unilateral resection of ribs and costovertebral joint, B) unilateral tethering between transverse processes of ipsilateral vertebrae, or C) unilateral tethering between ipsilateral pelvis and scapula. ....	60
Figure 1. 10 Motor signals are carried from the spinal cord to muscle fibres via the ventral nerve root. Proprioceptive information, including information related to the relative position of muscles, is relayed via the dorsal nerve root from muscle to the spinal cord. ....	61
Figure 1. 11 Compared to the deep location of the pineal gland within the human brain (A), its position in the chicken (B) and rodent (C) brain is significantly more superficial. This position facilitates surgical access for its excision in melatonin deficiency models of scoliosis. ....	70
Figure 2. 1 Following the administration of anesthetic the mouse was positioned prone. A marker was used to mark the location of the spinous processes, vertical line, and pelvic crest, horizontal line (A). A line drawn across the pelvic crests corresponds to the position of the L5-L6 interspace. An incision was made through the skin which was the held by a self-retaining retractor (B). A single incision was made through the thoracolumbar fascia over the spinous processes and the paravertebral musculature was dissected by scraping a blade down along the spinous processes and pulling laterally. The dissection of the local musculature forms a pocket on either side of the spine, bounded medially by the spinous	

processes and inferiorly by the articular processes (D). The articular processes are consequently exposed and visualized allowing decortication with a 1mm round diamond burr until punctate bleeding is observed. Following decortication of the visualized articular processes, a 7mm x 2mm collagen sponge impregnated with either saline or saline/rhBMP-2 solution is inserted into each of the pockets in contact with the posterior elements of the spine (E). The muscle and skin are then closed with continuous sutures using 5.0 Vicryl®.....85

Figure 2. 2 Three-dimensional reconstructions of CT images demonstrating the anatomy of murine lumbar spine (left) vs human lumbar spine (right). (A) Anterior vertebral body. (B) Transverse process. (C) Inferior articular process. The position and orientation of the transverse process of the mouse spine differs significantly from the human spine. Both the murine inferior articular process and the human transverse process share a lateral orientation. ....88

Figure 2. 3 Volume of the BMP induced fusion mass was assessed via microCT using a Skyscan 1174 scanner. A fusion mass was only produced in groups in which BMP was implanted. No new bone was observed at 1 week post op, while maximum fusion volume was achieved by week 2 and maintained at week 3. Decortication of the articular processes alone was insufficient to achieve novel bone formation. ....90

Figure 2. 4 Histological samples retrieved from fused murine vertebrae. Samples have been stained with Pico Sirius red and Alcian blue stain to differentiate between bone and collagen. At 1 week, a large collagen mass overlaying the posterior elements of the vertebrae forms with disruption of local musculature. By the second week postoperatively, a large bony mass that was continuous with the cortex of the vertebrae was present. This mass exhibited a resorptive marrow-like center by week 3. No novel collagen or bone was observed in the decortications only spine. ....92

Figure 2. 5 AP and lateral microCT images demonstrating the volume of new bone formed in response to rhBMP-2 dose. To the right of each set of microCT images was a cross sectional image of the spine taken at its widest point in the transverse plane. An increase in the size of the fusion mass was observed with increasing rhBMP-2 dose. It was noted that at a dose of 0.5 µg sufficient bone was formed to bridge the L4-L6 vertebrae resulting in successful fusion. ....93

Figure 2. 6 Volume of spine fusion bone mass as a function of rhBMP-2 dose. A dose-response relationship was observed with consistent bone mass being formed with a dose as low as 0.5 µg of rhBMP-2. Bone volume data for the 10 µg dose (n=6) is included from the first phase and was consistent with the dose-response trend. ..93

Figure 3. 1 MicroCT reconstructions of harvested spines. ZA treatment led to an increase in the opacity of the rhBMP-2 induced fusion mass relative to controls. Spine fusion was achieved in all samples..... 106

Figure 3. 2 MicroCT assessment of bone volume (A) and bone mineral density (B). BV was significantly increased with ZA treatment (a, p<0.01) and in the ZA treated groups significantly less bone was associated with the *Nf1*<sup>+/-</sup> genotype (b, p=0.02). Likewise, BMD was significantly increased with ZA treatment (a, p<0.01) relative to untreated controls of the same genotype..... 107

Figure 3. 3 Transverse sections of fusion masses with a TRAP stain, counterstained with fast green. .... 109

Figure 3. 4 Osteoclast surface relative to bone surface was quantified from tissue sections. Without ZA treatment, *Nf1*<sup>+/-</sup> mice showed an increase in OcS/BS relative to wild type controls (a, p=0.05). Treatment with ZA led to significant decreases in OcS/BS for both genotypes (b, p<0.01). .... 110

Figure 4. 1 Animals were divided as per the table into groups (A) and subjected to a posterolateral intertransverse spine fusion surgery in which rhBMP-2 and AdCre virus are delivered to the lumbar spine via implantation of paired collagen sponges (B) as per previous publication. Dosing with ZA and the MEK inhibitor PD0325901 began 2 days prior to the date of surgery. .... 121

Figure 4. 2 Spines were harvested from all animals 21 days post operatively. Representative reconstructions of the bony anatomy using uCT data demonstrates that AdCre treatment at the time of surgery results in a visually smaller and less robust fusion mass. Axial cross sections are taken from the midpoint of the fusion mass where it was the most substantial. .... 124

Figure 4. 4 Bone volume of the fusion masses, as determined with uCT (A), demonstrated that in saline/BMP-2 co-dosed animals, treatment with the MEK inhibitor PD0325901 significantly increases the volume of bone formed in the fusion mass relative to controls (301%). A similar increase in the volume of the fusion mass was noted when mice cotreated at the time of surgery treatment with AdCre/BMP-2 were dosed with PD0325901 (194%). uCT analysis demonstrated that co-treatment with AdCre/BMP-2 yielded a fusion mass that was 14% smaller than saline treated mice, though this difference was not found to be significant. Treatment with the bisphosphonate Zoledronic Acid yielded a significant increase (10%) in the bone mineral density of the fusion mass (B) in mice treated with AdCre virus and BMP-2 at the time of surgery. .... 128

Figure 4. 6 Quantification of the number of osteoclasts located at the perimeter of collagen sponge revealed that the MEK inhibitor PD0325901 and the bisphosphonate ZA led to an 81% and 43% reduction respectively. Animal groups which did not receive AdCre delivery did not generate a fusion mass with infiltration of marrow space by fibrous tissue and did not exhibit a significant volume of collagen sponge remaining at the 21 day cull. There was, therefore, no population of osteoclasts located remote from bone to be quantified. .... 131

Figure 5. 1 Confocal fluorescent images of *Tie2*-lineage cells (tdTomato, red) in rhBMP-2 induced muscle, native bone, bone marrow, and rhBMP-2 induced ectopic bone. Images are shown at the muscle/ectopic bone interface (A) within an ectopic bone nodule (B), and within the native bone of the femur (C). Text labels, m = muscle, eb = ectopic bone, bm = bone marrow, cb = cortical bone. Scale bar = 50  $\mu\text{m}$ . .... 146

Figure 5. 2 Fluorescent images of ectopic bone showing *Tie2*-lineage cells (tdTomato) overlaid with vascular marker CD31 (A) or chondrocyte marker SOX9 (B). *Tie2*-lineage cells were found to demarcate the new blood vessels in the ectopic bone but not cartilage islands. Scale bar = 50  $\mu\text{m}$ . .... 147

Figure 5. 3 Fluorescent images of ectopic bone showing *Tie2*-lineage cells (tdTomato) overlaid with tartrate-resistant acid phosphatase/TRAP activity stain (ELF97, green) to label osteoclasts (A, zoom in B). No overlap was seen between *Tie2*-lineage cells with an alkaline phosphatase/AP activity stain (ELF97) to label osteoblasts (C, zoom in D). Scale bar = 50  $\mu\text{m}$ . .... 148

Figure 5. 4 rhBMP-2 induced ectopic bone formation in *Tie2-cre-Osx<sup>fx/fx</sup>* mice and littermate controls. Representative XRs (A, B) and microCT reconstructions (C, D) are shown for the specimens corresponding to the median bone volume for each group (A, C = littermate controls, B, D = *Tie2-cre-Osx<sup>fx/fx</sup>* mice). The bone formed in all cases showed a cortical shell with some trabecular-like elements visualized using Picro Sirius Red/Alcian Blue staining (E). MicroCT quantification revealed no

significant difference in bone volume of ectopic rhBMP-2 induced bone with deletion of the *Osx* gene in *Tie2*-lineage cells (F). ..... 150

Figure 5. 5 X-ray (XR) images showing the progression of rhBMP-2 induced spine fusion. After implantation of collagen sponges loaded with rhBMP-2, no mineralized bone was seen at D2, but a fusion mass was apparent in all specimens by D10 and D17. Anterior-posterior and lateral views are shown for all time points. .... 151

Figure 5. 6 Fluorescent images of spine fusion bone masses with co-labeling for  $\alpha$ SMA-lineage cells expressing tdTomato (red), *Col2.3*-GFP (green), and a TRAP activity stain (blue). Based on the image overlays, *Col2.3*-GFP+ cells are demonstrated to originate from  $\alpha$ SMA-lineage progenitors. In contrast, no overlap was seen with TRAP+ cells previously shown to originate from the *Tie2*-lineage. Scale bar = 50  $\mu$ m. .... 153

Supplementary Figure 5. 1 Fluorescent images of *Tie2*-lineage cells (tdTomato) with TRAP activity (ELF97) in spine fusion masses showing recapitulates the findings seen in ectopic bone nodules (Figure 3). Osteoclasts were observed in the fusion mass from D10 onwards. Scale bar = 50  $\mu$ m ..... 157

Supplementary Figure 5. 2 Fluorescent images of *Tie2*-lineage cells (tdTomato) with CD31 immunohistochemistry in spine fusion masses showing recapitulates the findings seen in ectopic bone nodules (Figure 2A). Scale bar = 50  $\mu$ m. .... 158

Supplementary Figure 5. 3 Control fluorescent images of rhBMP-2 induced spine fusion masses in Tamoxifen untreated  $\alpha$ SMA-CreERT2*Col2.3*-GFP: Ai9 mice at d17. (A) DAPI staining (blue) of nuclei, (B) tdTomato (red) is not seen without Tamoxifen treatment, (C) *Col2.3*-GFP+ expression (green) is seen in the new bone, and (D) an overlay with light microscopy to visualize the bone. Scale bar = 50 ..... 159

## Glossary of Abbreviations

AAV9	Adeno-Associated Virus 9
ACVR1	Activin A receptor, type I
AIS	Adolescent idiopathic scoliosis
ANOVA	Analysis of variance
AP	Alkaline phosphatase
BMD	Bone mineral density
BS	Bone surface area
BV	Bone volume
Cre	Cre recombinase
CRISPR	Clustered Regularly Interspaced Short Palindromic Repeats
<u>DKK1</u>	Dickkopf-related protein 1
DMD	Duchenes muscular dystrophy
EDTA	Ethylenediaminetetraacetic acid
EMT	Endothelial-mesenchymal transition
EOS	Early onset scoliosis
EPC	Endothelial progenitor cells
ERK	Mitogen-activated kinase
ERT	Human estrogen receptor
FLNB	Filamin B
GFP	Green fluorescent protein
HCl	Hydrochloric acid
HO	Heterotopic ossification

IS	Idiopathic scoliosis
IVD	Intervertebral discs
JNK	c-Jun NH2-terminal kinase
KO	Knock out
Lox/P	locus of X-over P1
MEK	Mitogen-activated kinase kinase
MPH	methylphedinate
MRI	Magnetic resonance imaging
NF1	Neurofibromatosis
NHMRC	National Health and Medical Research Council
NSAIDS	Non-steroidal anti-inflammatory agents
OcS	Osteoclast surface area
Osx	Osteoblast-specific transcription factor osterix
Pax1	Paired Box 1
PCR	Polymerase chain reaction
PDGF	Platelet-derived growth factor
SMMHC	Smooth muscle myosin heavy chain



# 1. Literature Review

## 1.1 Bone and Orthopaedic Biology

The bony skeleton provides a scaffold upon which the tissues of the body are supported and protected. It serves as the rigid component of the musculoskeletal system that, coupled with the muscles, tendons and ligaments, allows for motion. Bone is also a biologically active tissue that serves as a storage unit for minerals (calcium in particular) and houses bone marrow, the production centre of the body's blood cells. It therefore plays important roles in mineral homeostasis and haematopoiesis. [2-4]

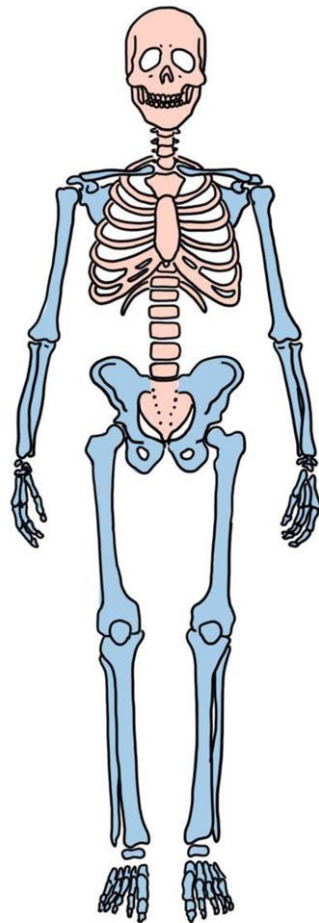


**Figure 1. 1** Human skeleton with axial (pink) and appendicular (blue) divisions.

### **1.1.1 Skeletal anatomy**

The adult human skeleton (figure 1.1) comprises approximately 206 bones [5] and associated cartilage and can be organizationally divided into the axial skeleton and the appendicular skeleton. The axial skeleton, as the name implies, is the axis of the body and is formed by the skull, ribs and vertebral column. Its functions are to maintain posture and to protect vital organs from external injury. Attached to this are the bones of the limbs that form the appendicular skeleton, which is responsible for mobility. Bones can also be categorized based upon their morphology - that is whether they are long, short or irregular in shape. [2]

### **1.1.2 Bone anatomy and histology**

The external surfaces of bones are enveloped in a complex and highly specialised connective tissue called the periosteum. The periosteum comprises two distinct layers: a thick outer, fibrous layer, which protects the bone and serves as an anchor point for tendons and ligaments and a thin inner layer which is rich in osteoprogenitor cells and plays an important role in bone growth and fracture repair. Beneath this cellular layer is compact cortical bone that provides most of the material stiffness and strength and constitutes about 80% of the weight of the skeleton. Running longitudinally through the cortical bone are a series of central or Haversian canals which are encircled concentrically by lamellae, or rings of bone. Bones gain additional strength from an internal sponge-like lattice of bone tissue called cancellous or trabecular bone. In long bones, cancellous bone is principally located in the metaphyses or end-regions. Cancellous bone comprises approximately 20% of bone weight and while less dense than cortical bone has a significantly greater

surface area. It is a highly vascular tissue and stores the bone marrow, where haematopoiesis occurs, within its bony lattice. [3]

### **Cellular composition of bone**

Bone is a metabolically active organ. Its structure is maintained through continuous remodelling, which involves a balance between the ongoing processes of bone formation and resorption. Each of these activities is primarily mediated by a specific cell type. Osteoblasts regulate formation of new bone, while osteoclasts perform the opposing action, controlling bone resorption. Remodelling may be activated by mechanical force, microdamage to the bone, or by changes to plasma concentrations of calcium and phosphorus. The purpose of remodelling is to yield a structure of maximal strength and minimal mass, while in the process also effecting important repair to any microdamage that arises from everyday function. [3, 6-9]

Osteoblasts or bone forming cells, are derived from osteoprogenitors - stem cells that have committed to the osteogenic lineage. Osteoprogenitors are present in many tissues, but are greatly enriched in the cellular inner layer of the periosteum. The primary function of osteoblasts is to produce and secrete osteoid, an extracellular collagen-based matrix, and then calcify that osteoid to produce mineralized bone tissue. As osteoblasts complete their cycle of differentiation and secretion of osteoid, they become buried in the lacunae of their matrix and become known as osteocytes. Osteocytes regulate bone metabolism by exchanging nutrients and waste with the vascular system via extensions of their plasma membrane and are critical to the maintenance of fluid flow through the bone. The flow of this fluid

may also be important to the process of remodelling by signalling mechanical stresses. [9]

Osteoclasts, the bone resorbing cells, are derived from the differentiation of haematopoietic macrophages/monocytes precursors located near the surface of bone. Once activated, osteoclasts migrate and bond to the surface of mineralized bone. Osteoclasts then release HCl and lysosomal enzymes into the resorptive microenvironment, creating a low pH (4.5) and degrading the components of the bone matrix. The products of degradation are taken up by the osteoclast and released from its free surface [6, 8, 9].

### **1.1.3 Embryonic development of bone**

Ossification is the process by which new bone is formed. The embryonic formation of bone is an important point of discussion and its principles are revisited in a subsequent section on bone repair. Developmentally, bones can form by either endochondral or intramembranous processes. With some overlap, long and short bones are formed via the former, while flat bones and irregular bones are formed via the latter. Bones are formed from the embryonic connective tissue known as mesenchyme, from which all connective tissue of the body ultimately is formed. Initially, mesenchymal cells are arranged loosely in the shape of bones. These mesenchymal templates will either differentiate directly into bone, via the process of intramembranous ossification, or will do this via a cartilaginous intermediary template by the process of endochondral ossification. [3]

### **(i) Endochondral ossification**

Endochondral ossification (figure 1.2) is the process by which most bones of the body are formed. This process involves the formation of a cartilaginous bone template which is replaced with bone matrix by proliferating osteoblasts. It is best illustrated using the example of a long bone. In the embryo, mesenchymal cells aggregate into the shape of the bone and differentiate into cartilage producing chondroblasts which lay down a cartilage extracellular matrix. When surrounded by extracellular matrix, the chondroblasts are called chondrocytes. Chondrocytes undergo hypertrophy, degradation and mineralization, producing the primary ossification centre. The mineralized matrix is then removed by osteoclast-like cells.[10] Osteoprogenitor cells in the periphery of the bone are stimulated by the penetration of a nutrient artery to differentiate into osteoblasts. Osteoblasts migrate into the spaces of the mineralized ossification centre and the consequent trabeculae and secrete osteoid, which hardens over a period of several days as calcium and other mineral salts are deposited. As the primary ossification centre grows towards the ends of the bone, osteoclasts (bone destroying cells) break down some of the newly formed bone in the centre of the shaft, leaving a cavity which is later filled with bone marrow. [3, 11]

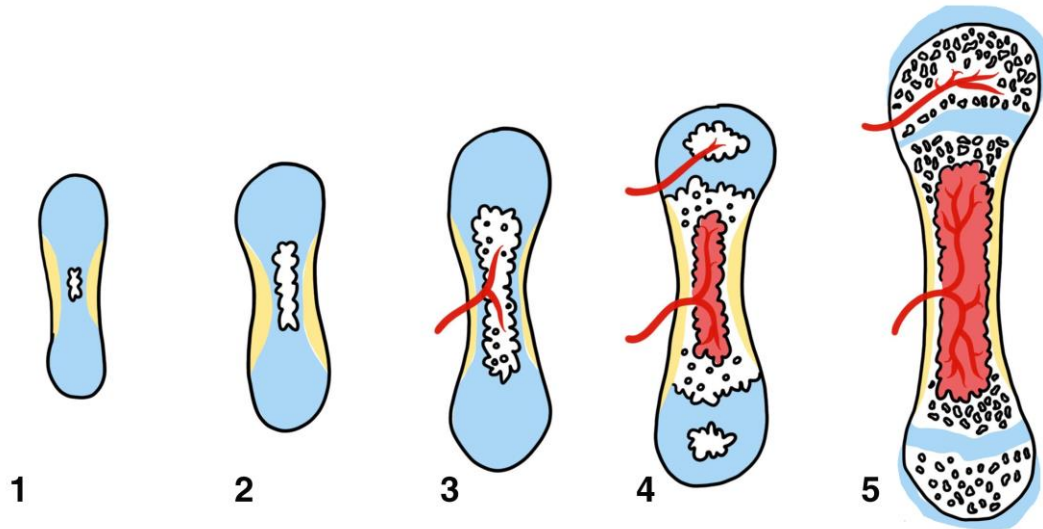


**Figure 1. 2** Endochondral ossification. Hyaline cartilage model with bone collar (1) ; Cavitation within cartilage model (2) ; Internal cavity invaded by periosteal blood supply with cancellous bone formation (3) ; medullary cavity formation and appearance of secondary ossification site in epiphysis (4) ; ossification of epiphyses and remainder of cartilage at physeal plates and articular surfaces.

## **(ii) Intramembranous ossification**

The flat bones of the body, including the skull and ribs, are formed by the process of intramembranous ossification (figure 1.3). Ossification occurs between sheets of mesenchymal cells at multiple ossification centres. Beginning at the ossification centre, a cluster of mesenchymal cells form and subsequently differentiate into osteoprogenitor cells, which in turn differentiates into osteoblasts. As in endochondral ossification, the osteoblasts in an ossification centre lay down osteoid which mineralizes, forming new bone. Continued bone formation allows the multiple ossification centres to coalesce and fuse. [3, 10]

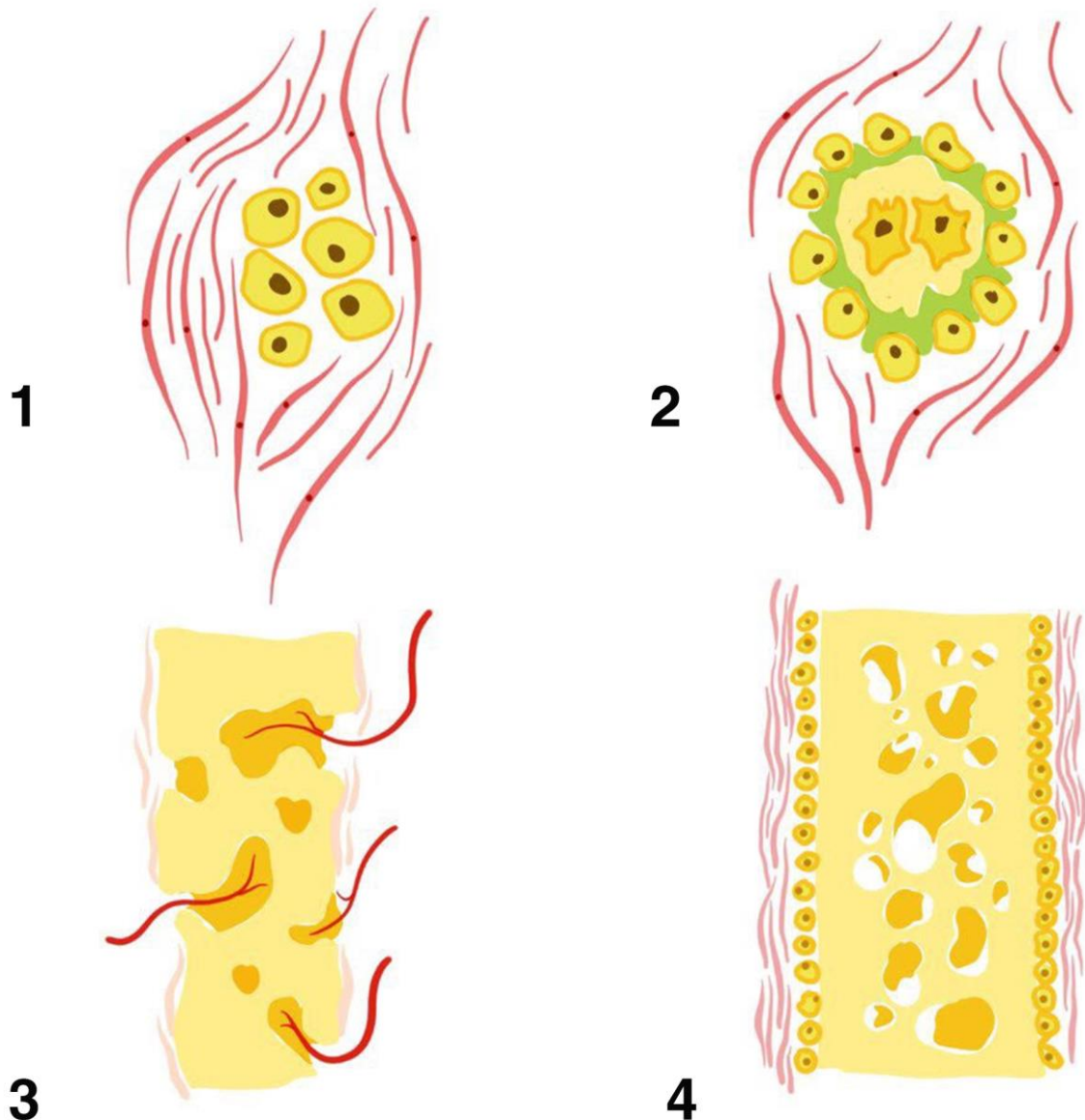


**Figure 1. 3** Intramembranous ossification. (1) Ossification centre appears within connective tissue membrane. (2) Osteoblasts secrete osteoid which mineralizes to form bone. Trapped osteoblasts become osteocytes (3) Random laying down of osteoid results in a poorly organized trabecular network of bone. Vascularized mesenchyme is laid down on the surface of the bone. (4) Dense mesenchyme becomes the periosteum and the bone deep to this thickens forming a cuff of mature lamellar bone.

### 1.1.4 Bone repair

Bone is repaired by a complex regenerative process involving the orchestration of multiple cell types which is stimulated as a response to injury. Unlike the healing of

other tissues which leaves a scar, bone repair implies the new formation of the original tissue. [12] The optimal result is repair with maximum strength and minimum weight with full restoration of skeletal function. During the repair process, the embryonic pathways of bone formation are repeated. All disrupted structures, including the periosteum, cortex, marrow and surrounding soft tissues contribute to bone regeneration. [13] Historically, fracture healing has been divided into primary and secondary fracture healing, though the former is rare and most fractures heal by the latter. [14] The process of bone repair may also be appreciated as a balance between anabolic (tissue forming), and catabolic (tissue remodelling), forces. [15]

### **(i) Primary fracture healing**

When bone fragments are reduced and immobilized with rigid fixation, the process of primary fracture healing may occur. Primary fracture healing attempts to restore the continuity of the Haversian system of the cortex. This process is callus-free and involves periosteal recruitment of osteoprogenitor cells. [13] It is also likely that contributing osteoprogenitor cells can originate from the surrounding soft tissues. [16]

### **(ii) Secondary fracture healing**

Secondary fracture healing (figure 1.4) involves a combination of intramembranous and endochondral bone formation, though the latter predominates. This process can be divided into 5 discrete stages, though there is considerable overlap between these chronologically. The process is initiated with the formation of a haematoma (1) and subsequent inflammation (2); this is followed by angiogenesis and the formation



of a soft cartilage callus (3). Hard callus formation (4) and bone remodelling (5) complete the process.

The trauma associated with a fracture tends to additionally injure surrounding soft tissues. At the moment of fracture, the blood vessels crossing the fracture line are disrupted leading to the production of a haematoma. Platelets in the haematoma release the cytokines TGF- $\beta$  and PDGF, initiating an inflammatory cascade which recruits osteoclasts and phagocytes to remove the newly dead tissue. Following this, fibroblasts and chondrocytes migrate to the fracture site from the periosteum and produce a collagen cuff around the fracture which is called the *callus*. The callus provides mechanical support to the fracture site as well as a scaffold for the formation of new bone. As an apparent recapitulation of embryonic processes, osteoblasts differentiate from osteoprogenitor cells and migrate into the collagen callus where they lay down osteoid. Once mineralized, the result is a hard callus uniting the bone fragments. The process of bone remodelling completes the process of fracture healing. Osteoclasts continue to remove dead bone and areas of callus that are not under mechanical load from the body, such as the periphery, are resorbed. Under normal healing conditions, the result is a perfect union of the fracture without any radiographic signs of previous fracture. [3, 13, 14, 16]

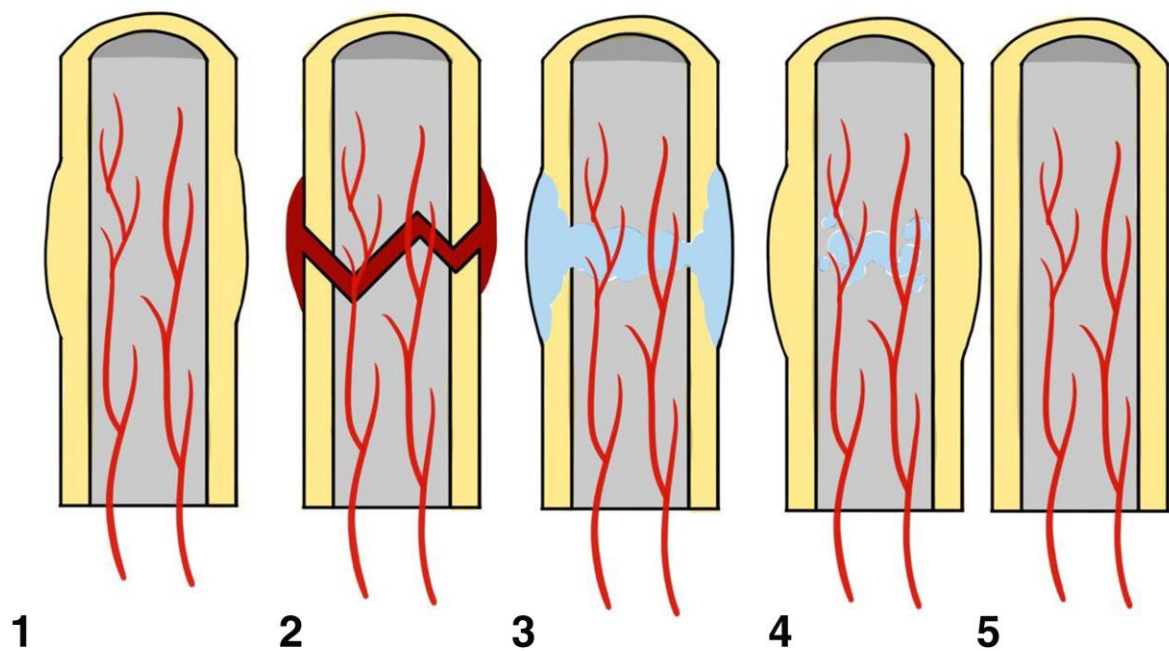


**Figure 1. 4** Secondary fracture healing. (1) Normal bone. (2) Fracture with disruption of blood vessels and haematoma formation. (3) Cartilaginous callus. (4) Replacement of cartilaginous callus by bony callus. (5) Remodelled bone.

### 1.1.5 Failure of the bone repair process

As bone repair is a multifactorial process, success depends upon the orchestration of many factors. Disruption of the bone repair pathway may result in the development of a delayed union or non-union of the fracture ends. At the point of non-union, all reparative processes have ceased. [17] The incidence of impaired healing has been reported as being 5-10%, resulting in significant morbidity. [18] Non-union occurs in the context of a poor biological and mechanical environment, though the specific cause for a particular failure of healing is often never known. Grossly, the predominant factors that determine successful outcome are blood supply and stability of the fracture site. [12]

### **(i) Blood supply**

During the process of endochondral ossification, osteoblast differentiation is stimulated by the penetration of a nutrient artery. Blood supply is similarly important to the success of fracture healing. Immediately following fracture, the blood supply is disrupted leading to necrosis of the fracture ends. Angiogenesis is an important phase of the fracture healing cascade and is responsible for restoring local blood supply to the fracture site. [18, 19] There is evidence to suggest that angiogenesis is stimulated by the same factors that stimulate osteogenesis and that the fracture haematoma is itself directly angiogenic. [20] Furthermore, it has long been appreciated that adequate blood supply to a fracture site is required for the formation of a strong callus. [21]

There is strong clinical evidence demonstrating a correlation between vascular impairment and unsuccessful bone healing. [18, 21, 22] The tibia offers an excellent example of how the rate of bone healing correlates with vascular supply. The upper metaphysis has a rich vascular supply. Fractures in this area tend to heal very well while fractures in the distal tibia, notorious for having one of the poorest vascular supplies in the body, have a tendency to develop non-unions and pseudoarthroses. [21, 23]

Experimental evidence has supported clinical findings regarding bone healing and vascular supply. Angiogenesis has been disrupted in animal models via physical impairment [24, 25], irradiation [26-28], disease [29] and pharmacological intervention [29, 30]. Interruption of angiogenesis in these models results in significantly impaired fracture healing.

## **(ii) Mechanical stability**

Reduction of a fracture, with the apposition of fragment ends, is an important factor governing subsequent successful healing. The degree to which primary or secondary healing contributes to the repair of a given fracture is determined largely by the relative motion between the fragments. When a fracture is stabilised with rigid, compressive fixation, primary fracture healing dominates. Bone is thus repaired by direct cortical reconstruction without formation of stabilising callus. When less rigid stabilisation is employed, secondary fracture healing via a cartilaginous intermediate callus is observed. [31, 32] Secondary healing is accepted as being the quickest method of restoring strength and form to a bone. Multiple studies have shown that delayed fixation of a diaphyseal fracture results in quicker healing when compared with immediate fixation. [33], [16, 34] Furthermore, numerous studies and clinical evidence support the finding that small amounts of relative movement between fragment ends promotes the formation of abundant callus, thereby enhancing the chance of union. [9, 32, 35, 36] These observations are likely the result of the *secondary injury phenomenon* which attributes these changes to the re-injury of the fracture site imposed by excessive motion without fixation. [12] However, excessive motion of unstable fragments impairs bone repair by not permitting soft tissue healing and periosteal revascularization, resulting in non-union. [37] The cellular mechanisms by which the mechanical micro-environment of a fracture dictates healing are largely unknown.

### **1.1.6 Cellular contributors to bone repair**

Bone repair depends upon the differentiation of osteoblasts from osteoprogenitor cells. Traditionally, these cells have been thought to be derived from the bone marrow and periosteum. [13, 14, 37-39] There exists clinical and experimental evidence however suggesting that extraosseous tissues contribute progenitor cells to the bone repair process.

#### **(i) Clinical evidence for extraosseous cell contribution to osteogenesis**

Heterotopic ossification (HO) is a phenomenon in which mature trabecular bone forms in extraosseous tissues. Bone may form in tissues adjacent to skeletal bone, as in the case of periarticular HO [40], or in more distant tissues of the skeletal muscle [41], skin [42], mesentery [43], or blood vessels [44, 45]. HO is significant to our understanding of osteogenesis because bone formation occurs at sites that are remote from the bone marrow and periosteum, the traditionally accepted location of osteogenic precursor cells. It has been proposed that HO is a reactive process that is stimulated in response to tissue injury, prompting the differentiation of osteoblasts and chondroblasts from non-committed mesenchymal stem cells located in injured tissue via protein signalling. [42]

A breakthrough in the understanding of the protein signalling that underlies HO was made by Urist in 1965. It was demonstrated that demineralised and lyophilized bone implanted into rabbit muscle pouches induced ectopic bone formation. [46] He determined that this was due to the effect of a mixture of proteins located in the extracellular matrix of bone which he named the 'bone morphogenetic proteins'. In recent decades, the proteins have been isolated from the decalcified matrix and the

BMP genes have been cloned. The resultant recombinant proteins (BMP-1, BMP-2) have been shown to be biologically effective at inducing the ectopic formation of new bone (Wozney, Rosen et al. 1988). As of 2002, the use of BMP in a collagen sponge vehicle has been approved for use in human patients in the forms of BMP-2 and 7. [47]

## **(ii) Experimental evidence for extraosseous cell contribution to osteogenesis**

Urist demonstrated that BMP was capable of inducing osteogenesis in extraosseous soft tissue when introduced experimentally. These results have been reproduced in vivo via both the physical implantation of BMP-2 into muscle [48-52] as well as via retroviral delivery of BMP-2 to target cells [49, 53, 54]. The ability of a BMP solution and retroviral delivery of BMP to stimulate differentiation of muscle cells into an osteoblastic phenotype is also supported by in vitro data. [49, 53-55] In vitro studies used ALP activity and osteocalcin production as markers of osteoblastic differentiation.

Wang et al [52] purified and characterized the osteogenic activity of rhBMP-2. Following implantation of the protein under the skin of rats in incremental doses between 0.46 $\mu$ g and 3 $\mu$ g, the implants were removed between day 5-21 and examined histologically. At day 5, immature and some hypertrophic cartilage cells were observed in the implants. At 7 days post implantation, chondrocytes were hypertrophic and the cartilage was mineralized. Osteoblasts surrounded by osteoid and vascular elements were also noted. By 14 days, removal of cartilage was nearly complete and bone was abundant. Osteoblasts and osteoclasts were widespread.

The implants were highly vascular and some haematopoietic cell maturation was identified. Implants removed at 21 days showed highly matured bone architecture. Doses of rhBMP-2 of 6µg and above were noted to yield consistent ectopic bone formation, though even at the lowest dose of 0.46µg ectopic bone was detected in half of implants removed at 21 days. They suggest that 0.6µg is the lowest dose that can reliably produce bone formation.

### **(iii) A genetic basis for HO**

HO is not associated with any known metabolic disorders (ie: hypercalcaemia) but is manifested extensively in individuals with *fibrodysplasia ossificans progressiva* (FOP) and *progressive osseous heterodysplasia* (POH). FOP is an autosomal dominant disease, though it may arise by spontaneous mutation [42], that is characterized by progressive ossification of the tendons, ligaments, fasciae and skeletal muscle, resulting in significant morbidity and suffering. [56] An understanding of the genetics that underlie these disorders may provide greater insight into the pathogenesis of HO as well as skeletal osteogenesis.

Patients with FOP have been shown to over-express BMP-4 [57]. The BMP-4 transcription rate in the cells of affected has been demonstrated to be 4-7 times greater than in unaffected controls. [58] Several mutations have been identified in genes that are associated with this disease. [42] Feldman [59] found an association between the FOP phenotype and a mutation at 4Q27-41 in four families with familial FOP. At least one of these genes is proposed to be linked with the BMP-signalling pathway. Shore [60] found that the mutation was specific to the gene for ACVR1, a receptor for BMP-4. Constitutive activation of ACVR1 results in the induction of

alkaline phosphatase activity in C2C12 cells upregulating BMP-4 and downregulating BMP antagonists.

#### **(iv) BMP and vascular calcification**

The association between endogenous (as opposed to implanted) BMP and HO has also been demonstrated in patients who are not affected by a BMP related mutation. Vascular calcification is a common condition that is associated with significant morbidity and mortality in the population. Traditionally it has been believed that vascular calcification occurs via a passive crystallization process involving the precipitation of minerals from calcium and phosphate saturated extracellular fluid. [61] There is evidence that vascular calcification is not the result of a passive process, but rather an active biologic mechanism involving BMP-stimulated osteogenesis. Prompted by the observation that these calcifications frequently contained fully formed bone tissue (including bone marrow) Bostrom et al [62] found that calcific atherosclerotic plaques expressed BMP-2.

#### **1.1.7 Cellular tracking**

The *de novo* formation of bone in skeletal muscle and other extraosseous tissues implies that these tissues, and potentially circulating systemic cell populations, represent sources of non-committed precursor cells that are capable of contributing to osteogenesis. In order to prove that these cells feature in the repair process of bone, a cellular tracking system must be implemented that allows for the permanent and selective labelling of precursor cells, permitting identification regardless of final differentiated cell type.



Early techniques for tracking the lineage of a cell involved the intracellular injection of a dye and observing the progeny of the mother cell. This system was limited by issues of dilution of dye strength by cell division and by transfer between cells, resulting in a reduction in specificity of labelling. [63-65] Genetic cell marking using tissue specific promoters, such as with LacZ gene, [66] resolves many of the issues that impede dye labelling but ceases to work once a cell stops expressing a promoter. This is a significant limitation for lineage tracking. Transplantation of a labelled cell population from a donor animal to a recipient allows for lineage tracking, although the injection of single cell suspensions can be a limiting factor compared to transplanting tissue grafts. For this reason, transplantation of cell suspensions is often best suited to haematopoietic studies.

Genetic recombination via the Cre-Lox/P system is a system that permits permanent labelling of a cell population under the control a tissue specific promoter. This proved to be the most suitable technique for our purposes.

### **(i) The Cre-LoxP system**

The Cre-LoxP system allows the introduction of selective genome alterations in a reporter mouse. Cre-recombinase is a bacteriophage P1 derived 38 kDa protein that is capable of recognizing 34 bp sequences, called LoxP sites, along the genome. When Cre-recombinase is expressed, site-specific recombination between two LoxP sites is catalysed. [67] Depending on the orientation of the LoxP sites, Cre-mediated recombination may lead to deletion, translocation between chromosomes or inversion of the DNA segment. [68] This system can be used to label a population of

cells spatially (tissue specific) and temporally. This is illustrated especially well by the lab of Ivo Kalajzic using the  $\alpha$ SMA<sup>CreERT2</sup>/Ai9 transgenic mouse line.

In order to achieve tissue-specific cell tracking, Cre-recombinase expression is under the regulation of tissue-specific promoters. For example, a population of cells expressing smooth muscle actinin ( $\alpha$ SMA) has been identified that has osteogenic potential. Cells expressing this are known to reside in areas known to contain osteoprogenitor cells (perivascular niches, periosteum). Cre-recombinase may be 'knocked in' to the genome in such a way that it is promoted only in cells expressing  $\alpha$ SMA. [68] LoxP site recombination is therefore restricted to tissues in which  $\alpha$ SMA is expressed.

Temporal control of the Cre-mediated recombination of the LoxP site can also be achieved. In order to accomplish this, a ligand binding domain for human estrogen receptor (ERT) to the Cre enzyme. When tamoxifen (an ERT antagonist) is given systemically to the mouse, the Cre-ERT complex is able to penetrate the nucleus of the cell and induce mutation.

When crossed with Ai9 reporter mice, this temporal and spatially specific Cre-mediated recombination results in the red fluorescence of the target cells, due to the expression of the TdTomato gene. This fluorescent labelling permits a permanent way of tracking a target cell population, regardless of transdifferentiation and ultimate cell fate.

## **1.2 Scoliosis**

### **1.2.1 The anatomy of the spine**

The vertebral column, is a component of the axial skeleton. It consists of 33 vertebrae can be divided into 5 regions based upon the morphology of their respective vertebrae: cervical (7 vertebrae), thoracic (12 vertebrae), lumbar (5 vertebrae), sacral (5 vertebrae), and coccygeal (4 vertebrae) (figure 1.5). These regions of the spine are in turn associated with natural anterior-posterior curvatures. The spine exhibits what Hippocrates called “ithiscolios”, meaning that it is straight in the coronal plane and curved in the sagittal plane. Specifically, when viewed front-on the cervical and lumbar spines are associated with convex curvature while the thoracic and pelvic (sacral and coccygeal) spines demonstrate concave curvature. Prior to birth only the Thoracic and Pelvic curves (concave curvatures) are present. The cervical curvature develops as the infant begins to raises its head, causing a convexity in the spine. The lumbar curve develops as the child begins to stand upright.

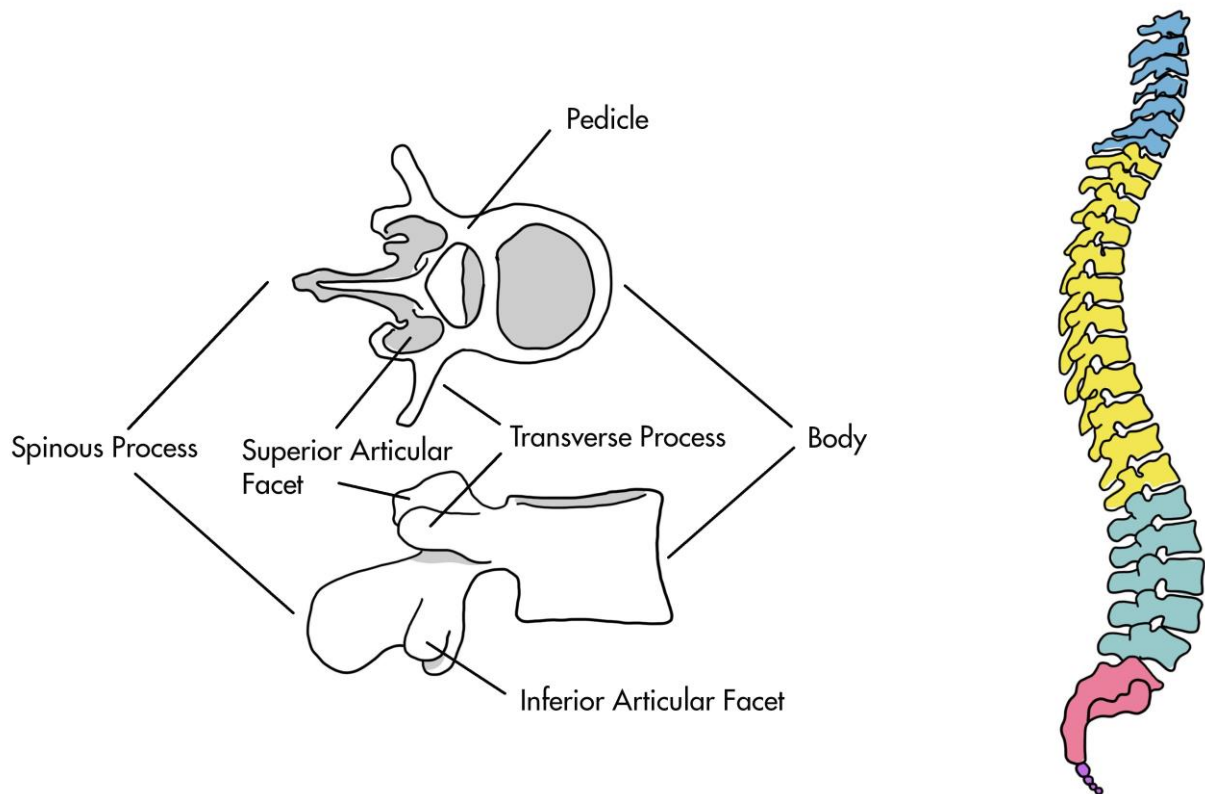


**Figure 1. 5** Anatomy of the spine and morphology of a typical lumbar vertebra.

The morphology of vertebrae differs subtly between regions, reflecting their function. The body of the vertebrae constitutes the bulk of the volume of the bone and bears the majority of the weight of the spine. It is roughly cylindrical in shape with superior and inferior surfaces bearing a thin cartilaginous layer. Adjacent vertebral bodies are separated via an intervertebral disc forming a joint which allows for flexion and compression. The vertebral arch attaches to the body posteriorly and is formed by the fusion of twin pedicles and laminae. The space bounded by the vertebral arch and posterior vertebral body is the vertebral foramen, in which the spinal cord lies protected. The spinous process projects posteriorly from the vertebral arch and is formed by the fusion of the laminae. At the union of the laminae and pedicles rise a pair of transverse processes which project laterally, and two pairs of articular

processes (superior and inferior). The first two cervical vertebrae, named the atlas and the axis, are exceptions. In place of a vertebral body, the atlas (Cervical vertebrae 1) possesses an anterior arch in which lies the odontoid process, a strong bony post arising superiorly from the vertebral body of the axis (C2). This joint is responsible for 90% of the rotation of the head from left to right. Intervertebral discs allow motion in any direction. The articular processes of adjacent vertebrae form synovial joints, limiting the spines motion in certain planes. In the cervical and lumbar spines they are positioned in such a fashion that facilitates flexion and extension with limited rotation. In the thoracic spine they guide lateral bending and rotation. The spinous and transverse processes provide anchor points for the ligaments and tendons of the spinal musculature. [69]

### **1.2.2 Scoliosis**

Scoliosis is a physical disorder of the spine that is characterized by lateral curvature, typically appearing during adolescence. [70] When combined with excessive kyphosis or lordosis, which are exaggerated curvatures of the thoracic and lumbar spine in the sagittal plane respectively often referred to as 'hump back' and 'sway back', the result is a complicated three dimensional deformity. Scoliosis is not a disease in itself, but is rather is the manifestation of one of a number disease processes which result in spinal asymmetry. It is a common disorder, with an incidence in the background population as high as 4.5%. [71]

Scoliosis is a diagnosis that comprises one of several aetiologies (figure 1.6). Congenital deformities result from primary physical abnormality of the vertebrae which develop during the first 6 weeks of intrauterine growth and manifest as spinal

curvature from birth. [72] These deformities are referred to as ‘dystrophic’. The spinal curvature of neuromuscular scoliosis is progressive and arises secondary to the muscular weakness or spasticity of the trunk as is seen for example in patients with cerebral palsy, muscular dystrophy, or spinal cord injury. [73] The causes of the appropriately named idiopathic scoliosis (IS) are still not clear. Metabolic, hormonal, mechanical and genetic factors have been proposed. [74] Some speculate that it may in fact be a late onset subtype of neuromuscular scoliosis. [75]

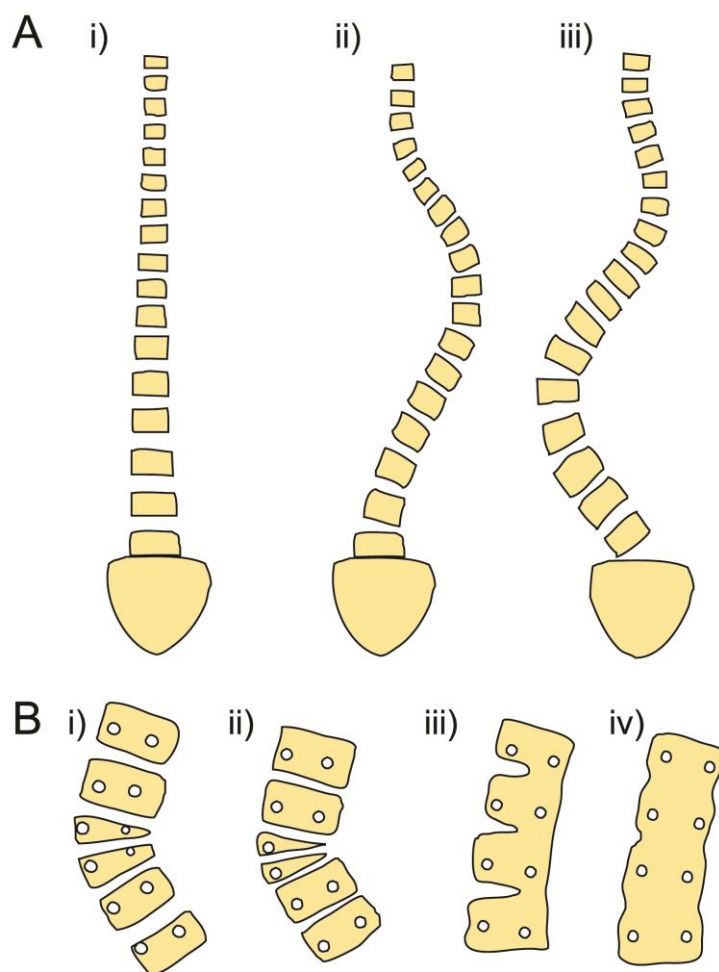


**Figure 1. 6** A) Normal spine (i) compared with thoracic (ii) and lumbar (iii) scoliotic deformity. B) Congenital deformity of spine secondary to partial unilateral failure of formation (i) complete unilateral failure of formation (ii), unilateral failure of segmentation (iii), and bilateral failure of segmentation (iv).

Lateral curvature of the spine is also evident as a sign in some well described conditions including, Osteogenesis imperfecta (OI) [76], Duchenne Muscular Dystrophy [77], Marfan Syndrome [78], Charcot-Marie-Tooth disease [79], Prader-Willi syndrome [80], Ehlers-Danlos disease, and [81] Filamin B (FLNB) associated disorders. Of particular note is the high prevalence of spine curvature requiring intervention in Neurofibromatosis type 1 (NF1).

## **1.3 Spine Fusion**

### **1.3.1 Indications for spinal fusion**

Spinal fusion is a procedure that immobilizes segments of the spine via the formation of bone bridges between adjacent vertebrae. Early implementation of spinal fusion focused on preventing the increasing deformity associated with scoliosis, as well as infections and traumatic injuries. [82] Scoliosis is a deformity of the spine characterized by a lateral curvature. When combined with the natural kyphosis and lordosis of the spine, the result is a complicated three-dimensional deformity. The disease is typically progressive, worsening as the vertebrae grow. Bamfield observed that progression of the disease occurred during growth of the vertebral body and suggested that it is caused by the asymmetrical growth of one side of the body with a conjugate resorption of the other side secondary to increased pressure on the growth plate. [70] With the cessation of vertebral growth, so ends the progressive deformity of scoliosis. However, a worsening of scoliosis may be noted through adulthood which is due largely to degeneration of the intervertebral discs with age. [83]

Spine fusion surgery has since been implemented in the treatment of pain secondary to unstable motion or degenerative change of the spine. [82]

#### **1.3.4 Historical treatments for spinal deformity**

Scoliosis is amongst the oldest diseases known, and early treatments are referenced in literature dating back as far as 3500 BC. Hippocrates (460 -370 BC) was the first to document the anatomy of the disease.[84] Early interventions encompassed a range of combinations of traction, casting and bracing and therapy for spinal deformity had evolved little until the 20<sup>th</sup> century. [85]

The development of x-rays by Röntgen as well as the emergence of modern surgery encouraged the surgical manipulation of spinal deformities. For the first time, surgeons were able to visualize and compare patients' deformities and formulate evidence-based approaches to treatment. The first surgical approaches focused on instrumented correction of deformity. Richard von Volkmann (1830–1889) and Hadra [86] used silver wire to correct deformity in Pott's disease (spinal manifestation of extrapulmonary tuberculosis) while in 1902 Fritz Lange splinted the spine with bilateral 4 mm steel rods secured at either end with silver wire (Lange 1910, suggesting that bracing systems should be placed under the skin.

#### **1.3.5 Early instrumentation for spinal correction**

##### **(i) The pioneering work of Hibbs, Albee and DeQuervain**

Spine fusion surgery was pioneered in 1911 independently by Hibbs, Albee, and De Quervain. Hibbs observed that a tuberculosis infected spine that has been treated with casting and bracing displayed a tendency towards a natural bony ankylosis [87] .



He proposed that surgical acceleration of this process may assist the healing process. Later, he commented on its potential use in the treatment of the advancing deformity that results from scoliosis. By splitting the spinous processes and laminae and elevating them to come into contact with adjacent spinous processes and laminae he attempted to induce fusion. He assisted this bridging effect with bone graft harvested from spinous processes. In 1917, he applied spinal arthrodesis to the treatment of scoliosis and eventually to fracture dislocations and spondylolisthesis [87]. Around the same time as Hibbs' first surgeries, Albee created an internal splint by inserting a section of tibial graft between adjacent spinous processes for the purpose of treating Potts disease. He had noted that bony union of joints elsewhere in the body caused the tuberculous process to disappear rapidly. His poor experience with infection and failure of implanted screws and other foreign bodies led him to use autologous tissue as a means of securing fixation. [88] De Quervain used scapular spine for his graft. The use of arthrodesis as therapy for joint pain and deformity was well established at this time but had not yet been applied to the spine.

## **(ii) Early instrumented spinal fusion procedures**

The practice of spine fusion evolved to incorporate the use of internal fixation devices (figure 1.7). As suggested by Lange, there were benefits to braces being put under the skin. Internal fixation yields a more stable construct than external bracing. In 1955, Allan built upon the work of Lange and began to use internal fixation devices to stabilise the fusion site with the intention to provide a quicker and more effective means of correcting spinal curvature. He devised a means of lengthening the concavity of a curvature via an expanding device. The device consisted of a jack formed by two Y-shaped pieces which are connected by a threaded sleeve. The

forked ends sat at a 30 degree angle from the shaft of the tool. The jack was placed between adjacent transverse processes along the concave side of the joint to be fused. As the sleeve rotated, the jack expanded and increased the distance between the transverse processes, lengthening the concavity of the deformity. Bone graft could then be positioned as for a standard fusion procedure. [89] Harrington subsequently developed a set of instrumentation (Harrington instrumentation) that consisted of a distraction bar and a compression rod with ratcheted hooks placed on either side of the curvature to incrementally achieve correction in the absence of vertebral fusion. [90]

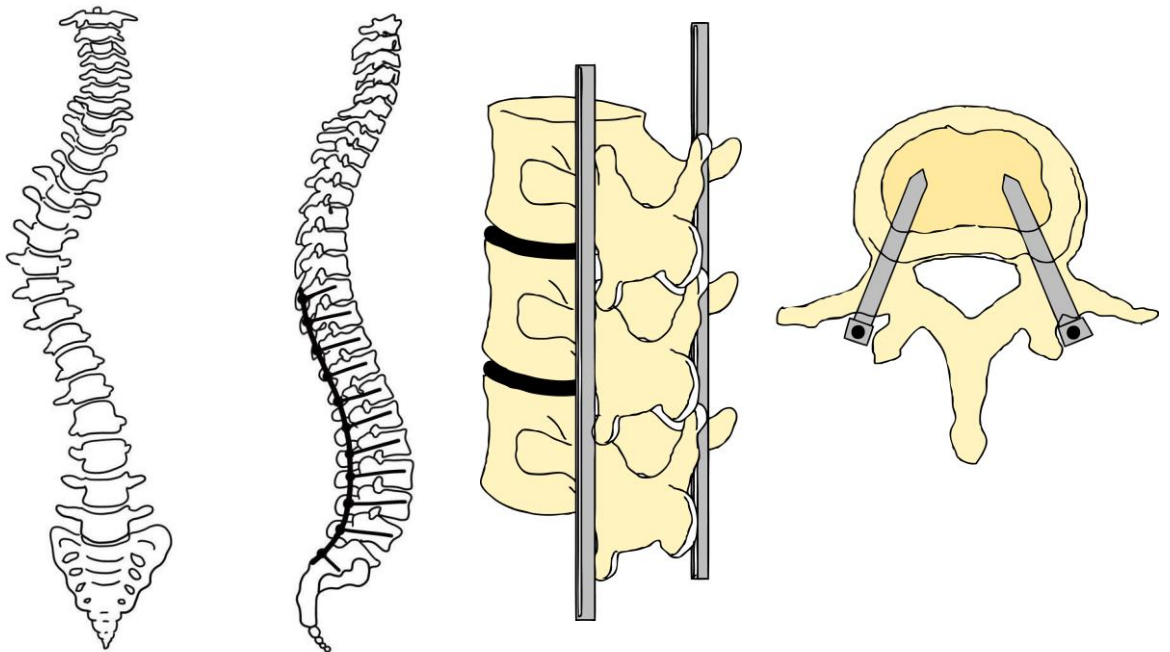


**Figure 1. 7** Instrumented spine fusion permits correction of scoliotic deformity with fixation of bilateral rods via pedicle screws extending into vertebral body.

### **1.3.6 Anabolic approaches for spinal fusion**

The use of autogenous bone as a graft material was ubiquitous in early fusion surgeries and is still the gold standard grafting substrate. In the context of spine fusion, autologous bone graft possesses several qualities that make it a desirable grafting material. It provides immediate structural support allowing for the splinting of adjacent vertebrae, therefore limiting motion. Autologous bone also has osteogenic, osteoinductive, and osteoconductive properties. [91] When autologous bone is harvested and transferred to a graft site, it carries with it its native osteogenic cells which, in the correct environment, are capable of forming bone. Native bone also has osteoinductive proteins which stimulate the proliferation of undifferentiated mesenchymal cells and formation of osteoprogenitor cells. The structure of bone consists of an osteoconductive three dimensional matrix that provides a scaffold that can support the ingrowth of new bone as well as new capillaries and perivascular tissues. The osteoconductive property of bone is thought to result from its physical architecture, chemical structure and surface charge. [92].

Autologous bone may be harvested from the iliac spine, as well as the ribs, fibula, and distal tibia. In addition to being limited in availability, its harvesting comes at the cost of significant morbidity. The frequency of major complications following autologous bone harvest has been reported to be 8.6%, with minor complications occurring in 20.6% of cases [93]. Numerous substitutes have been used that possess one or several of the qualities of autologous bone. The matrix of trabecular bone has been replicated using synthetic (such as calcium based porous ceramics) and biologic alternatives. Bone in the form of allograft (from a non-genetically identical individual of the same species) and xenograft (from a member of a different species) are examples of biologic substitutes. These materials provide immediate

structural support for surrounding tissue but in the process of cleaning and sterilising to prevent disease transmission and rejection, lose their osteogenic potential and do not function as well as native bone. [94] Their structural lattice remains intact, however, and they are effective osteoconductive substitutes for autograft.

BMPs are amongst the more popular anabolic bone graft substitutes. When compared against iliac crest autograft in posterolateral intertransverse lumbar spine fusion, BMP treated individuals yielded significantly higher fusion rates while reducing donor site morbidity [95].

### **1.3.7 BMP delivery systems**

BMP must be introduced into the body by way of a carrier material. The role of the carrier is to deliver and localise the drug to the target site, where it can exert its biological activity, and to provide a substrate for the bone forming cells. The quality of the BMP induced bone mass is largely dependent upon the quality of the carrier. Under optimal conditions, the bone mass will closely mimic the carrier in size and shape [4]. Kwon et al have proposed a series of criteria to define the ideal carrier material. A carrier must be biocompatible to limit inflammatory response and should localize the drug to the target site while maximizing its osteoinductive and osteogenic properties. These properties can be amplified if the carrier material provides an osteoinductive scaffold with a porosity mimicking native bone, promoting the ingrowth of bone forming cells and vasculature. Additionally, the structure of the carrier should limit the local effects of space occupying delivery systems and not compete with or limit bone formation. Finally, an ideal carrier will be biodegradable allowing timely removal from the body.

It is likely that the previously discussed adverse events associated with BMP use may be mitigated by the use of an improved carrier system. In current practice rhBMP-2 (marketed under the INFUSE® brand by Medtronic©) is distributed as a powder which is reconstituted into aqueous form at the time of surgery and impregnated into an absorbable collagen sponge. It has been suggested that adverse events are contributed to by the tendency of aqueous BMP to diffuse rapidly from the collagen sponge resulting in migration of the drug to sites remote from the fusion bed [96, 97]. In this way, BMP exerts its osteogenic and proinflammatory properties on extraosseous tissues, resulting in ectopic bone formation and soft tissue swelling respectively. Ectopic bone formation is a predictable result of the user of BMP and examples include foraminal and spinal canal bone deposition [98, 99] which may result in neurological impairment. The proinflammatory properties of BMP are responsible for the perivertebral soft tissue swelling. Cervical tissue swelling has been associated with dysphagia and airway oedema [100, 101], which has resulted in patient intubation and occasional mortality [102]. Inflammatory response disrupting the superior hypogastric plexus following anterior interbody lumbar fusion has been associated with an increased incidence of retrograde ejaculation in male patients [50]. Immobilization of BMP at the site of fusion is critical in achieving adequate local drug concentrations and preventing diffusion associated adverse events [97]. In order to better control BMP delivery at the target site, alternative delivery mechanisms have been investigated. Compression resistant carriers such as collagen/calcium phosphate composites [103-105], calcium sulphate biomaterials [75] and biodegradable polymers [72, 73, 106] are of particular note as they promote localised delivery of BMP as well as maintain a potential space for bone growth by preventing soft tissue compression.

### **1.3.8 Adverse effects associated with BMP induced spine fusion**

Due to its efficacy in forming new bone and the eliminated donor site morbidity associated with harvesting iliac crest bone graft, BMP is increasingly used to augment spine fusion procedures. It is currently only approved for use in anterior interbody lumbar cage fusions (AILF). In this procedure, the intervertebral disk is removed completely and is replaced with a metal cage which maintains intervertebral space and vertebral alignment. The cage, which has historically been iliac crest bone graft, may be filled with a BMP-impregnated carrier which promotes fusion of the adjacent vertebral bodies. Increasingly, BMP has been used off-label in alternate spine fusion techniques, including cervical fusion and lumbar posterolateral intertransverse fusion (PLF).

The initial peer reviewed, industry sponsored safety reviews of BMP in spine fusion suggested that its recommended use was not associated with any adverse effects or that any adverse effects noted were unrelated to its use. In these initial studies, 780 patients received BMP augmented spine fusion (including AILF and PLF techniques), without adverse effects reported. Due in large part to the promising findings of these trials, the use of BMP jumped dramatically from use in 0.7% of all fusions in 2002, to 25% in 2006. With the rising use of BMP in spine fusion there have been many reports of serious complications arising secondary to the use of BMP in the spine. Most complications arose between day 2 and 14 post-op. Early events were associated with what appeared to be a pro-inflammatory activity of BMP. When used in the context of cervical spine fusion, patients were reported to develop a swelling of the neck soft which could progress to airway obstruction requiring emergency intervention. Patients were also known to report difficulty in breathing and speaking

as well as pain while swallowing. Smucker et al noted a 27.5% incident of clinically significant swelling. Other significant events observed were related to overgrowth and uncontrolled bone formation, and to the negative effect of BMP on exposed nerves and dura which may result in nerve symptoms including pain, loss of function and retrograde ejaculation. [71]

### **1.3.9 Failure of Spine Fusion Surgery**

Since the first pioneering operations for spinal fusion performed by Hibbs and Albee 100 years ago, the procedure has been plagued by high failure rates.[88, 107] Pseudoarthrosis is the name given to the 'false joint' created by non-union of two bones at a site of desired fusion. The rate of pseudarthrosis has been estimated to be between 5% and 35% [108]. Successful fusion is dependent upon a multifactorial process. The process of osteogenesis involved in the fusion of adjacent vertebrae involves the same mechanisms discussed in bone repair. As with bone repair, vascularity and mobility are important factors which determine the success of the fusion procedure.

#### **(i) Influence of vascularity on spinal fusion success**

##### **Blood supply and the fusion bed**

The importance of vascularity to the bone repair process has been described. Cytokines released immediately following vascular injury associated with bone trauma promote an influx of osteogenic cells, while intact vessels provide a conduit

for their migration. In the case of spinal fusion surgery, bone trauma is induced by the surgeon during decortication of the fusion bed.

Decortication of the graft site establishes the contact surface area available for the growth of the bony bridge between adjacent bones. A greater decorticated surface area will encourage the growth of a larger fusion mass [109] , by exposing a greater amount of osteogenic cells which will be available for subsequent bone formation. The decorticated fusion bed must expose and traumatise viable and vascular bone to be effective. Use of power burrs may induce thermal necrosis of the bone, limiting the effective surface area available to participate in bone healing. (Boden 1998) The transverse processes are difficult to decorticate and have a smaller available surface area compared to the body of the vertebrae, resulting in a smaller fusion bed. Posterolateral fusion beds, therefore, represent a comparatively poor bone environment for bone growth. [110]

### **Osteoporosis is a condition associated with poor vascular supply and poor surgical outcome**

Osteoporosis is the most common metabolic bone disease. It is characterized by bone that has a lower density and decrease turnover rate, resulting in decreased healing capacity when compared with healthy tissue. There is a strong association between osteoporosis and vascular disease. [111] Men and women with known peripheral arterial disease have been shown to have lower bone mineral densities and present with more fractures than matched controls. [112, 113] Cancellous bone is affected more than cortical bone by the decreased turnover and its effects are more pronounced in the vertebrae, which have a relatively high ratio of cancellous to



cortical bone. Additionally, the trabeculation in affected bone are sparser and significantly more brittle than non-affected bone resulting in a poor anchor site for instrumentation used to secure vertebrae. [114, 115]

### **Factors influencing bone vascularity**

Circulating drugs, nicotine and irradiation are amongst the most prominently investigated factors which threaten bone vascularity. The rate of their investigation is surely associated with their incidence in the population and strong association with impaired bone healing.

Non-Steroidal Anti-inflammatory agents (NSAIDs) are commonly used in the perioperative period for pain relief. Several studies have shown an association between high dose NSAIDs, specifically Ketorolac and non-union in spinal arthrodesis. [116] [117-119] There is strong evidence suggesting that NSAIDs inhibit angiogenesis [120, 121] and interfere with the inflammatory cascade which is critical for initiating the early stages of bone healing. Furthermore, it has been proposed that these agents may have a direct inhibitory effect on osteoblast and osteoclast function. [122-124]

Similar effects on bone vasculature have been shown secondary to circulating nicotine.[125] The correlation between cigarette smoking and non-union after attempted spinal arthrodesis is well established.[125-128] Nicotine is thought to inhibit the revascularization of bone graft. [30] A non-union rate of 26.5% in smokers has been compared with 14.2% in non-smokers. [129] Patients who ceased smoking for 6 months showed non-union rates comparable to their non-smoking counterparts.

Irradiation during the peri-operative period has long been appreciated to have deleterious effects on bone. Post-operative radiotherapy has greatly decreased the incidence and recurrence of soft tissue sarcomas [27] but has been shown to have an adverse effect on bone healing. Arnold et al [26] demonstrated an inversely proportional relationship between preoperative irradiation and the healing of rat femoral fractures. Similar relationships have been established by Emery and Bouchard using canine and rabbit models, respectively [130]. They found that irradiation administered in the immediate postoperative period was detrimental to successful bone growth. They proposed that this was due to the adverse effect of irradiation on bone vascularity resulting in a graft bed of diminished viability. They also suggested that irradiation was directly deleterious to dividing mesenchymal stem cells and immature osteoblasts.

## **(ii) Mechanical stability**

Immobilization is critical in the establishment of union between the bony fragments of a fracture [16]. The fusion of adjacent bones united by a bony bridge is analogous to the fracture scenario with respect to the need for immobilization. In non-instrumented spine fusion, splinting of adjacent vertebrae is accomplished solely by the mechanical properties of the graft material. There is consequently a greater propensity for relative motion between the vertebrae that are intended to be fused.

It has been observed that when interlocking cortical or cortico-cancellous grafts are used in lumbosacral sheep spine, union always occurs at the interlumbar joints and never occurs at lumbosacral joints. Nagel et al concluded that this was the result of increased relative motion at the lumbosacral joints relative to interlumbar joints. Their

study showed that a strain of approximately 10% at the joint site will be tolerated and result in successful fusion. A strain of approximately 36% or greater, which is observed at the lumbosacral joint, will result in the development of a pseudoarthrosis [131]. Similar observations have also been made in dogs [132, 133] where it was noted in a segmental spine fusion model that more cranial interlumbar fusion segments yielded stiffer fusion masses compared to their caudal counterparts. Excessive motion in the rabbit spine yielded similar inhibition of fusion [134] This effect is evidenced in human patients in the extreme case of spinal fusion in patients with Muscular –Dystrophy. These patients exhibit a higher rate of union which is likely due to their decreased voluntary movement relative to non-affected patients.

Evidence suggests that the effects of motion may be mitigated by the use of immobilising instrumentation. Using a canine model, Gurr and McAfee demonstrated that 6 months postoperatively, fusion was more probable if spinal instrumentation were used [135, 136]. The fusion mass was also shown to be more rigid compared with the non-instrumented fusion mass. It was noted, however, that the use of instrumentation resulted in a degree of device-related osteoporosis. Fuller [137] demonstrated in a study of canine anterior spine fusion that ceramic implants showed a significantly increased degree of revascularization and new bone growth when used with instrumentation, compared with no vascularisation or growth when used without, suggesting the importance of fixation when using non-biologic graft substitutes.

The stress and mechanical load at the fusion site have an effect on the resultant union. In the spine, compressive forces are transmitted from vertebrae to vertebrae by way of the intervertebral disc. Consequently, nearly 80% of the mechanical load of a segment is sustained by the intervertebral disc. Interbody fusion, therefore, is

subject to higher mechanical load and responds with a high degree of bone formation. It is proposed that the increased compressive forces stimulate vascularisation and mesenchymal cell proliferation into the graft. [138] Additionally, these forces act to stabilise the graft between adjacent vertebrae, thereby decreasing relative motion that may impede new bone formation. Posteriorly placed grafts along a transverse process fusion bed are subject to primarily tensile force and little compressive force and thus demonstrate poor bone formation.[139] Bone formation at these sites are primarily dependent upon the biological (osteogenic, osteoinductive) activity of the graft. [138]

With respect to pseudoarthrosis, DePalma suggested that the "...condition is iatrogenic; its responsibility lies entirely in the hands of the surgeon." [108] Technical choices made by the surgeon, including location of fusion site, degree of immobilization, and quality of bone bed, will affect the result of a fusion procedure. Anterior interbody fusions, for example, show a lower probability of developing non-union than do posterior fusions.

## **1.4 Neurofibromatosis type 1 (NF1)**

### **1.4.1 NF1 is characterized by scoliosis**

Neurofibromatosis type 1 (NF1) is a common genetic disease with an incidence of 1 in 3000-3,500 which results from mutations in the NF1 tumour suppressor gene [140]. The *Nf1* gene encodes the protein neurofibromin which is expressed in all tissues of the body. Although NF1 exhibits high penetrance, its expression is variable resulting in a wide spectrum of tissue manifestations, including bone.

Though the pattern of inheritance and nature of the genes involved has only been described recently, its relatively high incidence has meant that it has been observed and discussed extensively as far back at the thirteenth century. [141]

Early descriptions of NF1 made note of its cutaneous manifestations, in particular the neurofibromas that are characteristic of the disease. These present as cutaneous nodules, are often present in infancy, and may cover the body extensively in a disfiguring fashion. These early descriptions compared patients to amphibians, reptiles and monsters. Early accounts are sufficiently vague that it is not known for certain that they pertain to NF1, and retrospective diagnosis employs a degree of conjecture (figure 1.8).



**Figure 1. 8** Illustration from Aldovandri's 'Monstrorum Historia' depicting of an individual with what is now been thought to be NF1. [1]

The 1700s saw descriptions of NF1, become more scientific with a focus on the experience of the patient. In this fashion, Akenside observed that the skin wens (presumably neurofibromas), were at times associated with neurological symptoms [142]. Smith correlated these symptoms of numbness with pathology described on autopsy of patients suffering from NF1 [143]. He concluded that the lesions were subcutaneous and originated in the nerve, though he suggested incorrectly that they developed in response to a cancer of the surrounding connective tissue. Virchow further refined these observations and suggested that these lesions were fibromas of the connective tissue that contained nerves and noted that the disease was inherited by familial transmission[144]. However, it was von Recklinghausen who the disease came to be named for. Von Recklinghausen, a student of Virchow, performed a meticulous dissection of the cadaver of a patient with Nf1 and described in great detail the location, morphology and contents of the neurofibromas. He also was the first to note the pigmented café-au-lait spots and axillary and inguinal freckling that are utilised diagnostically today. [145]

It has since been documented that in addition to the cutaneous signs and associated neurological symptoms, patients with NF1 exhibit a host of other complications including cognitive impairment [146] and musculoskeletal problems.

The most common musculoskeletal manifestations include tibial bowing or pseudarthrosis, sphenoid wing dysplasia and dystrophic scoliosis [147]. With respect to the spine, as many as 25% of patients with NF1 will demonstrate a degree of scoliotic deformity. This deformity may be divided into either non-dystrophic or dystrophic types. [148] Non-dystrophic deformities present in a fashion similar to idiopathic scoliosis - that is to say without significant morphologic change to the vertebrae or surrounding soft tissues. This is contrasted with the dystrophic type in

which vertebrae may show failure of formation or segmentation, and surrounding soft tissues may contain large tumour masses. The deformity associated with dystrophic scoliosis is more severe and challenging to treat than its non-dystrophic counterpart. Approximately a quarter of these individuals will require spine fusion surgery to correct the curvature and prevent deformity [149].

#### **1.4.2 NF1 is a RASopathy that is plagued by poor bone healing**

Pseudarthrosis in the spine may develop in as many as 13% of patients with NF1 in whom fusion is attempted, with solid fusion seen in as few as 7% of patients [93]. This is likely associated with primary defects in bone metabolism that is seen in NF1. It has been shown in multiple studies that patients with NF1 demonstrate a reduced bone mineral density (BMD) [71, 150-153]. Impaired bone anabolism via reduced osteoblastogenesis, and augmented bone catabolism via increased osteoclastogenesis have been proposed as contributing factors [154]. When the Nf1 gene is intact, it acts to downregulate the Ras family of proteins. Ras proteins are critically involved in cell survival, proliferation, differentiation and apoptosis. When the Nf1 gene is faulty or missing, Ras activity is uninhibited [155]. It has been proposed that the upregulation of osteoclasts function in NF1 occur secondary to uninhibited Ras activity, as occurs in NF1 [147, 155-157]. Yang et al. observed a gain in function by osteoclasts in Nf1+/- mice, including increased survival, proliferation, migration, adhesion, and lytic activity [158]. Similar processes are likely to contribute to the poor bone healing that is characteristic of the fractures in patients with NF1. NF1 patients requiring spine fusion for the correction of scoliotic curvature and the prevention of future deformity demonstrate a high rate of complication including the formation of spinal pseudarthrosis. In these cases adjacent vertebrae



are united by fibrous tissue rather than with a bone bridge. The Ras-ERK pathway has been implicated in uncontrolled cell proliferation and fibrosis [159] .

Historically, bone graft (crushed up bone harvested from the patient or cadavers) has been used as an osteoinductive agent to induce the formation of new bone to unite adjacent vertebrae. In recent years recombinant human bone morphogenetic proteins (rhBMPs) such as rhBMP-2 and rhBMP-7 (OP-1) are now clinically approved for use in anterior interbody fusions when paired with a tapered spinal fusion cage. Increasingly, these agents are being used off-label in posterior interbody, posterolateral intertransverse, and anterior cervical fusions. Bone graft and rhBMPs have been used separately or in combination to achieve successful fusion in some NF1 patients.

## **1.5 Animal Models of Scoliosis**

### **1.5.1 Biomechanical forces in scoliosis modelling**

Multiple animal species have been used to model the pathogenesis of idiopathic-type scoliosis. Historically, IS has only been observed in humans though there is limited evidence that it may also occur in the chicken. [15] Spinal deformities seen in other animals are typically classified as congenital, suggesting that IS may be exclusive to bipeds. [16] Consequently, it has traditionally been accepted that the mechanisms implicated in IS act in concert with axial loading along the spine to produce deformity. Weakening of the vertebral bone, of the surrounding supporting tissues or positional asymmetry is exploited by the force of gravity acting upon the vertebral column of a biped. The force of gravity is resolved in the spine as dorsal shear forces causing the

natural column to fail, resulting in lateral curvature. [16, 17] Burwell et al describe this as The Nottingham Concept. [17]

## **1.5.2 Quadrupedal Models of Scoliosis**

### **Mechanical models**

Quadrupedal animals are not subject to the same axial loading and dorsal shear stress as bipeds. Despite this, cost and efficiency have favoured their use in experimental research. They are, without question, the most utilised systems for the purpose of modelling scoliosis.

The majority of scoliosis models have been developed around techniques designed to create a mechanical asymmetry in the spine. This has been accomplished via several techniques. In 1961 Langenskiold et al [18] described a series of mechanical methods with which to induce scoliosis in a quadruped. He proposed that the primary techniques for inducing scoliosis in quadrupedal animals include (i) the excision or denervation of local musculature, (ii) the resection of ribs, or (iii) the fixation of vertebrae or ribs to each other. Each of these approaches serves to create an asymmetry in the natural column of the spine or supporting tissues without altering the structure of the vertebral bodies themselves. The development of spine curvature in these animal models is consistent with clinical evidence showing that humans in prolonged recumbence can develop scoliotic deformity, suggesting that gravity is not in fact a prerequisite. To date, the majority of experimentation to produce models of scoliosis in animals has followed these techniques, although with varied success.

Langenskiöld, in a landmark paper in which he performed 15 surgical interventions on rabbits (figure 1.9), found that deformity could not be induced by sectioning of the phrenic nerves or the lower intercostals muscles. Unilateral resection of the erector spinae muscles, sectioning of the lower intercostals nerves (6-11) with or without sectioning of the associated ribs, and unilateral tethering of the transverse processes of T6-11 only seldom produced a curvature which was generally quite slight. He found that only by resecting the posterior end of ribs 6-11, including the costovertebral joints, was he able to create significant spinal deformity in all subjects. However, Langenskiöld acknowledged that despite achieving scoliosis consistently in these subjects, little was known about the deforming forces that were released by the operation. It was understood that an asymmetry of forces on the spine resulted in a deformity, but the nature of these forces was not clear. Michelsson [19] has since proposed that the dorsal rib acts as a lever. When the costovertebral joint is disrupted, the lever mechanism of the rib fails and an asymmetry of forces upon the spine results.

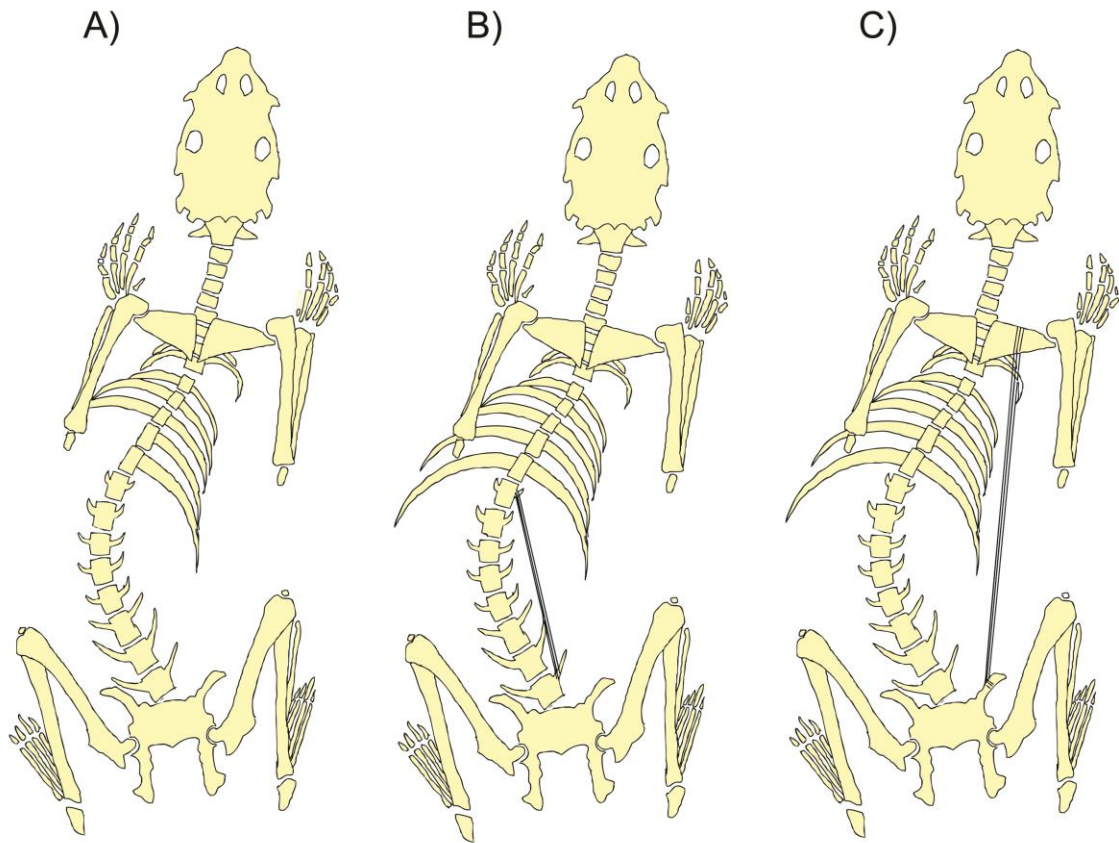


**Figure 1. 9** Mechanical asymmetry along the spine of a quadruped can be created via A) unilateral resection of ribs and costovertebral joint, B) unilateral tethering between transverse processes of ipsilateral vertebrae, or C) unilateral tethering between ipsilateral pelvis and scapula.

While others have expanded upon the early work of Langenskiold, there have been few fundamental advances with respect to the modelling of scoliosis in quadrupeds. Multiple studies have examined the effects of dorsal rhizotomy in rabbits on spinal deformity. [20-22] Dorsal rhizotomy (figure 1.10) involves the ablation of the dorsal nerve root which is responsible for the transmission of proprioceptive information. These studies tend to show that damage to the dorsal root ganglia produce a deformity with the convexity on the side of the injury. It has been proposed that individuals with idiopathic scoliosis have an abnormality of postural equilibrium which is likely mediated by proprioceptive loss on that side. The cause of the deformity in this instance was presumed to be related to unilateral muscle weakness secondary

to this deficit. Abnormal proprioception has been detected in adolescents with IS relative to age matched controls. [23-25] and post-mortem investigation of the spines of individuals with AIS showed abnormal dorsal root ganglia. [26] Alexander suggested that with respect to experiments that induce scoliosis via dorsal rhizotomy, it was not the proprioceptive loss from damage to the dorsal root that caused the weakness, but paralysis of the trunk muscles as a result of surgical damage to the anterior horn. [20] Similarly, the causal association made in observational studies of humans has been challenged, with suggestions that it is the curvature of scoliosis that results in proprioceptive imbalance rather than vice versa. [27]

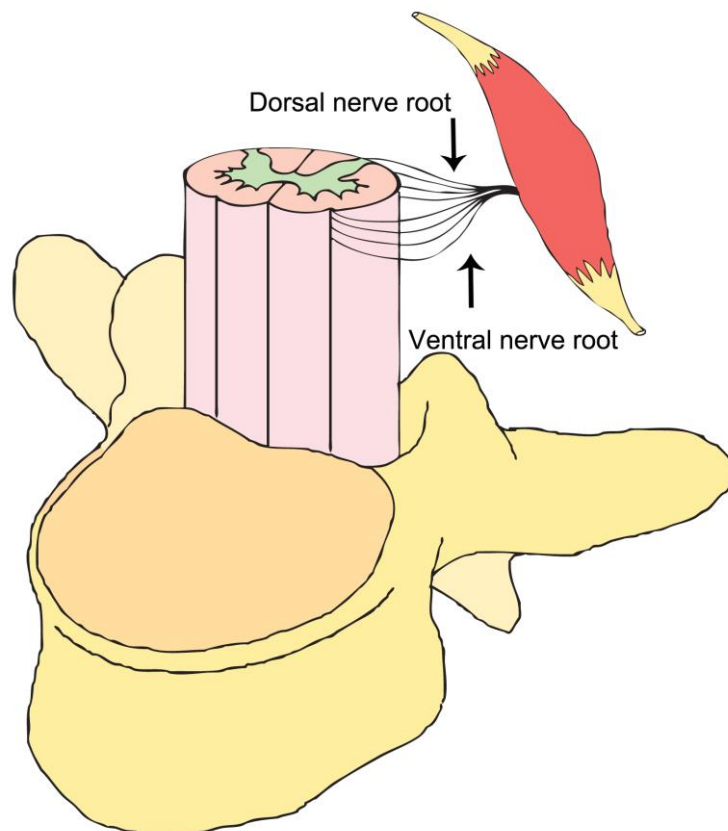


**Figure 1. 10** Motor signals are carried from the spinal cord to muscle fibres via the ventral nerve root. Proprioceptive information, including information related to the relative position of muscles, is relayed via the dorsal nerve root from muscle to the spinal cord.

Following the success of Langenskiold experiments with the resection of lower ribs, which yielded a severe deformity in all subjects, this has become a popular technique for modelling scoliosis in animals. [28-36] All studies which have applied this technique have produced similar data with a high incidence of scoliosis produced. These experiments have typically done so using rabbit subjects, though it has also been performed on chickens. [37, 38] Common amongst this work is the conclusion that the curvature created by resection is dependent upon the continued non-union of the costovertebral joint. In animals where union developed, and presumably stability was restored, deformity was attenuated or reversed.

Although Langenskiold achieved only moderate success with unilateral tethering, this has since become one of the preferred methods for inducing scoliosis in an animal model. It has certainly been applied to the broadest range of species including calves, [39, 40] goats, [28-30, 36, 41] pigs, [32, 33] dogs, [42] rabbits, [18, 31, 35, 43, 44] and rats. [45, 46] In these models, a lateral curvature is created along a juvenile spine by fastening a series of adjacent vertebrae to each other or of the pelvis to the ipsilateral scapula. As the animal grows and the vertebral column elongates it is forced into a rotational lordosis which is resolved as a lateral curvature with the convexity facing the tether. In these experiments, all animals will develop an immediate post-operative scoliosis as curvature is ensured during the procedure. Persistence of the deformity is dependent upon the strength and durability of the fixation. Failure or intentional release of the tethering results in a reduction of the Cobb angle, occasionally with complete correction, followed by steady progression of the curve. [31, 47]

The models that have achieved the highest incidence of scoliosis have been those that induce a mechanical asymmetry, in particular the tethering models which have been discussed. Consequently, they are the most frequently used. As with the work of Langenskiold, these experiments provide a reliable and reproducible technique for producing a lateral curvature in a spine of an otherwise healthy mammal. Though the pathogenesis of the curvature in these animals may not mimic the human condition, the utility of these models is that they produce a consistent deformity upon which to investigate curvature reversal and straightening. By this measure they are very successful. Braun et al. created an experimental scoliosis in immature goats using a rib tether technique. They successfully attempted to correct the deformity using a shape memory alloy staple in the anterior thoracic vertebrae. [29, 48, 49] This experiment has been repeated several times with consistent success. [49, 50] The techniques designed to initiate a spinal deformity have also been proposed as treatments when applied to an established deformity in the opposite direction. [40]

### **Genetic models**

Langenskiold observed bedridden patients and noted that scoliotic deformity could arise and progress in a spine orientated in a horizontal plane, and free from the dorsal shear forces of gravity. A central tenet of most scoliosis modelling is the concept that bipedalism is a requisite. Models that do not use an animal with erect posture, have either tried to induce such a posture, or mimic the deforming forces of gravity in the horizontal plane. Recent research involving observation of the curveback guppy [51] has demonstrated that spinal deformity closely mimicking AIS can develop in non-bipeds. The curveback guppy is a small live bearing fish whose young are born with fully ossified skeletons. Like humans, they develop a lateral

curvature of the spine at variable times after birth with predominance in females with distortion of the apical vertebra. Gorman suggests that although this deformity can arise in the absence of a bipedal gait, the biomechanical forces acting on the spine of the guppy may in fact be similar to those in the human. In humans the force acting on the spine is along the cranio-caudal axis as gravity acts vertically upon the head and upper body. The force on the guppy spine also acts along the cranio-caudal axis but is independent of gravity, instead originating from the power of the tail-beat motion pushing the animal through the dense medium of water. The result is a compressive force along this axis. As axial loading is not unique to humans as curveback guppies, it is likely that there is at least one secondary component acting in parallel with these forces to create spinal deformity. Humans and fish share many developmental pathways and many gene sequences isolated in the fish have analogues in humans. Several of these sequences, including those involved in osteoblast and chondrocyte differentiation, bone and muscle formation, pineal gland development, have been implicated in human scoliosis.

Mice represent one of the least used animal species in scoliosis modelling. The example of the curveback guppy suggests that a genetic predisposition is likely to play a role in the development of AIS. The genome of the mouse has been sequenced and extensively studied. The ability to generate knock-out and transgenic mice provides the opportunity to study the function of various genes in vivo. We have only begun to apply this technology to the study of scoliosis. Giampetro et al performed a search of the Mouse Genome Database by phenotypic category yielding 100 mouse mutations. [52] Of the 66 of these whose genome had been mapped, 27 demonstrated a scoliotic phenotype. The loci of the mutations responsible for the deformities in these mice have analogues in humans, including



Pax1, Dll3, Wnt3a, Ky, Lmx1a, Fbn-2, and Sim2. The phenotypes associated with these mutations generally yield structural malformation of the vertebrae and ribs, consistent with congenital scoliosis rather than IS.

NF1 (formerly von Recklinghausen's disease) is a common genetic disease that is associated with a 20-25% rate of scoliosis in addition to a characteristic range of other clinical features. 4-43% of patients with NF1 will exhibit a degree of spinal deformity [53-57] with many of these requiring correction via external bracing or surgery depending upon the severity of the curvature.[58, 59] The pathogenesis of the deformities seen in NF1 are not easily classified into the scoliotic divisions presented earlier. Suggested causes include one or a combination of compressive or erosive effects of adjacent neurofibromas, osteomalacia, endocrine disruption and muscular imbalance. Aetiological classification is further complicated by the fact that there are now two recognized subtypes of scoliosis in NF1 as determined by clinical and radiographic data. Dystrophic and non-dystrophic types are differentiated by the presence or absence of dysplastic changes in the vertebrae, including scalloping or wedging of the vertebral bodies, spindling of the transverse processes and rib pencilling. [60] Non-dystrophic scoliosis in NF1 patients is clinically and radiologically similar to idiopathic scoliosis and may therefore share a common pathogenesis.

Animal models have reproduced the orthopaedic manifestations of NF1 with varying success [61-65], with scoliosis only demonstrated in one. An Nf1<sup>-/-</sup> genotype was induced in osteochondroprogenitor cells using the Col2 $\alpha$ 1-cre promoter to yield a severe phenotype with radiographic parallels to the human orthopaedic manifestations of NF1 [66]. Mice showed reduced growth, tibial bowing and progressive scoliosis and kyphosis. These changes were associated with increased cortical porosity, increased osteoclastogenesis and decreased osteoblast number.

The scoliosis observed in this model closely mimicked the features of dystrophic scoliosis seen in patients with NF1 demonstrating primary structural defects of the vertebrae, including fusion of adjacent vertebrae, as well as of the intervertebral discs. Histology of day 16.5 embryos showed that ossification centres were not present in all vertebral bodies unlike wild type controls where their presence was ubiquitous. A similar model involving targeting of osteoblast precursor cells using 2.3kb promoter of Col1 [36] produced a vertebral phenotype with shorter vertebrae with reduced cortical and trabecular bone mass. When strength tested, a reduced peak load and peak stress to failure was noted in L5 vertebrae. However, it was not able to create spinal deformity. This was proposed to be the result of the quadrupedal gait of the mouse which did not mimic the axial loading in humans. The cortices of the bone in these mice has been noted to have increased microporosity which may be due to increased lacunae size. [160]

Nf1<sup>-/-</sup> is an embryonically lethal condition secondary to cardiac abnormalities. Nf1<sup>+/-</sup> mice are viable, fertile and demonstrate a mild phenotype with minimally impaired bone healing [62], impaired spatial learning [63] and predisposition to tumour development [64]. Consequently several models have been created which are capable of inducing an Nf1<sup>-/-</sup> genotype that is localized to either a specific tissue, or to a specific location within the body with correspondingly more severe phenotypes. Impairment in healing can be simulated by local transduction of Nf1<sup>flox/flox</sup> mice with cre-expressing adenovirus [65] which initiates heterozygosity for Nf1 deletion in cells of preosteoblast lineage.

The modelling of scoliosis in other genetic diseases with known bone phenotypes has proved more challenging. Scoliosis is a recognized feature of OI (brittle bone

disease), and CypB knockout mouse developed as a model of OI showed decreased bone mineral density and body mass as well as prominent kyphosis. [67]

Mutations in Filamin B (FLNB), a gene that encodes a cytoplasmic actin-binding protein, is responsible for several skeletal disorders which are characterized by a degree of scoliosis, including spondylocarpotarsal syndrome, Larsen syndrome, and atelosteogenesis phenotypes I and III. Zhou et al [68] created a mouse in which FLNB is disrupted. While a majority of these mice did not survive to term, the few that survived were very small and showed severe skeletal manifestations with evidence of kyphosis, scoliosis, lack of intervertebral discs (IVD) and fusion of vertebral bodies. The degree of kyphosis and scoliosis was not defined in this experiment. The deformity was likely to have arisen secondary to the fusion of the vertebral bodies and the absence of IVDs. The dystrophic bone phenotype of these mice was sufficiently severe that they had to be euthanized at 4 weeks of age.

Duchenne Muscular Dystrophy (DMD), which is caused by a loss of functional dystrophin and is primarily known for its muscular manifestations, is associated with an incidence of scoliosis of 75-90%. [8, 69] A dystrophin-utrophin double knockout mouse was created as a model of DMD [70]. This mouse exhibited a range of musculoskeletal abnormalities, including premature degeneration of the intervertebral discs, but did not show any spinal deformity.

The dystrophic changes in the spine produced by these models, with and without an associated spinal deformity, are reminiscent of those seen in congenital scoliosis. With the exception of NF1 model in which scoliosis was reproduced, the difficulty achieving deformity in other models supports the concept that scoliosis is a multifactorial process that is particularly challenging to model when investigating variables in isolation. It is conceivable that the primary deficiencies created using

these genetic models may have yielded to the axial forces of gravity and produced a scoliotic deformity in a bipedal model.

Most models to this point have been dependent upon some form of surgical intervention. The use of mice has presented a technical challenge that can be readily overcome with the use of larger animals. Knock out and transgenic mice likely represent a future direction for scoliosis research. These mice permit the investigation of the activity of specific genes, directed by observational genomic mapping of affected individuals and mice. Additionally, the breeding and lifecycles can produce a large volume of data over a short period of time, making them a potent tool for the investigation of the aetiology of the many varieties of scoliosis affecting humans. The development of murine models of NF1 that demonstrate orthopaedic phenotypes is an excellent example of the modelling power of transgenic mice. By targeting a specific cell lineage and obtaining an accurate representation of the human histology and morphology, significant information is obtained regarding the aetiology of dystrophic scoliosis in NF1.

In summary scoliosis research has been enhanced by the development of both mechanical and genetic models. Mechanical models \permit the study of primarily surgical interventions that are aimed at reducing established deformity. Genetic models present a unique opportunity to develop disease specific interventions to treat and/or prevent the development of spinal deformity.

### **1.5.3 Bipedal Models of Scoliosis**

#### **Mechanical models**

Bipedal animals are subject to axial forces upon the spine, secondary to gravity, as humans. They are therefore an attractive option for the modelling of human spine deformity. Following the success of quadrupedal rib resection models, this technique has been applied to bipedal animals, specifically the chicken [37, 38] and non-human primates. [71, 72] Deguchi first applied this model to chickens in which he either resected or transected the dorsal ribs. He found that at 20 weeks, animals with transected ribs showed healing of the bone and no scoliosis. In those animals that received resection, marked scoliosis was observed. The degree of scoliosis was increased with decreased age at surgery and with increasing number of ribs resected. Animals showing regeneration at the resection site were noted to have milder scoliosis. These results are consistent with similar experiments involving quadrupedal animals.

Although the Langenskiold technique for inducing scoliosis via rib resection has been successfully applied to the bipedal chicken, translation to primates has proven more challenging. A study was conducted on 10 young baboons, aged 2-3 months in which the heads of 4-5 ribs were resected unilaterally. At one year post-op, no subjects developed any degree of scoliosis. [72] Another study, involving 30 monkeys of unspecified type, divided the subjects into three treatment groups of n=10. These groups consisted of: removal of dorsal end of lower 6 ribs on the right side, removal of costo-transverse ligaments of lower 6 costo-vertebral joints on the right side, and removal of the dorsal end of the lower 6 ribs on the right side followed by the same procedure on the left side 6 weeks later. Subjects from the first two groups only developed a mild rotational deformity. However, at 6 weeks post

operatively, all subjects from the third group had developed a severe scoliosis with an average angle of 46°. [71]

### Neuroendocrine models

The most common model of bipedal scoliosis involves inducing a state of melatonin deficiency in test animals, often by removal of the pineal gland. The progression to scoliosis following pinealectomy was first observed in chickens [73-79] by Thillard [79] in 1959. Animals were subjected to pinealectomy (figure 1.11) upon hatching and were observed to develop a high incidence of spinal deformity of between 52% and 100%. In animals such as the chicken and rodents, the pineal gland has a superficial location relative to its position in the human and is more readily surgically accessible. The scoliosis produced in these animals can be prevented by melatonin therapy or reimplantation of the pineal gland into a skeletal muscle pouch. Grossly, the curvatures evident in these animals appeared very similar to those seen in IS, characterized by similar distributions of single and double curves, location of curves, degree of rotation and degree of stability. [74, 76]

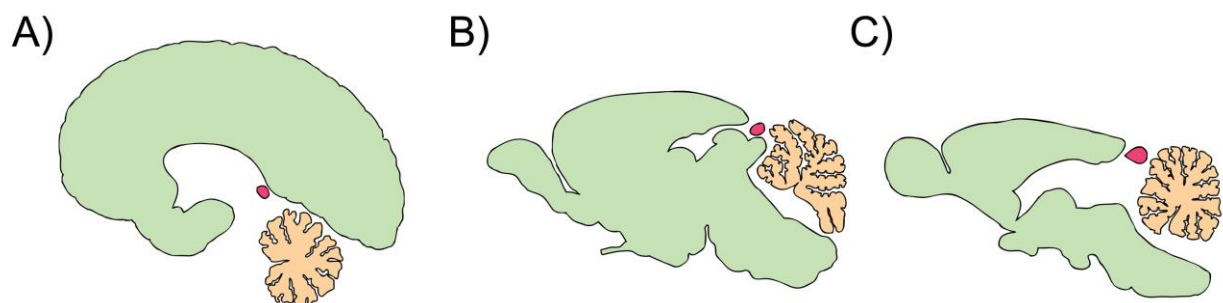


**Figure 1. 11** Compared to the deep location of the pineal gland within the human brain (A), its position in the chicken (B) and rodent (C) brain is significantly more superficial. This position facilitates surgical access for its excision in melatonin deficiency models of scoliosis.

Nevertheless, the dissimilarities in the morphology of the chicken and human models are worth noting. The source of the deformity in human IS is initially predominantly due to wedging of the intervertebral discs and later from a slow progressive vertebral body wedging. [80] Chickens, unlike humans, have very small discs and the histology of their intervertebral joint has been described as being more like a synovial joint than a fibrous joint as seen in humans. As a result, there is no abnormality noted in the discs of pinealectomized vs control chickens. The lateral curvatures in the spines of pinealectomized chickens arises completely from wedging deformity of the vertebrae which is associated with significant morphologic asymmetry of the other vertebral structures including pedicles and processes. [74]

The utility of the pinealectomized chicken as a model for IS has been cast into doubt when the same technique has been applied to non-human primates. Following pinealectomy in 18 rhesus monkeys between 8 and 11 months of age, 10 were melatonin deficient for 29 months during which time none of them developed scoliosis. [81] These results suggest that data obtained from pinealectomized lower animals may not be extrapolated to humans. Observational studies involving humans with both scoliosis and underactive pineal glands support this. In a prospective study, 48 Australian children with pineal lesions aged one to 18 were followed up for 80 months (30 for non-survivors). Two of the surviving boys developed scoliosis, one of which corrected itself spontaneously over 2 years, and none of the deceased were shown to have developed scoliosis on their final X-Rays and MRI. [82]

Several cross sectional studies have been performed comparing melatonin levels between adolescents with and without scoliosis. While some studies support the theory that low melatonin secretion is associated with the development of AIS [83, 84], the majority show that there is no correlation. [85-89]

Though research into melatonin deficiency as a cause of scoliosis is inconclusive, it fulfils Langenskiold criteria for a good model of scoliosis in that it constitutes a reliable and reproducible method for creating scoliotic deformity upon which experimental interventions may be applied. Deguchi et al successfully performed experiments in which they induced a scoliotic deformity in the spines of chickens via rib resection [38] and pinealectomy [90]. Subsequently, in a cohort of pinealectomized chickens, they performed rib resection on the concave side of the curvature in animals that showed  $>20^\circ$  at 4 weeks of age. Chickens treated with rib resection developed milder scoliosis ( $6-56^\circ$ ) vs controls ( $24-85^\circ$ ).

Research into melatonin deficiency and scoliosis has supported the concept that bipedalism is a prerequisite for deformity. In a series of experiments conducted by Machida et al. [75, 83, 91], scoliosis was induced in rodent following pinealectomy. Animals that were allowed to ambulate on 4 limbs did not develop any incidence of deformity. However, deformity could be produced in animals that had been made bipedal by amputation of the forelimbs and tail. Following amputation, animals were drawn into a bipedal stance by the gradual raising of food and water. The same held true when quadruped hamsters were subjected to pinealectomy. [92] These findings have been recapitulated by Akel et al using melatonin deficient C57BL6/NCrl mice which were made bipedal by forelimb and tail amputation with gradual raising of food. The bipedal rodent model has also been applied to another neuroendocrine theory of scoliosis. It has been observed that Adolescent girls with IS have low circulating leptin. [93-95] Wu et al performed an experiment in which they injected the hypothalamus of 8 bipedal mice with lentivirus vectors expressing leptin. These mice were noted to have high circulating levels of serum leptin relative to controls (n=8) which were injected with lentivirus vectors expressing physiologically inactive GFP.



100% of leptin lentivirus injected mice were noted to develop scoliotic deformity, a result which is in contrast to the clinical evidence.

#### **1.5.4 Summary**

There have been, over the years, many attempts to develop animal models to investigate scoliosis in humans. The aetiology of this deformity has thus far remained largely elusive, particularly with regard to idiopathic scoliosis which develops in youth and may progress to a debilitating degree. Most early research into scoliosis modelling can be characterized by attempts to reproduce the curvature that is seen in human scoliosis but not necessarily its pathogenesis.

Scoliosis, in particular idiopathic scoliosis, is a common but poorly understood condition and is a sign expressed by several different disease processes rather than a diagnosis in itself. Intrinsic and extrinsic forces acting upon the spine, genetic predisposition, neuroendocrine dysfunction have been implicated in scoliosis and have been modelled with varying degrees of success. As proposed by Schimandle et al [96], the utility of a model is dependent upon the intention of the experiment. If the intention is to investigate mechanical factors, a larger animal of benefit as it will approximate the size and anatomy of the human. Several models, including tethering and melatonin deficiency models have been very successful at producing reliable deformity which can then be used to test a variety of interventions targeted at curve reduction. Smaller, skeletally immature animals, such as mice, are better for investigating biological questions.

It is likely that the aetiology of scoliosis in humans is a multifactorial process. The impact of mechanical factors upon the spine with respect to scoliosis has been

extensively studied. Correspondingly, the only treatments for scoliosis today involve mechanical correction of curvature. The investigation of the biological causes of scoliosis is in its infancy. The use of mice to investigate the genetic factors influencing spinal deformity has just begun to be exploited and represent a valuable tool for future investigation.

## **1.6 Hypothesis and Aims**

Neurofibromatosis type 1 may produce a scoliotic deformity of the spine that is challenging to treat. [93] The most successful method for correcting the deformity and limiting its progression involves the surgical implantation of paraspinal rods that act as internal braces. In the short term, these rods immobilize the spine such that bony union of adjacent vertebrae may be achieved. Failure to unite, pseudarthrosis, represents a failure of fusion and over time the repeated stresses places on the hardware will result in its weakening and breaking. Such failures are a significant source of morbidity and cause for reoperation, often in the setting of a paediatric population. [161-163]

The reason for failure of spine fusion in NF1 scoliosis is multifactorial. First, the dystrophic scoliosis seen in NF1 is associated with significant deformity and often is subject to asymmetrical muscular forces secondary to tumour infiltration of the paraspinal tissues. Deformities of this severity are challenging to treat even in a non-NF1 population.

Second, patients with NF1 show defects in bone metabolism, including impaired anabolism and augmented catabolism via reduced osteoblastogenesis and increased osteoclastogenesis respectively. [105] Clinically, patients receiving

revision surgery for failed spine fusion are found to have fibrous tissue in place of bone uniting adjacent vertebrae. This must be excised to prepare the vertebrae for a second attempt at fusion. This process is similar to that seen in the case of pseudarthrosis of the tibia in NF1. It has been proposed that the unopposed action of Ras in NF1 patients may be implicated in these orthopaedic manifestations of the disease. [164, 165]

Third, the formation of a successful fusion mass is dependent upon recruitment of osteoprogenitor cells. The source of this population of cells is largely considered to be the periosteum and bone marrow. It has been suggested that other tissue may be a source of progenitor cells that are able to contribute to bone formation and repair, including skeletal muscle, smooth muscle and vascular endothelial cells. [166-170]

The cell populations that contribute to the formation of a spine fusion mass has not been well characterized.

In this thesis, we will investigate methods to improve spine fusion outcomes in patients with NF1. In Chapter 2, we will explore the history of animal models used to model spine fusion surgery. We will build upon this in Chapter 3 to develop our own murine model of spine fusion. This model will specifically be developed to model posterolateral lumbar spinal fusion.

The role of NF1 in bone metabolism and healing is well documented, primarily in the context of tibial pseudarthrosis. The effect of NF1 in the setting of spine fusion is not well researched. In Chapter 3, we will employ the developed surgical model for spine fusion in a transgenic mouse line that is *Nf1*<sup>+/-</sup> systemically. We will investigate the phenotype of this mouse line with respect to spine fusion and attempt to address the anticipated catabolic imbalance with the bisphosphonate Zoledronic acid.

Tumours analysed from patients with NF1 have shown double inactivation of the Nf1 gene (*Nf1<sup>-/-</sup>*) in keeping with the two-hit hypothesis in which one allele is constitutionally inactivated and the other the subject of mutation. In mouse models, double inactivation of the Nf1 gene is associated with development of a more severe phenotype. In Chapter 4, we will apply the spine fusion procedure to a transgenic mouse in which we will initiate double inactivation of the Nf1 gene in the tissues local to the lumbar spine. Neurofibromin is known to downregulate Ras pathways, inactivation of the Ras-MEK pathways may represent an opportunity to correct the orthopaedic phenotype of NF1 in the spine. Animals will be dosed with the MEK inhibitor PD0325901 and the bisphosphonate to attempt to correct the unopposed activity of Ras and the excessive catabolism witnessed in NF1.

The mobilisation of extra-osseous populations of osteoprogenitor cells may represent a niche that may be exploited to enhance bone formation. In chapter 5 we will apply the spine fusion surgical model to *Tie2-Cre: Ai9* and *αSMA-creERT2: Col2.3-GFP: Ai9* reporter mice and observe the distribution of lineage-labelled cells. We hypothesize that Tie2 and αSMA cells will contribute to the osteoprogenitor cell population in the fusion masses of experimental mice.



**(i) Posterolateral intertransverse lumbar fusion in a mouse model**

Justin Bobyn <sup>1,2</sup>, Anton Rasch <sup>1</sup>, David G. Little <sup>1,2</sup>, and Aaron Schindeler <sup>1,2§</sup>

<sup>1</sup> Orthopaedic Research & Biotechnology Unit, The Children's Hospital at Westmead, Sydney, Australia

<sup>2</sup> Discipline of Paediatrics and Child Health, Faculty of Medicine, University of Sydney, Sydney, Australia

Published in *Journal of Orthopaedic Surgery and Research*, 10 January 2013

## **Abstract**

**Background:** Spinal fusion is a common orthopaedic procedure that has been previously modeled using canine, lapine, and rodent subjects. Despite the increasing availability of genetically modified mouse strains, murine models have only been infrequently described.

**Purpose:** To present an efficient and minimally traumatic procedure for achieving spinal fusion in a mouse model and determine the optimal rhBMP-2 dose to achieve sufficient fusion mass.

**Method:** MicroCT reconstructions of the unfused mouse spine and human spine were compared to determine a surgical approach. In phase 1, posterolateral lumbar spine fusion in the mouse was evaluated using 18 animals allocated to three experimental groups. The spine was accessed via a midline excision with Group 1 receiving decortication only (n=3), Group 2 receiving 10µg rhBMP-2 in a collagen sponge bilaterally (n=6), and Group 3 receiving 10µg rhBMP-2 + decortication (n=9). The surgical technique was assessed for intraoperative safety, efficacy, access and reproducibility. Spines were harvested for analysis at 3 weeks (Groups 1, 2) and 1, 2, and 3 weeks (Group 3). In phase 2, a dose response study was carried out in an additional 18 animals with C57BL6 mice receiving sponges containing 0, 0.5, 1, 2.5, 5 µg of rhBMP-2 per sponge bilaterally.

**Results:** Based on structural differences observed between the murine and human spines, exposure, decortications, and sponge insertion was placed upon the murine articular processes, found to be structurally more analogous to the human transverse processes and easily accessible via the midline. Decortication alone (Group 1) yielded no novel bone formation but introduction of rhBMP-2 (Groups 2 and 3)

yielded significant bone mass bridging the L4-L6 vertebrae by at week 3. For Group 3 where longitudinal examination of bone formation was examined, no additional bone increase was seen between weeks 2 and 3. The dose response experiment revealed that all doses down to 0.5 $\mu$ g were sufficient to create a fusion mass.

**Conclusion:** We describe a new approach for mouse lumbar spine fusion that is safe, efficient, and highly reproducible. The technique we employed is analogous to the human midline procedure and may be highly suitable for genetically modified mouse models.



## Introduction

Spinal fusion surgery has been performed since the pioneering work of Hibbs [171], Albee [88] and DeQuervain in the early 20<sup>th</sup> century. When successful the procedure has significantly reduced the morbidity associated with spinal deformity and, controversially, discomfort. Historically, the procedure has suffered from high rates of non-union. It has been estimated that 5-30% of spinal fusion procedures result in pseudarthrosis [108], the causes of which are certainly multifactorial.

Animal surgical models have been utilized extensively to improve surgical technique and gain insight into the mechanisms of spinal fusion failure. Larger animals such as canine [110, 130, 132, 136, 172] and ovine subjects [131, 173] have traditionally been employed due to their close approximation of the size and anatomy of human patients. Rat and rabbit studies [30, 40, 134, 138, 174-180] typically represent the lower limit with respect to size that spine fusion procedures have been attempted. Mouse models have rarely been studied, likely owing to the technical difficulty associated with surgical access and technique demanded by their small size. Until recently, spinal fusion attempts in mice have been limited to percutaneous injection of BMP solution and mesenchymal stem cells into the paraspinal musculature [181, 182], thereby obviating the need to surgically expose and manipulate the vertebral structures.

Advancements in transgenic mice have encouraged the use of surgical models that explore the impact of genetics on repair and regeneration. Rao et al ([183]) were the first to publish a consistent technique for performing posterolateral lumbar spinal fusion in mice, using a modified version of the paraspinal approach described by Wiltse [184].

Fusion was induced via autogenous bone graft from donor mouse of same strain or rhBMP-2 delivered in a collagen sponge. Radiographic assessment demonstrated that a dense fusion mass was formed in 62% of fusion sites, although no specific breakdown was given for the bone graft and rhBMP-2 groups. This model also featured a prolonged operating time of 60 min.

In this study we have utilized a surgical approach involving a single midline incision through the thoracolumbar fascia that more closely approximates the current human midline surgical technique. Such an approach aimed to minimize tissue trauma as well as increase visibility and access to the articular processes. One other aim of this modified procedure was to minimize the operative time and maximize the experimental reproducibility between subjects and the rate of spine fusion.

## **Methods**

### **Anatomical Analysis by MicroCT**

The spines of 5 C57BL6 mice, aged between 8 and 10 weeks, were harvested and analyzed via microCT using a SkyScan 1174 compact microCT scanner (SkyScan, Kontich,

Belgium). Samples were scanned in 70% ethanol at 21.3  $\mu\text{m}$  magnification, 0.5 mm aluminium filter, 50 kV X-ray tube voltage and 800  $\mu\text{A}$  tube electric current. The images were reconstructed using NRecon, version 1.5.1.5 (SkyScan). A global threshold was used representing bone tissue. Representative three-dimensional fractures were reconstructed with sagittal slices using CTVol Realistic Visualisation software version

2.1.0.0 (SkyScan). The structure of the lumbar spine was documented and compared with the relevant human anatomy. Subsequently, 5 additional mice were culled and the lumbar spine was dissected. The relationships of the soft tissue to the bone were observed and documented with a view to establishing a clear and efficient surgical access to the lumbar vertebrae which would allow secure positioning of a collagen sponge for the delivery of osteoblast stimulating factors.

### **Surgical Model**

18 C57BL6 mice (male and female aged 8-10 weeks) had posterolateral lumbar spine fusion surgery performed. Surgery was performed by a two surgeons in a single sitting with anesthetic support from an experienced animal technician.

Mice were anaesthetized with ketamine (35mg/kg) / xylazine (5 mg/kg) solution administered intraperitoneally. Hair overlying the operative site was shaved with an electric razor once anaesthetized and the area prepped with iodine. Animals were positioned prone with folded gauze beneath the abdomen, increasing the excursion of the lumbar spine to facilitate access to and visibility of the surgical field. The head was covered with saline soaked gauze to protect the ears from overheating under operating lights. rhBMP-2 marketed under the brand name Infuse® (Medronic Australasia) was used in this study. Prior to surgery, the collagen sponge that was supplied with the vial of BMP for human use was cut into 2mm x 7mm sections. A solution of saline and BMP was made allowing the accurate pipetting of 10 mg of BMP onto each sponge intraoperatively.

With the intention of fusing the lumbar spine from L4-L6, surface anatomy was located to determine incision point. The iliac crest is approximately level with the L5-L6 interspace [183]. This level as well as the midline was marked with surgical pen (Figure 1A). The procedure was performed under an operating microscope or surgical loupes at 2.5x magnification. A 15 mm incision was made in the skin made along the midline, centered over the line running between the iliac crests (Figure 2.1 B). The skin was opened and held in place with a self-retaining retractor (Figure 2.1 C). At this point, the midline was identified by the spinous processes. The iliac crest was directly visible. A second 15 mm incision, through the dorsolumbar fascia, was made in the midline, along the spinous processes. The spinous processes and lumbar paravertebral muscles have now been accessed. The paravertebral muscles overlying the articular processes of L4-L6 were separated from the spinous processes in a single motion by scraping a # 10 blade down the lateral border of the spinous process and pulling the muscles laterally (Figure 2.1 D). This motion shears the muscle at its junction to the bone minimizing trauma to the tissue. This was performed bilaterally exposing the articular processes and creating a potential space between muscle and bone. Muscle was retracted bilaterally with a purpose-built micro-retractor allowing controlled and gentle retraction while maintaining maximum visibility of all articular processes. A pneumatic 1 mm round tip diamond burr was used to decorticate the visible articular processes until punctuate bleeding was observed. Care was taken not to disturb surrounding muscle tissue.

Two collagen sponges, impregnated with either saline or an rhBMP-2/saline solution (containing 10mg of BMP per sponge), were placed bilaterally in the potential space which has been created (Figure 2.1 E). The fascia was apposed and closed with a

single line of continuous sutures using 6.0 Vicryl, The skin was subsequently closed in the same fashion. Mice were placed on a heat pad following surgery and monitored for recovery. Antibiotics were administered in the drinking water for 24 hours postoperatively.

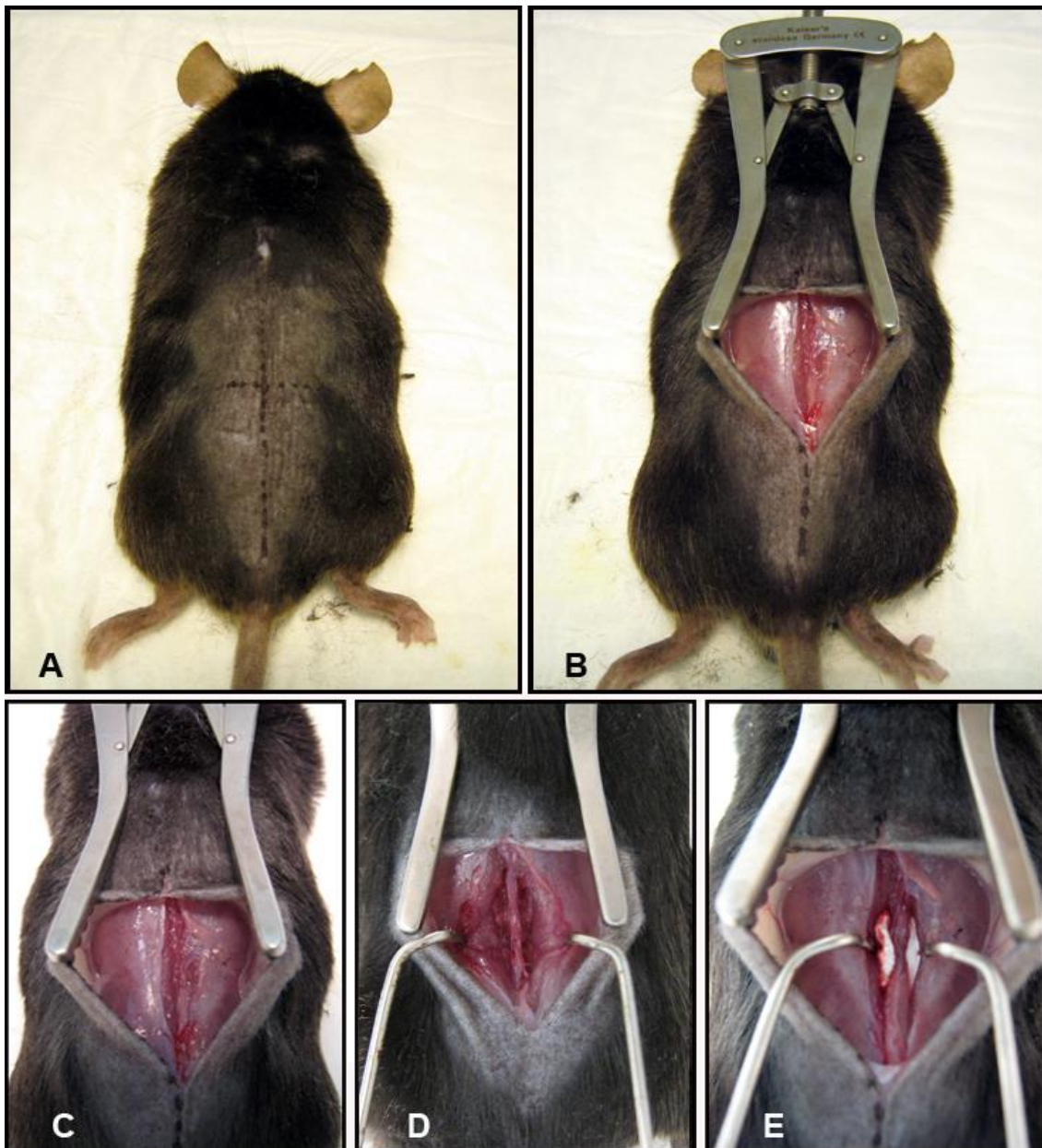


**Figure 2. 1** Following the administration of anesthetic the mouse was positioned prone. A marker was used to mark the location of the spinous processes, vertical line, and pelvic crest, horizontal line (A). A line drawn across the pelvic crests corresponds to the position of the L5-L6 interspace. An incision was made through the skin which was held by a self-retaining

retractor (B). A single incision was made through the thoracolumbar fascia over the spinous processes and the paravertebral musculature was dissected by scraping a blade down along the spinous processes and pulling laterally. The dissection of the local musculature forms a pocket on either side of the spine, bounded medially by the spinous processes and inferiorly by the articular processes (D). The articular processes are consequently exposed and visualized allowing decortication with a 1mm round diamond burr until punctate bleeding is observed. Following decortication of the visualized articular processes, a 7mm x 2mm collagen sponge impregnated with either saline or saline/rhBMP-2 solution is inserted into each of the pockets in contact with the posterior elements of the spine (E). The muscle and skin are then closed with continuous sutures using 5.0 Vicryl®.

### **Study Design**

Once the safety and efficacy of the surgical model had been demonstrated, it was applied to a small study involving 18 C57BL6 mice to determine the optimal dose of rhBMP-2 required to establish fusion of the spine. Mice were divided into dose groups of 0, 0.5, 1, 2.5, and 5 µg of rhBMP-2 per sponge bilaterally and culled at 3 weeks. Spines were harvested and fixed in 4% paraformaldehyde for 24 hours and then analyzed by X-ray and microCT were used to visualize novel bone formation.

### **Radiography**

Following harvesting and fixation in 4% paraformaldehyde, microCT data was obtained via SkyScan 1174 compact microCT scanner (SkyScan, Kontich, Belgium). Samples were scanned in 70% ethanol at 21.3 µm magnification, 0.5 mm aluminum filter, 50 kV X-ray tube voltage and 800 µA tube electric current. The images were reconstructed using NRecon, version 1.5.1.5 (SkyScan). A global threshold was used representing bone tissue. Representative three-dimensional fractures were reconstructed with sagittal slices using CTVol Realistic Visualization software version 2.1.0.0 (SkyScan).

## **Histology**

Harvested vertebrae and surrounding musculature were fixed in 4% paraformaldehyde for 24 hours at 4°C on a shaker were and then stored in 70% ethanol until ready for decalcification. Samples were decalcified in 0.34M EDTA (pH 8.0) solution at 4°C on a shaker for 30 days with solution changes every 2-3 days. Samples were next embedded in paraffin and sectioned transversely through the center of the fusion mass at a thickness of 5 microns. Mounted sections were stained via Picro Sirius Red/Alcian Blue to differentiate bone and cartilage.

## **Statistics**

The significance of the medians and distribution of bone volume data as a function of increasing dose was first analyzed via stringent non-parametric statistics (Kruskal-Wallis independent sample test; SPSS Statistics v18). Using an assumption of normally distributed data, an ANOVA with *post-hoc* Bonferroni test was then performed to compare individual groups. The limit for statistical significance was set at 0.05.

## **Results**

### **Anatomical examination of the unfused mouse spine**

MicroCT images of the mouse lumbar spine were compared to human anatomical scans (Figure 2.2). Comparison of both species showed shared similar vertebral structures, although their position and orientation differed between species. Of particular note was the positioning of the transverse process (TP) in the mouse lumbar vertebrae. In the human, the TP is located posterolaterally, and is therefore the anchor point in

posterolateral spine fusion. In contrast, in the mouse it is the inferior articular processes, rather than the transverse processes that share this orientation. For the purposes of modeling a human surgery in a mouse, we concluded that a posterolateral interarticular process spine fusion would more closely approximate the posterolateral intertransverse procedure used in humans today.

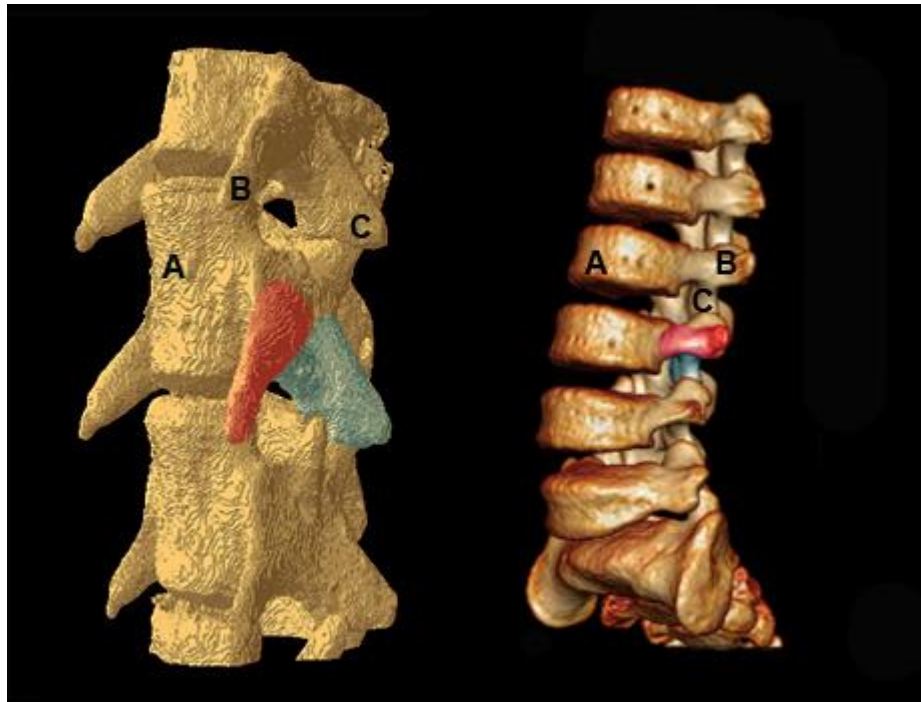


**Figure 2. 2** Three-dimensional reconstructions of CT images demonstrating the anatomy of murine lumbar spine (left) vs human lumbar spine (right). (A) Anterior vertebral body. (B) Transverse process. (C) Inferior articular process. The position and orientation of the transverse process of the mouse spine differs significantly from the human spine. Both the murine inferior articular process and the human transverse process share a lateral orientation.

### **Surgical timing and morbidity**

There was no intra- or post- operative morbidity or mortality in either the fusion outcome study or the rhBMP-2 dose response study. Animals were monitored for neurological impairment (particularly of the hind limbs), wound infection, weight loss and distressed



behavior. Operative time, in the hands of an experienced surgeon, was approximately 15 minutes skin to skin. We believe that the brief operating, and hence anesthetic time as well as the minimized trauma contributed significantly to the observed safety of the procedure.

### **Fusion outcomes**

Our results were consistent with previous studies [183], demonstrating little or no bone growth evident in decortication-only control animals on micro-CT reconstruction as well as in decortication/BMP animals culled at 1 week. By week 2, a significant volume of bone was observed in all animals which received BMP-2. The bone bridge typically united all vertebrae from L2/3-L6 with an AP dimension equal to or greater than that of the lumbar vertebrae to which it has fused (Figure 2.3). The bone mass was homogeneously of lower density than the vertebral cortical bone. At week 3, areas of centralized resorption were noted in the bone mass. Decortication does not appear to have contributed significantly to new bone formation. MicroCT reconstructions were supported by histology (Figure 2.4). Paraffin sections stained with Picro Sirius Red/Alcian Blue stain demonstrated an abundance of collagen, stained blue, overlying the posterior elements of the spine. The observed collagen is likely a remnant of the collagen sponge used to deliver the rhBMP-2 and was associated with lateral displacement of the perispinal musculature, stained green. No new bone formation, stained red, was observed at 1 week time points in any group. Overwhelming bone formation was observed at the 2 week end point in all groups dosed with rhBMP-2. The

size of the fusion mass was unchanged at 3 weeks. However, consistent with microCT data, an area of centralized resorption was evident. This was visualized as a reduction of red staining structures in the center of the fusion mass relative to samples obtained at 2 weeks.

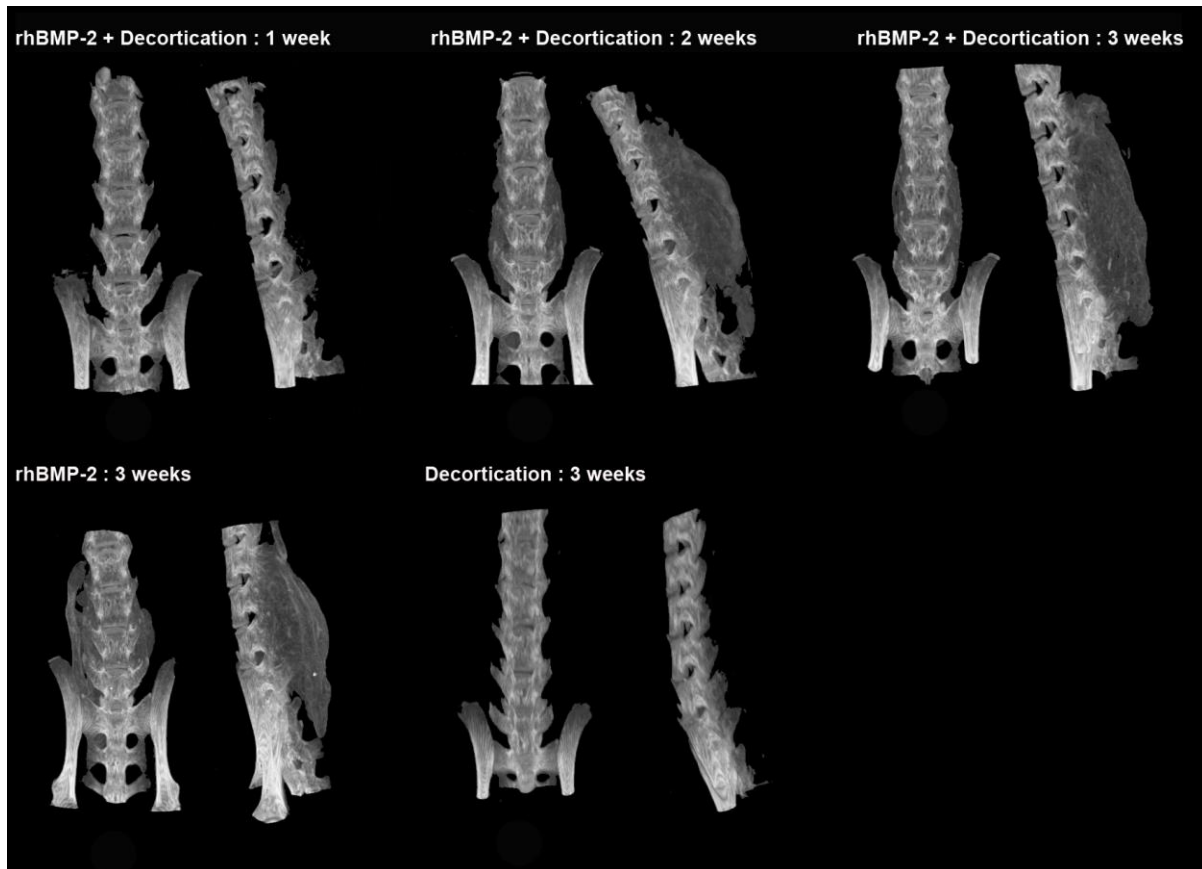


**Figure 2. 3** Volume of the BMP induced fusion mass was assessed via microCT using a Skyscan 1174 scanner. A fusion mass was only produced in groups in which BMP was implanted. No new bone was observed at 1 week post op, while maximum fusion volume was achieved by week 2 and maintained at week 3. Decortication of the articular processes alone was insufficient to achieve novel bone formation.

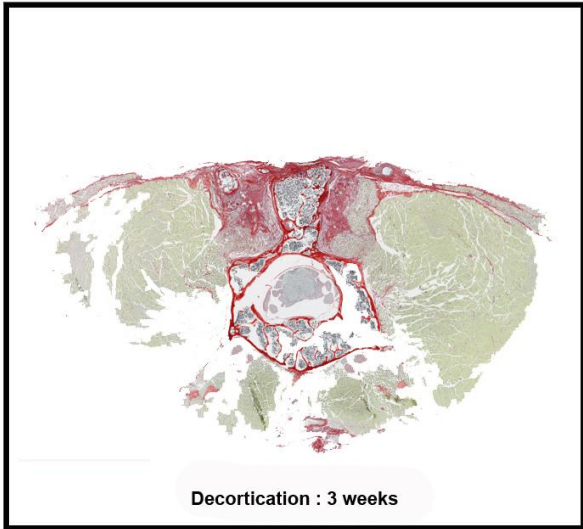
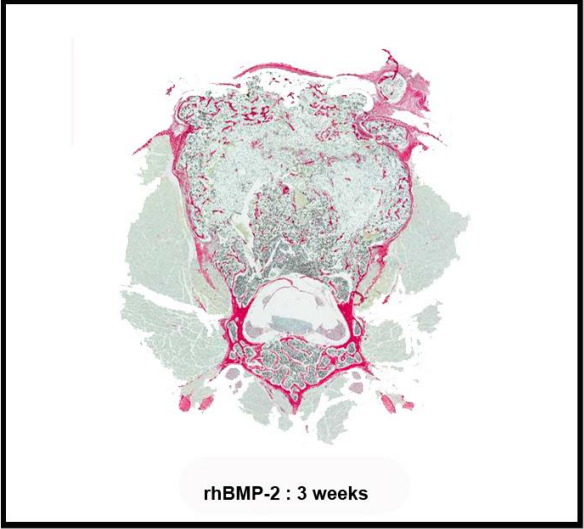
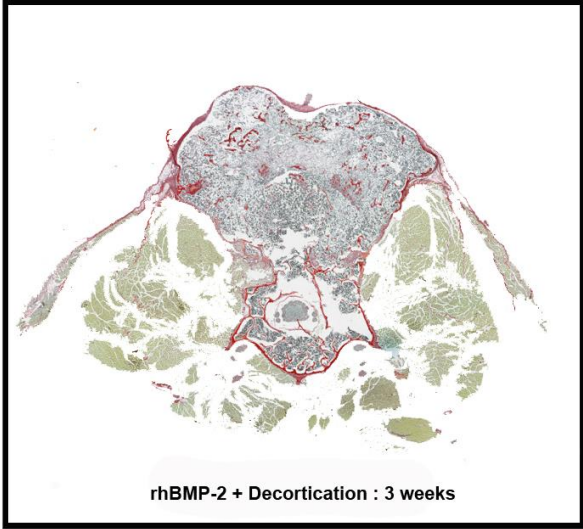
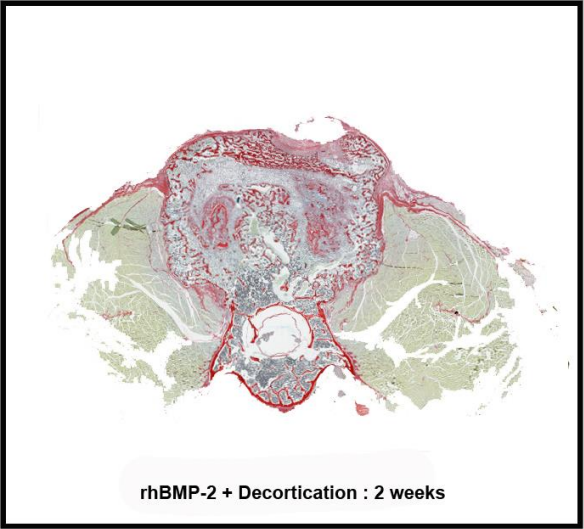
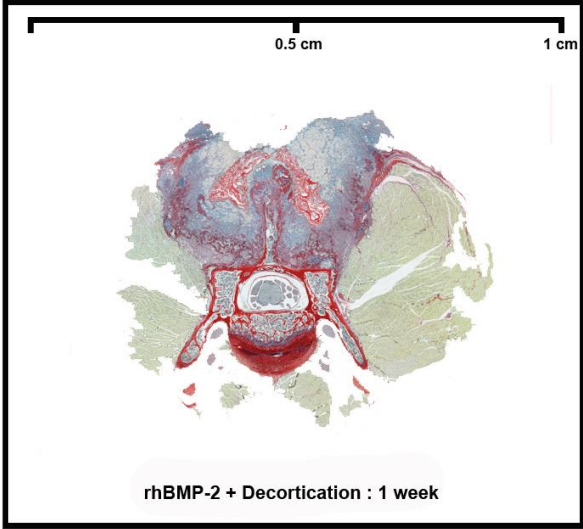


**Figure 2. 4** Histological samples retrieved from fused murine vertebrae. Samples have been stained with Pico Sirius red and Alcian blue stain to differentiate between bone and collagen. At 1 week, a large collagen mass overlaying the posterior elements of the vertebrae forms with disruption of local musculature. By the second week postoperatively, a large bony mass that was continuous with the cortex of the vertebrae was present. This mass exhibited a resorptive marrow-like center by week 3. No novel collagen or bone was observed in the decortications only spine.

### **rhBMP-2 dose response study**

A dose responsive relationship was observed between the rhBMP-2 dose and size of the fusion mass (Figure 2.5). When collagen sponges were added with 0 $\mu$ g of rhBMP-2, no fusion mass was observed. MicroCT data showed that a dose as low as 0.5 $\mu$ g was able to promote fusion and the amount of bone formed increased with increasing rhBMP-2 dose (Figure 2.6). The significance of the distribution of bone volume data as a function of increasing rhBMP-2 dose was found to be different by non-parametric independent sample analysis ( $P < 0.01$ ) and also by ANOVA ( $P < 0.01$ ). *Post-hoc* intergroup testing showed significant differences between the induced bone volumes between the 0  $\mu$ g (no treatment) group and the 2.5  $\mu$ g, 5  $\mu$ g, and 10  $\mu$ g rhBMP-2 groups (all  $P < 0.01$ ). Bonferroni *post-hoc* intergroup testing showed significant differences between the induced bone volumes between the 10  $\mu$ g groups and the 0  $\mu$ g (0.000), 0.5  $\mu$ g (0.005) and 1  $\mu$ g (0.051) groups as well as between the 0  $\mu$ g and the 2.5  $\mu$ g (0.008) and 5  $\mu$ g (0.005) groups.

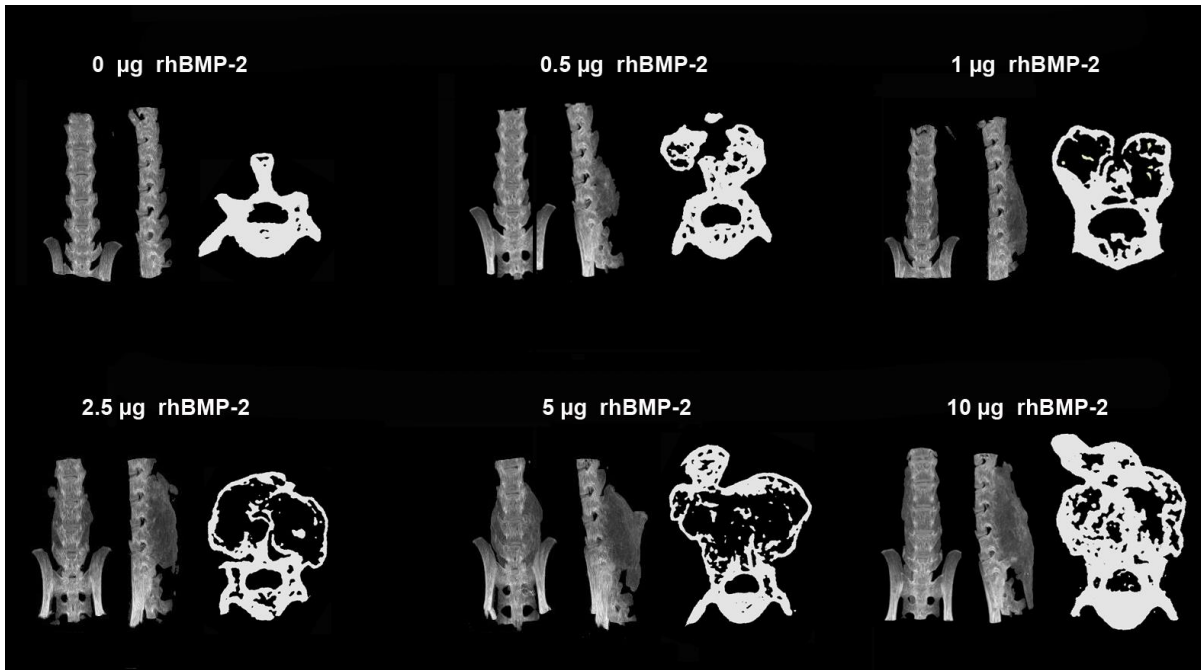


**Figure 2. 5** AP and lateral microCT images demonstrating the volume of new bone formed in response to rhBMP-2 dose. To the right of each set of microCT images was a cross sectional image of the spine taken at its widest point in the transverse plane. An increase in the size of the fusion mass was observed with increasing rhBMP-2 dose. It was noted that at a dose of 0.5 µg sufficient bone was formed to bridge the L4-L6 vertebrae resulting in successful fusion.

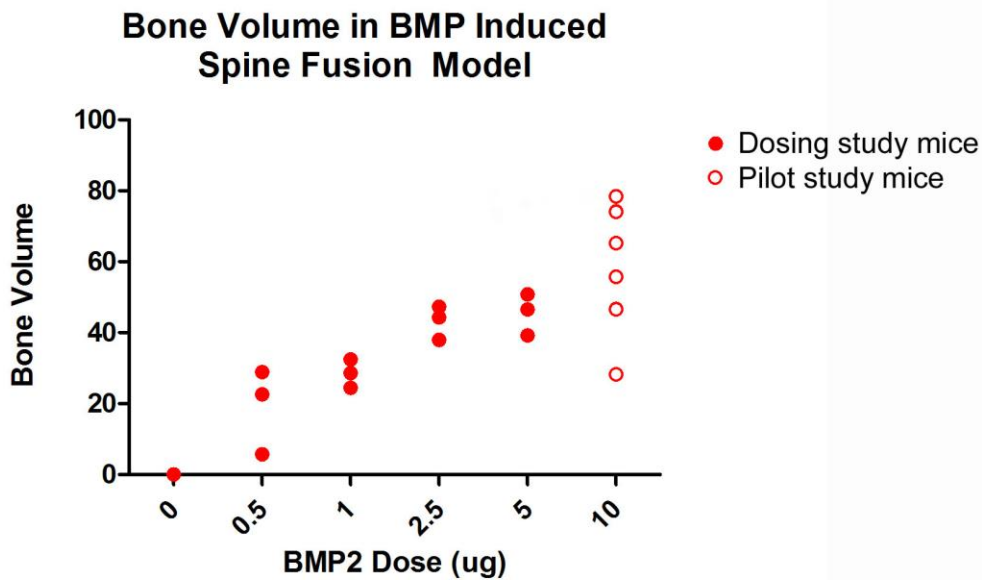


**Figure 2. 6** Volume of spine fusion bone mass as a function of rhBMP-2 dose. A dose-response relationship was observed with consistent bone mass being formed with a dose as low as 0.5 µg

of rhBMP-2. Bone volume data for the 10 µg dose (n=6) is included from the first phase and was consistent with the dose-response trend.

## **Discussion**

Historically, larger animals have been used to model spine fusion surgery due to their proximity in size and anatomy to humans. Recently, advancements in transgenic mice have generated an experimental niche for the use of murine surgical models. Knockout and transgenic mice offer a unique opportunity for insight into the genetic and cellular mechanisms underlying bone repair [185]. Idiopathic scoliosis (IS) is the most common cause of spinal deformity in children, but the etiology of the disease has remained elusive. Recent research has found a strong association between mutations of the CHD7 gene and the development of IS [186]. The potential exists to replicate CHD7-mutation dependent IS in transgenic mice and to investigate intervention therapies in an accurate murine model. Similar advantages are offered to the modeling of scoliosis in neurofibromatosis type 1 (NF1) patients. NF1 is the most common single gene disorder and at least 10% of patients diagnosed with NF1 will show signs of scoliosis in childhood [187]. A transgenic mouse model for human NF1 is currently available [188]. Additionally, there are several collateral advantages that may be gained by using mice for surgical modeling. As evidenced by this study, the small size of the mouse, though technically challenging, allows for a relatively quick operations which results in decreased intraoperative morbidity and mortality. Furthermore, this factor, when combined with the short generation time and the inexpensive housing costs of the mouse allows for a large volume of data to be obtained over a short period of time at little cost.

primary major drawback to using the mouse to replicate human surgery lies in the anatomical differences between the two species. With respect to the lumbar spine, our investigation into the murine anatomy yielded several distinct morphological differences between the mouse and the human lumbar vertebrae which have been previously overlooked, particularly the position and orientation of the transverse processes. However, the structural similarities of the mouse articular processes and the human transverse processes may be exploited to yield a procedure that is functionally analogous to that which is performed in humans.

Previous mouse and rat models of posterolateral spine fusion have adopted a modification of the Wiltse technique which utilizes a paraspinous approach to the transverse processes [178, 183, 184]. Given the anatomical differences between rodents and humans we don't believe that this is an optimal approach. Furthermore, the Wiltse technique uses twice as many incisions as a midline approach and is not currently in popular practice. The result is a procedure that does not mimic contemporary technique or relevant anatomy and leads to longer operating times with a consequent risk of increased morbidity and mortality. The surgical approach used in this study minimizes the number of incisions, tissue trauma and ultimately the total operative time.

In mice who only received articular process decortication as intervention, no bone formation was observed. Additionally, little difference was noted in the size of the fusion mass between the BMP-only group and the BMP + decortications group. This may suggest a limited contribution to the fusion mass by the periosteum. Local muscle and vasculature have been proposed as potential contributors of osteogenic cells to the

bone repair process [12, 18, 21, 45, 53, 55, 166-168, 185, 189-193] and may play a significant role in the context of spine fusion.

The initial study used an rhBMP-2 dose of 10 $\mu$ g per sponge. This dose was chosen by scaling down the dose currently used by our lab to achieve an rhBMP-2 mediated bone mass in rats. This yielded a very large amount of bone formation which is equal to or greater in volume than the spine itself. Such a large mass of bone suggests that the mouse spine is particularly sensitive to the osteogenic effects of rhBMP-2 and that a functional and stabilizing fusion mass could be achieved with a lower dose. We propose that the overwhelming response to the 10 $\mu$ g dose may be obscuring the influence of additional variables, such as decortications of the articular processes. A follow-up study was performed to determine minimum dose of BMP-2 required to obtain fusion. At 3 weeks a significant dose response relationship between rhBMP-2 and the volume of the fusion mass was observed. It was found that a dose of 0.5 $\mu$ g, equivalent to 5% of the original dose, was sufficient to achieve successful fusion. The resulting fusion mass was significantly smaller than that achieved using 5 $\mu$ g or 10 $\mu$ g rhBMP-2. This smaller fusion mass may be more sensitive to the effects of intervention. In our analysis we included bone volume data for a 10  $\mu$ g rhBMP-2 dose. This data was obtained from our initial pilot experiment which used identical mice and methods to the dosing study. In figure 5, the 10  $\mu$ g data is represented with hollow circles to identify these mice as having being operated on at a different point. The bone volumes for the fusion mass obtained from an rhBMP-2 dose of 10  $\mu$ g is consistent with the dose-response relationship exhibited by the 0-5  $\mu$ g groups.



We have demonstrated that a midline approach to posterolateral interarticular process spine fusion in a mouse model is safe, efficient, and yields consistent and reproducible results. A BMP-2 dose of 0.5µg per sponge is sufficient to achieve fusion of adjacent vertebrae. By exploiting anatomical similarities between the species, the technique closely mirrors that which is used in humans. The development of a surgical protocol in mice that is functionally analogous to the procedure in human patients is advantageous. This model permits the rapid observation of a large number of subjects over a relatively short period of time and allows valid extrapolation of reproducible data and results, thereby fulfilling the criteria for the ideal animal model as proposed by Schimandle and Boden [179].

## **Acknowledgements**

This work was supported by funding from Australian National Health & Medical Research Council Project Grants (1003478, 1003480).

Authors' roles: DGL, AS, JB and AR for study design and conceptualization. JB, AR, LP and MK for study conduct. JB for data analysis. DGL, AS, JB for data interpretation. JB for drafting manuscript. DGL and AS for manuscript revision and approval.

**(ii) Maximizing bone formation in posterior spine fusion using rhBMP-2 and zoledronic acid in wild type and NF1 deficient mice**

Justin Bobyn <sup>1,2\*</sup>, Anton Rasch <sup>1\*</sup>, Mikulec K <sup>1</sup>, David G. Little <sup>1,2</sup>, and Aaron Schindeler <sup>1,2§</sup>

<sup>1</sup> The Centre for Children's Bone Health, Sydney Children's Hospital Network, Sydney, Australia

<sup>2</sup> Discipline of Paediatrics and Child Health, Faculty of Medicine, University of Sydney, Sydney, Australia

\* Both authors contributed equally to this work

Published in *Journal of Orthopaedic Research*, 9 April 2014

## Abstract

Spinal pseudarthrosis is a well described complication of spine fusion surgery in NF1 patients. Reduced bone formation and excessive resorption have been described in NF1 and anti-resorptive agents may be advantageous in these individuals. In this study, 16 wild type and 16 *Nf1*<sup>+/-</sup> mice were subjected to posterolateral fusion using collagen sponges containing 5µg rhBMP-2 introduced bilaterally. Mice were dosed twice weekly with 0.02mg/kg zoledronic acid (ZA) or sterile saline. The fusion mass was assessed for bone volume (BV) and bone mineral density (BMD) by microCT. Co-treatment using rhBMP-2 and ZA produced a significant increase (p<0.01) in BV of the fusion mass compared to rhBMP-2 alone in both wild type mice (+229%) and *Nf1*<sup>+/-</sup> mice (+174%). Co-treatment also produced a significantly higher total BMD of the fusion mass compared to rhBMP-2 alone in both groups (p<0.01). Despite these gains with anti-resorptive treatment, *Nf1*<sup>+/-</sup> deficient mice still generated less bone than wild type controls. TRAP staining on histological sections indicated an increased osteoclast surface/bone surface (Oc.S/BS) in *Nf1*<sup>+/-</sup> mice relative to wild type mice, and this was reduced with ZA treatment.

## Introduction

Neurofibromatosis type 1 (NF1) is a genetic disease with an incidence of 1 in 3000 that results from mutations in the *NF1* gene. [194] *NF1* is expressed in many tissues and its deficiency is associated with a range of characteristic features that present with variable penetrance. Orthopedic manifestations are one of the standard diagnostic criteria for NF1. As many as 25% of individuals will go on to develop some degree of scoliosis. [195, 196] Spine fusion surgery to correct the curvature and prevent future deformity is not uncommon, however with NF1 this can have an increased complication rate. [197] Pseudarthrosis at the fusion site may develop in as many as 25% of NF1 cases; in these incidents the adjacent vertebrae are united by fibrous tissue rather than with a solid bone bridge. [163] Solid fusion is seen in as few as 7% of cases. [93]

These poor surgical outcomes are likely due to primary defects in NF1 bone metabolism. Up to 30% of adolescents and adults with NF1 show reduced bone mineral density (BMD), [198, 199] likely related to reduced bone formation and increased bone resorption. [50] Moreover, poor bone healing is observed in murine models of NF1-deficient and NF1-null fracture repair, and these feature delayed union and pseudarthrosis respectively. [159, 200] Orthopedic models have likewise shown a bone anabolic deficiency as well as excess resorption from abundant osteoclasts. [49] Consequently, combination therapies using recombinant human bone morphogenetic proteins (rhBMPs) together with bisphosphonates have been proposed for the treatment of tibial pseudarthrosis. This strategy is supported by both genetic mouse models of NF1 [201, 202] and a published case series of NF1 tibial pseudarthrosis patients. [203]

Currently therapeutic development for NF1 spine fusion is hampered by a lack of an appropriate pre-clinical model to test interventions. Such a system requires both a genetic model of NF1 deficiency as well as an established protocol for spine fusion surgery. We have previously described a novel protocol for spine fusion in mice which we have shown to be safe, reliable and reproducible. [204] This model utilizes rhBMP-2 delivered by surgically implanted collagen sponges to induce a posterolateral fusion. In this study we describe the application of this surgical model to *Nf1* deficient mice (*Nf1*<sup>-/-</sup>) with and without systemic bisphosphonate treatment. It was hypothesized that bisphosphonate treatment would maximize the retention of rhBMP-2 induced bone yielding a superior fusion outcome as determined by bone volume and density.

## **Materials and Methods**

### ***Nf1* Gene Knockout Mice**

*Nf1* knockout mice were a gift from L. Parada (UT Southwestern, Dallas, TX). [205] This mouse line possesses no tissue specificity in its *Nf1* deficiency. The mouse line was maintained on a C57BL/6J background and genotyping was performed using a PCR-based method. *Nf1*<sup>-/-</sup> heterozygous knockout mice aged 8-10 weeks were compared with wild-type (*Nf1*<sup>+/+</sup>) littermate controls. Female mice were used for all experiments. All animal experiments were approved by the local institutional ethics committee.

### **Study Design**

16 wild type mice and 16 *Nf1<sup>+/-</sup>* mice were used for the experiment. All mice underwent surgery for posterolateral fusion using bilateral paravertebral acellular collagen sponges (ACS, Medtronic), each loaded with 5µg rhBMP-2. This dose was specifically chosen to represent the lower limit of the dose used in pediatric surgery (4.2mg in a 40 kg individual). For each genotype, n=8 were dosed twice weekly with saline and n=8 with five doses of the bisphosphonate zoledronic acid (ZA, Novartis AG). ZA was given at 0.02 mg/kg (total dose 0.1 mg/kg) by biweekly subcutaneous injection commencing 3 days postoperatively. Mice were culled at 3 weeks and spines harvested for radiographic and histological analyses.

## **Surgery**

The surgical technique was performed with the intention of fusing the lumbar spine from L4-L6 using a published technique[204] modified from prior approaches in rodents. [183, 184] Surgery was performed on mice aged between 8-10 weeks old by two surgeons in a single sitting with the aid of a trained animal technician. Anesthesia, preoperative prep and postoperative observation were performed by the animal technician. The procedure was performed under an operating microscope at 2.5× magnification. A 15 mm incision was made in the skin along the midline, centered over a line running between the iliac crests. The skin was retracted and held with a self-retaining retractor. The paravertebral muscles overlying the articular processes of L4-L6 were separated from the spinal column by scraping a 10 mm blade down the lateral border of the spinous process and pulling the muscles laterally. A pneumatic 1 mm round tip diamond burr was used to decorticate the visible articular processes until punctate bleeding was observed. Two

collagen sponges, impregnated with either saline or a BMP/saline solution were placed bilaterally adjacent to the decorticated bone. The fascia was closed with a single line of continuous sutures using 6.0 Vicryl, and the skin was subsequently closed in the same fashion. Mice were placed on a heat pad following surgery and monitored for recovery. Antibiotics were administered in the drinking water for the duration of the experiment.

### **Radiography**

Bone volume (BV; mm<sup>3</sup>) and total bone mineral content (TMD; mg/mm<sup>3</sup>) of the fusion mass were measured by microCT using software that encompassed the fusion mass within a uniform region of interest (ROI). MicroCT data was acquired using a SkyScan 1174 compact microCT scanner (SkyScan, Kontich, Belgium). Samples were scanned in 70% ethanol at 21.3 um magnification, 0.5 mm aluminum filter, 50 kV X-ray tube voltage and 800 μA tube electric current. The images were reconstructed using NRecon, version 1.5.1.5 (SkyScan). The bone of the fusion mass was isolated from native bone by means of manually drawn regions of interest (ROI) and thresholded using CTAn software version 1.10.03. A global threshold of 0.3g/mm<sup>3</sup> was set for bone tissue. Representative 3-dimensional fractures were reconstructed with sagittal slices using CTVol Realistic Visualization software version 2.1.0.0 (SkyScan).

### **Histology**

Harvested vertebrae and surrounding musculature were fixed in 4% paraformaldehyde for 24 hours at 4°C on a shaker and were then stored in 70% ethanol until decalcification. Samples were decalcified in 0.34M EDTA (pH 8.0) solution at 4°C on a

shaker for 30 days with solution changes every 2-3 days. Spines were cut axially and the central 5mm of the fusion mass were isolated and embedded in paraffin. Axial sections were taken through the center of the fusion mass at a thickness of 5µm. Mounted sections were stained via Picro Sirius Red/Alcian Blue to differentiate bone and cartilage. Adjacent sections were stained for tartrate-resistant acid phosphatase (TRAP) expression to highlight osteoclasts, and counterstained with light green. Bone volume/trabecular volume (BV/TV) for the heterotopic bone and osteoclast number (OcN) and surface area (OcS) was calculated relative to bone surface (BS) in mm using Bioquant software.

### **Statistical Analyses**

The volume and density of bone present at 3 weeks was compared between *Nf1<sup>+/-</sup>* and wild type groups and between groups receiving ZA and saline. Statistical analysis and graphing were performed using Graphpad Prism. The influences of genotype and bisphosphonate treatment were examined by non-parametric Kruskal Wallis/Mann Whitney U tests between the relevant groups with a significance cutoff of 0.05. Error bars on graphs represent the 95% confidence intervals.

### **Results**



## ***Nf1*<sup>+/-</sup> mice and wild type mice develop a robust fusion mass in response to rhBMP-2**

Posterolateral inter-transverse spine fusion surgery was performed on 32 mice and, consistent with prior applications of the model, [204] there were no cases of morbidity or mortality. Two surgeons working in tandem were able to complete an operation in ~20 minutes. Animals showed no post-surgical complications or adverse reactions to bisphosphonate treatment. On examination at 3 weeks, a large, bony fusion mass was palpable, and occasionally visible overlying the lumbar vertebrae. Mice did not display any discomfort or neurological impairment as a result of the overwhelming bone formation, as can occur in human patients. [206]

MicroCT images of harvested mouse vertebrae obtained at 3 weeks were reconstructed from all spines recovered from both wild type and *Nf1*<sup>+/-</sup> mice (Figure 3.1). Analysis of the total bone volume of the fusion masses showed a -11% decrease in the bone volume and density of fusion masses of *Nf1*<sup>+/-</sup> mice relative to wild type controls ( $p=0.08$ ). While this did not reach significance, *post-hoc* power analysis indicated  $\beta=0.34$  suggestive of significance with a larger sample size. Notably, the effect size for *Nf1* genotype influencing spine fusion mass was less than that previously reported for rhBMP-2 induced ectopic bone nodules. [202]

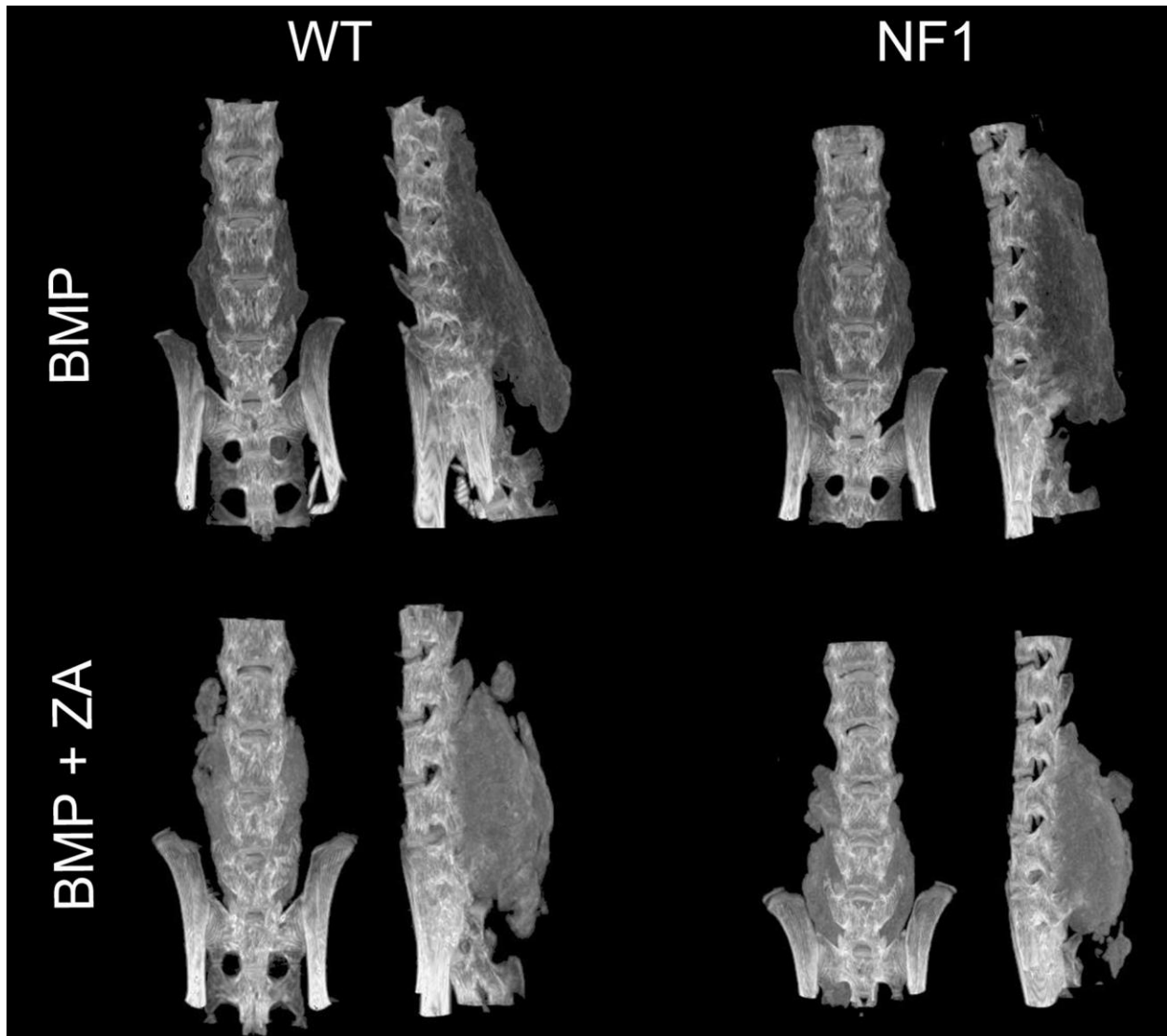


**Figure 3. 1** MicroCT reconstructions of harvested spines. ZA treatment led to an increase in the opacity of the rhBMP-2 induced fusion mass relative to controls. Spine fusion was achieved in all samples.

### Evaluation of the effects of ZA co-administration in wild type and *Nf1*<sup>+/-</sup> mice

Co-treatment with rhBMP-2 and systemic ZA was examined in the spines of wild type and *Nf1*<sup>+/-</sup> mice. Radiography (XR and microCT) obtained at 3 weeks postoperatively showed that co-treatment with ZA led to a more radio-dense fusion mass. The size of

the fusion mass, however, remained unchanged. Both the wild type and *Nf1*<sup>+/-</sup> mice showed significant improvements in fusion with ZA treatment.

Quantification of bone volume by microCT showed a +226% increase (wild type) and +174% increase (*Nf1*<sup>+/-</sup>) ( $p < 0.01$ , Figure 3.2 A). In addition, ZA treatment resulted in a consistent 1% increase in BMD that was statistically significant ( $p < 0.01$  for WT and *Nf1*<sup>+/-</sup> groups, Figure 2B). Despite the substantive increases in net bone with ZA treatment, *Nf1*<sup>+/-</sup> animals showed a -20% reduction in bone compared to wild type controls ( $p = 0.02$ ).

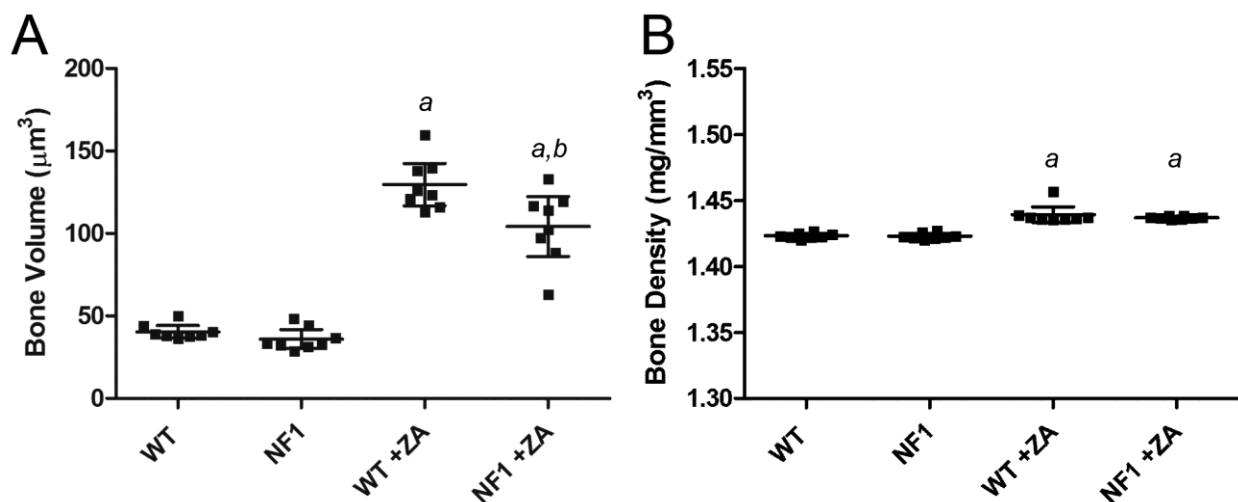


**Figure 3. 2** MicroCT assessment of bone volume (A) and bone mineral density (B). BV was significantly increased with ZA treatment (a,  $p < 0.01$ ) and in the ZA treated groups significantly less bone was associated with the *Nf1*<sup>+/-</sup> genotype (b,  $p = 0.02$ ). Likewise, BMD was significantly increased with ZA treatment (a,  $p < 0.01$ ) relative to untreated controls of the same genotype.

### **ZA treatment reduces the resorption of rhBMP-2 induced bone in the fusion mass of *Nf1*<sup>+/-</sup> and wild type mice**

Transverse sections were taken from the widest level of the fusion mass and used for osteoclast quantitation (Figure 3). Osteoclast surface area (OcS) and bone surface area (BS) were calculated via Bioquant software. Analysis revealed an increase in the

osteoclast surface area to bone surface area ratio (OcS/BS) in *Nf1<sup>+/-</sup>* samples relative to wild type controls ( $p=0.05$ ).

Co-treatment with rhBMP-2 and ZA treatment led to a significant reduction in OcS/BS in both wild type mice ( $p < 0.01$ ) and *Nf1<sup>+/-</sup>* mice ( $p < 0.01$ ) with respect to animals treated exclusively with rhBMP-2 (Figure 4). The decreases in osteoclast surface with ZA treatment were consistent with the increases in net bone identified by radiography. With ZA treatment there was no difference between wild type and *Nf1<sup>+/-</sup>* mice with respect to OcS/BS ( $p=0.28$ ).



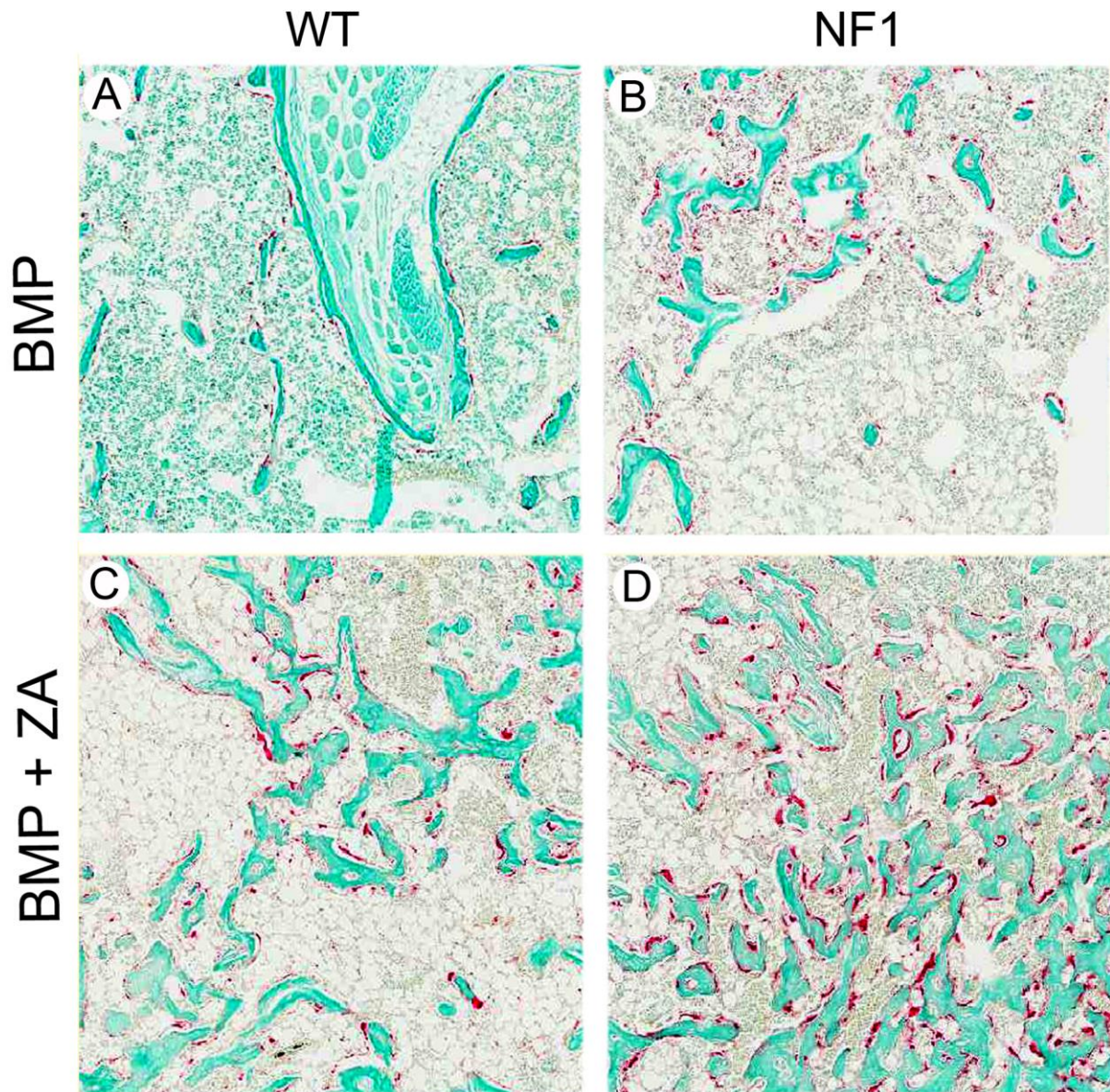


**Figure 3. 3** Transverse sections of fusion masses with a TRAP stain, counterstained with fast green.

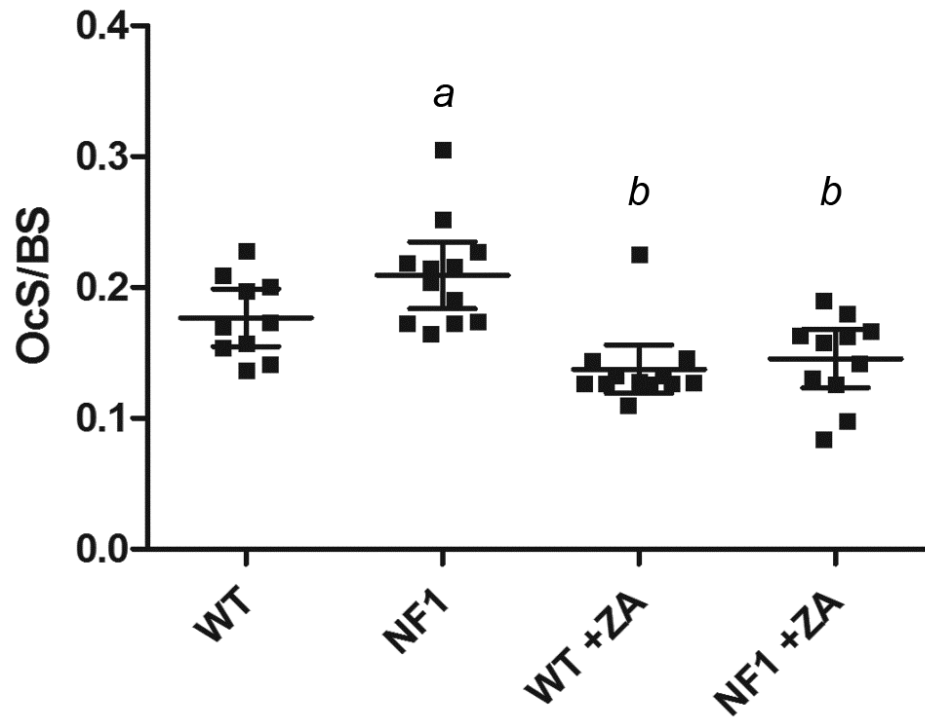


**Figure 3. 4** Osteoclast surface relative to bone surface was quantified from tissue sections. Without ZA treatment, *Nf1*<sup>+/-</sup> mice showed an increase in OcS/BS relative to wild type controls (a, p=0.05). Treatment with ZA led to significant decreases in OcS/BS for both genotypes (b, p<0.01).

## Discussion

The bone phenotype of NF1 is characterized by excessive resorption and decreased osteoblast activity. [165, 207] This poses a significant challenge in the context of spine fusion surgery, which is commonly used to correct the scoliosis that is associated with the disease. Although an *Nf1*<sup>+/-</sup> mouse model has been previously studied in the context of tibial fracture repair, [200] investigation of spine fusion therapies has been limited by the unavailability of a suitable model of posterolateral spine fusion. We have previously described a novel approach for mouse lumbar spine fusion that is safe, efficient, highly reproducible, and analogous to contemporary human surgery. [204] By applying this

model to *Nf1* deficient mice we have demonstrated that dual treatment with rhBMP-2 and ZA is superior to treatment with rhBMP-2 alone. The combination of rhBMP and bisphosphonate treatment has been previously applied in the context of NF1 pseudarthrosis, [201, 203] but this approach has also been shown to be generally effective in other orthopedic models. [208, 209]

This study confirms that at a dose of 5µg bilaterally, rhBMP-2 is able to reliably and reproducibly promote the formation of a large multilevel fusion mass in the lumbar spine in both wild type and *Nf1*<sup>+/-</sup> mice. Thus this model does not recapitulate the poor response to rhBMP and complications associated with spine fusion associated with NF1. While the differences in BV between *Nf1*<sup>+/-</sup> mice and wild type controls approached significance, the effect size was less than predicted based on prior studies [202] and did not reach significance with the sample size employed.

We propose two possible factors that may have contributed to this lack of difference. First, this could reflect species-dependent effects between humans and mice and may indicate an intrinsic limitation of this model system. Deletion of a single *Nf1* allele has been reported to be less impactful in mice than in individuals with NF1. The *Nf1*<sup>+/-</sup> mice do not show reduced bone density or develop spontaneous delayed or non-unions comparable to a clinical NF1 congenital pseudarthrosis. [200, 209] We have recently utilized a model of localized double inactivation of *Nf1* in the tibia to model tibial pseudarthrosis [159] and it is possible that such a localized genetic approach could be developed for the spine.

Second, it is possible that employing lower doses of rhBMP-2 could lead to more profound differences in the fusion rate of wild type and *Nf1*<sup>+/-</sup> mice. The selected dose of

5µg per side was comparable to other murine ectopic bone formation studies that model the clinical application of rhBMPs, [210-212] and human patients, particularly those with NF1, typically receive large doses of rhBMPs in order to stimulate a maximal response. [47]Comparable doses were used in ectopic bone studies that showed a difference between wild type and *Nf1*<sup>+/-</sup> mice, [202]but use of rhBMPs at a bony location can stimulate a greater response than in an ectopic/intramuscular location.

The addition of the bisphosphonate ZA, a known modulator of bone remodeling, effectively shifted the equilibrium of bone homeostasis in favor of bone formation by inhibiting resorption. The net effect was a measurable and significant increase in fusion mass bone volume and density when compared to controls receiving rhBMP-2 alone. Notably, a significant difference in fusion mass BV was observed between wild type and *Nf1*<sup>+/-</sup> mice treated with ZA. This implies that *Nf1* deficiency is associated with a *bona fide* anabolic deficiency in this mouse model. Nevertheless, inhibition of resorption led to considerable (+174%) increases in bone.

Translation of this concept could yield increased fusion success rates in the treatment of scoliosis in NF1 patients, reducing the incidence of pseudarthrosis which is a source of great morbidity in this population. Additionally, the robust fusion masses seen in wild type mice dosed with ZA suggest that uncomplicated cases of spine fusion may also benefit from bisphosphonate therapy. As an approved anti-resorptive drug, ZA is a candidate for translational application.



## **Acknowledgements**

This research was supported by funding from the National Health and Medical Research Council APP1003478, including salary support for Dr. Schindeler. Zoledronic acid used in the study was provided by Novartis AG. Prof Little has previously received research funding from Novartis AG for projects unrelated to this study.

### **(iii) Spine fusion in a murine model of double inactivation of NF1 in the spine**

Justin Bobyn MBBS <sup>1,2</sup>, Nikita Deo PhD <sup>1,2</sup>, David G. Little FRACS(Orth) PhD <sup>1,2</sup>, Aaron Schindeler PhD <sup>1,2§</sup>

- <sup>1</sup> Orthopaedic Research & Biotechnology Unit, The Children's Hospital at Westmead, Sydney, NSW, Australia
  - <sup>2</sup> Discipline of Paediatrics and Child Health, Faculty of Medicine, University of Sydney, Sydney, NSW, Australia
  - <sup>3</sup> Bone Unit, Musculoskeletal Disease Area, Novartis Institutes for BioMedical Research, Basel, Switzerland
- § Corresponding author

Submitted for publication to *Journal of Orthopaedic Research*, January 2018

## ABSTRACT

Spine fusion is a common procedure for the treatment of severe scoliosis, a frequent and challenging deformity associated with Neurofibromatosis type 1. Moreover, deficiencies in NF1-Ras-MEK signaling have intrinsic effects on bone formation and resorption that impact on spine fusion outcomes. In this study we describe a new model for AdCre virus induction of *Nf1* deficiency locally in the mouse spine in a fusion procedure. This model produces abundant fibrous tissue (*Nf1<sup>null</sup>* +393%,  $P < 0.001$ ) and decreased marrow space (*Nf1<sup>null</sup>* -67%,  $P < 0.001$ ). This was associated with a lesser histological quality anticipated to impact on union quality in humans, despite no significant impact on bone volume of the fusion mass (*Nf1<sup>null</sup>* -14%,  $P = 0.999$  n.s.). Similar to prior reports of multinucleated TRAP+ cells in NF1 fibrous tissue distal from the bone, we observed such cells in the fibrous tissues seen in *Nf1<sup>null</sup>* spines. Systemic adjunctive treatment with the MEK inhibitor PD0325901 and the bisphosphonate zoledronic acid were trialed in this model. MEK inhibitor increase bone volume (+194,  $P < 0.001$ ) whereas ZA increased bone density (+10%,  $P < 0.002$ ). Both MEKi and ZA decreased TRAP+ cells in the fibrous tissue (MEKi -62%,  $P < 0.01$ ; ZA -43%,  $P = 0.054$ ). In *Nf1<sup>null</sup>* spines, no adverse effects were seen with either treatment, however in wild type spines MEKi led to a 23-fold increase in residual cartilage in the fusion mass ( $P < 0.01$ ). In summary, the AdCre-virus induced knockout spine model has utility for modeling spine fusion, and allow screening of alternative adjunctive therapies for improving NF1 spine fusion.

## INTRODUCTION

Neurofibromatosis type 1 (NF1) is a common autosomal dominant genetic disorder with an estimated incidence of 1 in 2500 live births [213]. The *NF1* gene is expressed in numerous tissues and can thus affect a wide range of clinical features, each with variable penetrance. Individuals with NF1 are prone to tumor development, including cutaneous and subcutaneous neurofibromas, plexiform neurofibromas, optic gliomas, and peripheral malignant nerve sheath tumors [214, 215]. A subset of NF1 individuals are born with or develop osseous manifestations, with scoliosis and tibial pseudarthrosis being the most clinically challenging to treat [213].

The reported incidence of scoliosis in NF1 varies, but has been reported to be between 11% [216] and 64% [217], and may be classified into non-dystrophic or dystrophic types. Non-dystrophic scoliosis is similar in presentation to idiopathic scoliosis while dystrophic scoliosis is associated with dystrophic changes to the vertebrae. Dystrophic scoliosis is associated with short, acute curves, due to the vertebral wedging and segmentation abnormalities which are seen in the disease. [218]. The dystrophic curves present earlier and with more severe deformity,[219] however despite the severe angulation of these curves, neurological compromise is not always present.

Intervention for scoliosis can be further complicated by intraspinal and paraspinal neurofibromas, that can be present in up to 50% of individuals with NF1-associated dystrophic scoliosis. Paraspinal neurofibromas are often found to the concavity of the curve and may present as massive soft tissue tumors which may invade the muscle and compress surrounding structures. [220, 221] [222-224] Similarly, intraspinal tumors may represent a source of significant morbidity as they compress neurological structures.

Dural ectasia is a widening of the thecal sack which may erode bony and soft paraspinal tissues. This is seen as vertebral scalloping on plain radiographs. In the presence of severe angulation, it may serve a protective function by limiting cord compression. [148, 221].

Surgery remains the primary means of correcting and preventing further deformity for NF1 individuals with worsening scoliotic curves. Positive surgical outcomes are primarily dependent upon establishing robust fusion between adjacent vertebrae [197]. As is seen in the case of tibial pseudarthrosis, patients with NF1 demonstrate impaired bone repair at the spine. Pseudarthrosis in the postoperative spine is seen in as many as 25% of cases [163], with as few as 7% of cases developing a clinically robust fusion [93].

To overcome the poor bone formation seen in NF1, combinations of anabolic bone agents (e.g. Bone Morphogenetic Proteins; BMPs) and anti-resorptive drugs (e.g. bisphosphonates) have been promoted as potent adjunctive agents. In animal models of tibial non-union, this has led to improved healing in *Nf1* knockout fractures [225]. Comparable positive outcomes were reported in a clinical tibial pseudarthrosis case series employing off-label BMPs and bisphosphonates [203]. Limited reports have attempted to model BMP and bisphosphonate use in the spine, with one report showing a significant increase in bone volume and mineral density of the fusion mass in *Nf1*<sup>+/-</sup> and wild type mouse fused spines [226]. However, this model featured heterozygosity for NF1, whereas recent clinical reports show double inactivation of *NF1* in tibial pseudarthrosis [227] and preclinical models affect *Nf1*<sup>null</sup> tissues in tibial fracture healing [159], [228].

Moreover, adjunctive treatments such as BMPs and bisphosphonates fail to target the specific cellular pathways associated with NF1 deficiency. The NF1 gene encodes for the protein neurofibromin, a negative regulator of the Ras oncogene. Impairments in osteoblast function have been linked to elevated Ras signaling [229], and the Ras-ERK cascade has been implicated in the uncontrolled cell proliferation and fibrosis [230, 231]. In pseudarthrosis surgery, invading fibrotic/mesenchymal tissue is recommended to be aggressively surgically resected [232] [203]. Fibrosis is also a complication of localized *Nf1<sup>null</sup>* fracture mouse models [159].

Ras canonically acts via a phosphorylation cascade through Raf, MEK (mitogen-activated protein kinase kinase), and ERK (mitogen-activated kinase). Thus it was speculated that downstream inhibition of the NF1-Ras-MEK axis using a MEK inhibitor (MEKi) could reduce fibrosis and enhance bone formation. The MEKi PD0325901 has been shown to reduce tumor growth in preclinical xenograft models [233, 234] and has subsequently been shown to be tolerated in human trials with a measureable effect on decreasing melanoma tumor size.[235]

In this study we further describe a new murine model that recapitulates the challenging clinical nature of NF1 spine fusion. NF1 is inactivated in the spine of *Nf1<sup>flox/flox</sup>* mice by employing cre-expressing adenovirus (AdCre) system, similar to prior tibial non-union studies [159]. This fusion model shows a lack of bony union and extensive fibrosis. Next, interventions combining rhBMP-2 with the MEK inhibitor PD0325901 or the bisphosphonate Zoledronic Acid were tested. Outcome measures were radiographic and histological. We submit that this model can be used not only for therapeutic testing, but as an archetypical approach to gene deletion in the context of spine fusion.

## **METHODS**

### **Animal Colony**

We sourced *Nf1<sup>flox/flox</sup>* mice, as originally generated by Prof Luis Parada, from the National Cancer Institute (NCI) mouse repository (Bethesda, MD, USA). The *Nf1<sup>+/-</sup>* strain was supplied directly by Prof Parada. Both colonies were maintained on a C57/Bl6 background. All animal experiments were approved by the Westmead Hospital Animal Ethics Committee.

### **Adenovirus production and purification**

Human embryonic kidney cells, HEK293, were grown in T175 culture flasks to 80% confluence and transduced with AdCre (gift from Dr Thomas Gajewski) [236]. 72 hrs after transduction, cells were harvested as it was observed that cells were beginning to detach. Harvested cells were pelleted and subjected to cell lysis and DNase treatment. The resulting supernatant was ultracentrifuged for 1 hr. Viral fractions were then pooled and re-spun for 20 hrs. Centrifugation was performed at 35,000 rpm in a standard CsCl gradient in a Beckman SW-41Ti rotor. Purified virus was dialyzed in a Slide-A-Lyzer Dialysis Cassette, 10 kDa cutoff (Thermo Scientific, USA) for up to three days in a 10mM Tris (pH 8.0) solution. Following dialysis, virus was titered using the Adeno-X titration kit (Clontech, USA) and used or frozen at -80°C in 10% glycerol.

## **Surgical model**

Female C57BL6 mice aged 8-10 weeks were subjected to a surgical spine fusion procedure using a published model.[237] Surgery was performed by a single surgeon over two sessions with support from an experienced animal technician. 15 mm midline longitudinal incision was made centered at the level of the iliac crests. Mice were anaesthetized with an intraperitoneal injection of ketamine (35mg/kg) and xylazine (5mg/kg) with a 27G needle. Anesthesia was maintained with inhaled isoflurane as required. Paraspinal muscles at the level of L4-L6 were swept laterally to expose the bony anatomy which was decorticated with a diamond tipped burr. A collagen sponge loaded with either saline, saline/rhBMP-2 or AdCre virus solution/rhBMP-2 was inserted into this paraspinal pocket (Figure 4.1). The rhBMP-2 was delivered at a dose of 10 µg in each sponge. Animals were culled at day 21 by CO<sub>2</sub> asphyxiation and spines from L1 to lower sacrum, were harvested for radiographic and histological analysis.



A

	Nil	PD0325901	ZA
Saline	4	0	0
Saline + BMP-2	4	4	0
AdCre	5	0	0
AdCre + BMP-2	7	5	8

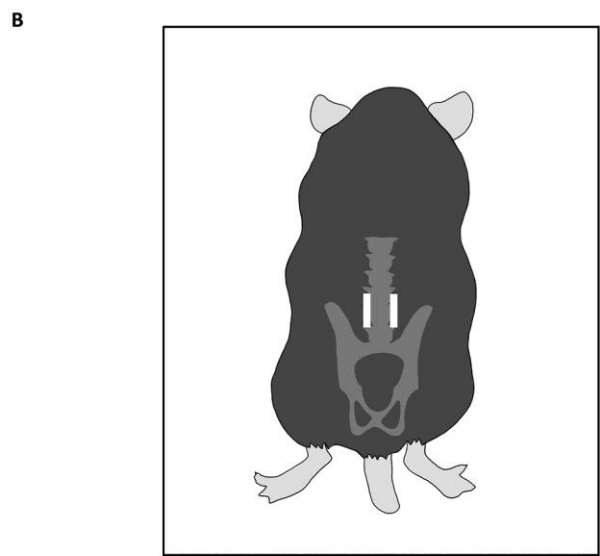


**Figure 4. 1** Animals were divided as per the table into groups (A) and subjected to a posterolateral intertransverse spine fusion surgery in which rhBMP-2 and AdCre virus are delivered to the lumbar spine via implantation of paired collagen sponges (B) as per previous publication. Dosing with ZA and the MEK inhibitor PD0325901 began 2 days prior to the date of surgery.

### Drug Treatments

Oral drug delivery with PD0325901 was performed as described by Sullivan *et al.* [238]. Prior to the experiment, mice were single housed to ensure that consistency in oral dosing of drug/vehicle. Strawberry jelly was used as a vehicle for drug delivery. Animals were trained to eat the jelly prior to the experiment and dosing began at day -2. Jelly was made with 0.8% DMSO (Sigma-Aldrich, St. Louis, MO, USA), 16% Splenda (Splenda® Low Calorie Sweetener, Johnson-Johnson Pacific Pty, NSW, Australia),

9.6% gelatine (Davis Gelatin, GELITA Australia Pty, NSW, Australia) and 7.9% flavoring (QUEEN Flavoring Essence Imitation Strawberry, Queen Fine Foods Pty, QLD, Australia). Jelly was loaded with PD0325901 dissolved in DMSO to be delivered as a daily dose per animal of 10mg/kg. Dosing began on day 1 post op and continued until cull at day 21.

Subjects in the bisphosphonate treatment group received a five doses of 0.02mg/kg ZA (total dose 0.1mg/kg) (Novartis AG) by biweekly subcutaneous injection commencing 3 days postoperatively, as previously published [202].

### **MicroCT analysis**

MicroCT analysis was performed as described in our previously published study of NF1 spine fusion. [226] Spines and surrounding soft tissue were harvested at day 21 and fixed in a 4% paraformaldehyde solution for 24 hours at 4°C and then stored in 70% ethanol. Samples were scanned using a SkyScan 1174 compact microCT scanner (SkyScan, Kontich, Belgium). Samples were scanned in 70% ethanol at 21.3 um magnification, 0.5 mm aluminium filter, 50 kV X-ray tube voltage and 800 µA tube electric current. The dicom images were reconstructed using NRecon software, version 1.5.1.5 (SkyScan). The fusion mass was isolated from native bone by manually drawing regions of interest (ROI) and thresholded using CTAn software version 1.10.03. A global threshold of 0.3g/mm<sup>3</sup> was set for bone tissue. Representative 3-dimensional fractures were reconstructed with sagittal slices using CTVol Realistic Visualization software version 2.1.0.0 (SkyScan).

## **Tissue histology**

Following microCT scanning, samples were decalcified in 0.34M EDTA (pH 8.0) solution at 4°C on an agitation tray for 30 days with solution changes every 2-3 days. Spines were cut axially at the level of the largest portion of the fusion mass. This typically coincided with a vertebral level of L5-6. Samples were embedded in paraffin and sectioned in the axial plane at a thickness of 5µm and were stained via Picro Sirius Red/Alcian Blue [159] to differentiate bone and cartilage. Adjacent sections were stained for tartrate-resistant acid phosphatase (TRAP) expression to highlight osteoclasts, and counterstained with light green. Histology was quantified using BioQuant Osteo software 2016 v16.1.60 (BioQuant Nashville, TN, USA). Representative regions of interest (ROI) were selected for each sample and volumes of target tissue were measured and expressed proportionately against the ROI. Outcomes included bone volume (BV/ROI), fibrous tissue volume (FV/ROI), cartilage volume (CV/ROI), marrow volume (MV/ROI) and Osteoclast number (OcN/ROI).

## **Statistical Analysis**

Statistical analysis was performed using GraphPad Prism 7 (GraphPad, La Jolla, USA) using one-way ANOVA with multiple comparisons. Statistical significant was calculated using a cut-off of  $\alpha < 0.05$ .

## RESULTS

### Fibrosis following spine fusion surgery is considerably increased in *Nf1<sup>null</sup>* spines

Spine fusion surgery was performed involving the implantation of collagen sponges containing rhBMP-2 to promote bone formation. All mice were of the *Nf1<sup>flx/flx</sup>* genotype, with groups featuring *Nf1<sup>null</sup>* tissue having AdCre virus co-administered during surgery via the implanted sponges. No morbidity or mortality was noted in any of the test animals up until the cull date of 21 days. At the experimental endpoint, all of the animals possessed a palpable fusion mass (Figure 4.2).

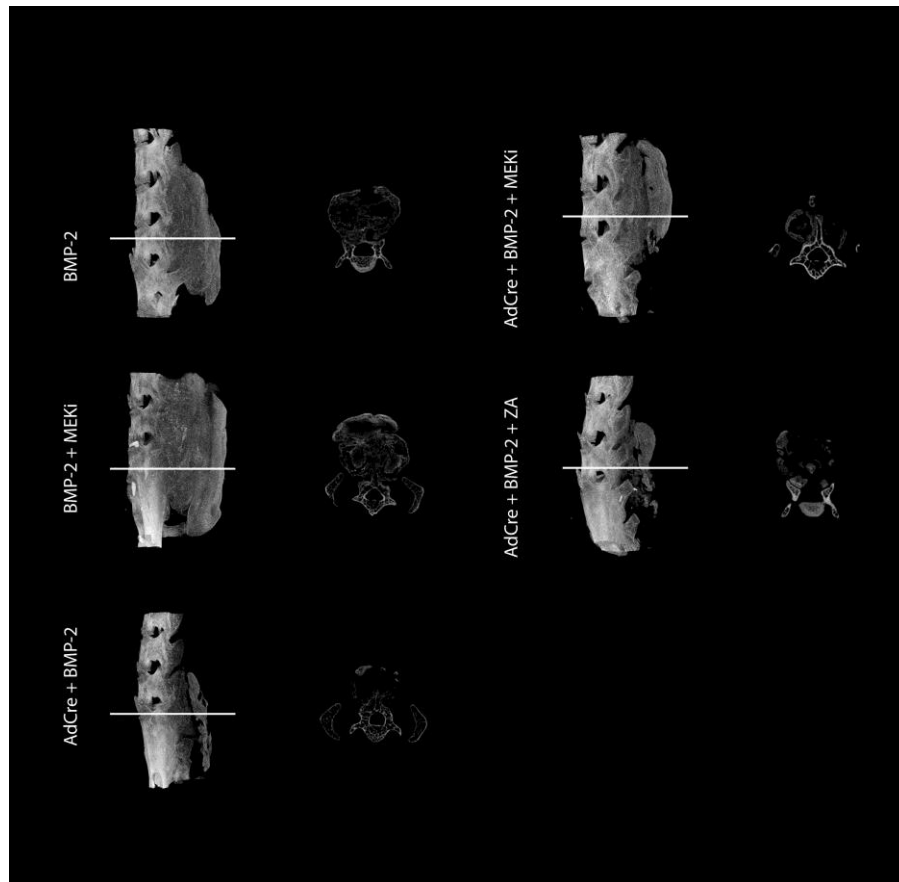


**Figure 4. 2** Spines were harvested from all animals 21 days post operatively. Representative reconstructions of the bony anatomy using uCT data demonstrates that AdCre treatment at the time of surgery results in a visually smaller and less robust fusion mass. Axial cross sections are taken from the midpoint of the fusion mass where it was the most substantial.



Fibrous tissue showed a significant increase in Nf1null spines compared to untreated controls, as quantified on histological sections (Nf1null +393%,  $P < 0.001$ ) (Figure 3B). Furthermore, fibrous tissue accounted for 48% of the fusion mass area in Nf1null spines, where it was only 10% of the fusion mass area in control spines. Nf1null spines showed a significant decrease in marrow space compared to controls (Nf1null -67%,  $P < 0.001$ )(Figure-4.3C).

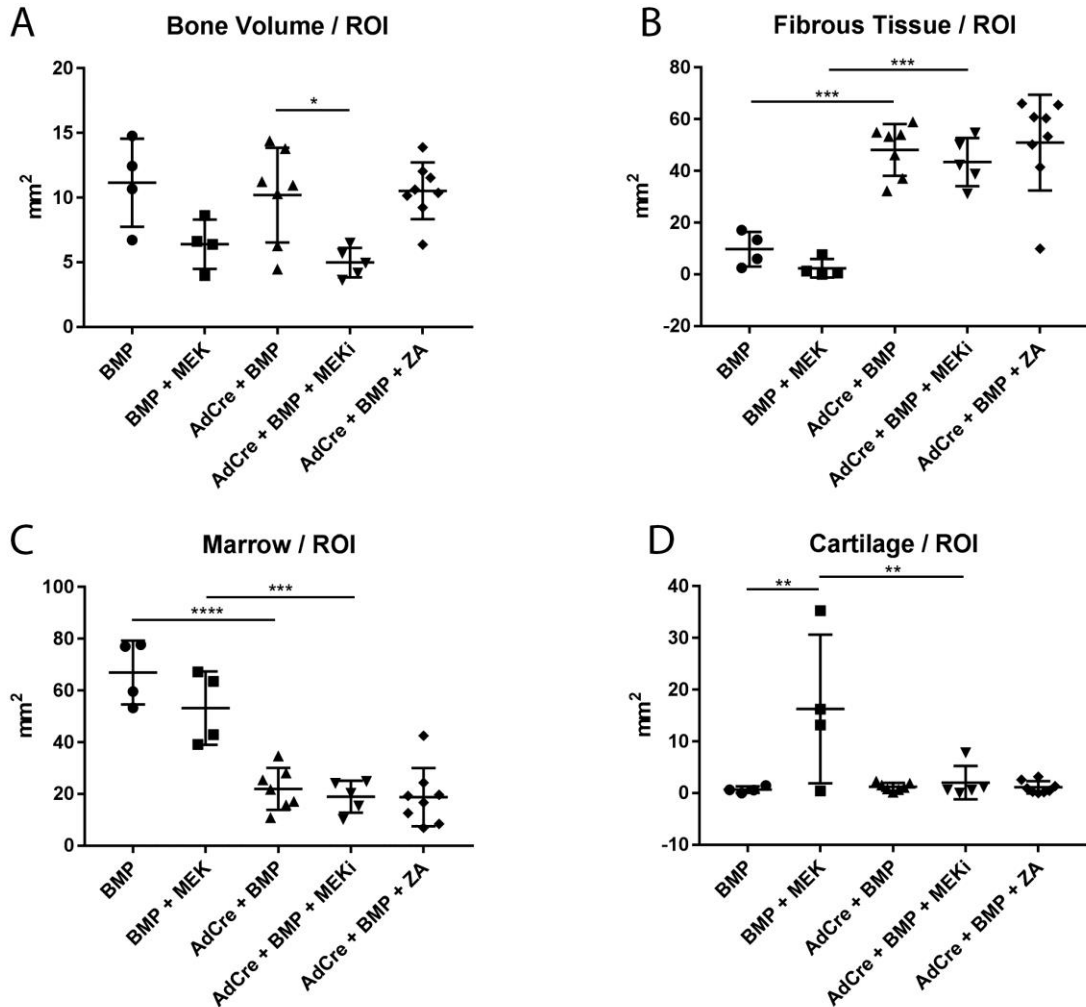


**Figure 4.3** Significant findings in uCT analysis of fusion mass volume were not reproduced by histological analysis (A).

Histology confirmed that a significant increase of fibrous tissue was found in the fusion masses of all AdCre treated mice (B) relative to mice that did not receive AdCre virus. This trend is mirrored by the relative proportion of marrow space measured in the fusion masses (C). All groups that receive treatment with AdCre virus showed significantly less marrow space than control groups suggesting that the volume of fibrous tissue seen in the AdCre groups is infiltrating the free marrow space of the fusion mass.

A significant increase in the relative proportion of cartilage in the fusion mass was noted only in the BMP-2 + MEKi group (D). This increase was dramatic (2304%) and was not reproduced in the AdCre + BMP-2 + MEKi group.

Qualitatively, *Nf1<sup>null</sup>* spines exhibited fibrous tissue invading the remnants of the collagen sponge. This was rarely observed in control spines, where this space was largely replaced by trabecular bone and marrow. Within the fibrous tissue of *Nf1<sup>null</sup>* spines, abundant multi-nucleated TRAP+ cells were seen (Figure 4.5), comparable to prior models of pseudarthrosis [159] and clinical biopsies [239].

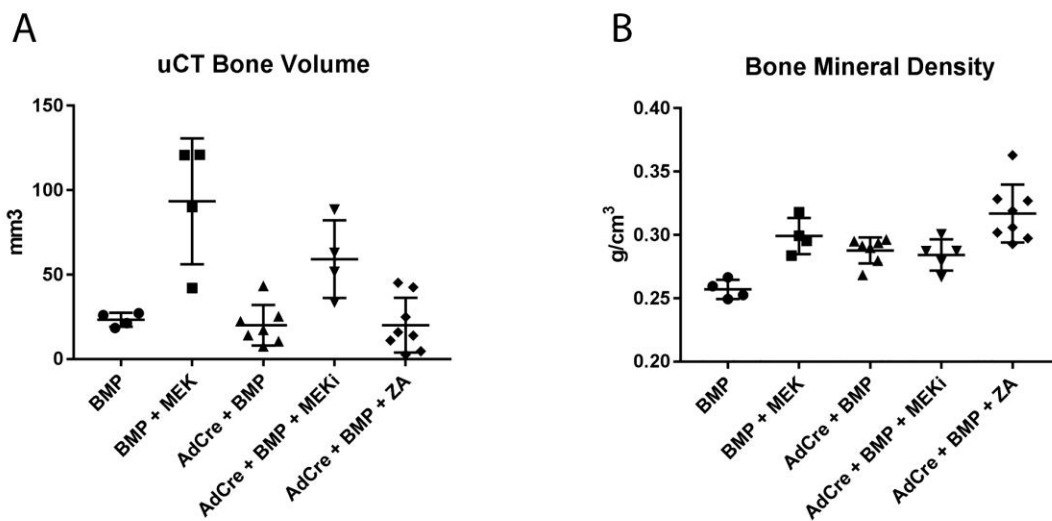


**Figure 4. 4** Bone volume of the fusion masses, as determined with uCT (A), demonstrated that in saline/BMP-2 co-dosed animals, treatment with the MEK inhibitor PD0325901 significantly increases the volume of bone formed in the fusion mass relative to controls (301%). A similar increase in the volume of the fusion mass was noted when mice cotreated at the time of surgery treatment with AdCre/BMP-2 were dosed with PD0325901 (194%). uCT analysis demonstrated that co-treatment with AdCre/BMP-2 yielded a fusion mass that was 14% smaller than saline treated mice , though this difference was not found to be significant. Treatment with the bisphosphonate Zoledronic Acid yielded a significant increase (10%) in the bone mineral density of the fusion mass (B) in mice treated with AdCre virus and BMP-2 at the time of surgery.



## **Bone volume and mineral density were increased by MEKi and bisphosphonate in *Nf1<sup>null</sup>* spines**

Bone volume, as quantified by microCT, showed no significant decrease in *Nf1<sup>null</sup>* spines relative to controls (*Nf1<sup>null</sup>* -14%,  $P=0.999$  n.s.) (Figure 4.5A). This contrasts with prior findings in the *Nf1<sup>+/-</sup>* spine fusion [226] and in *Nf1<sup>null</sup>* pseudarthrosis [159].

However, both adjunctive pharmacotherapeutic interventions impacted on the fusion mass, as quantitatively assessed by microCT (Figure 4.2, Figure 4.4). In *Nf1<sup>null</sup>* spines, MEKi dosing increased bone volume. Bone volume was increased by +194% ( $P<0.001$ ) compared to saline controls. Similarly, ZA treatment increase bone density in *Nf1<sup>null</sup>* spines by +10% ( $P<0.002$ ) relative to saline treated controls (Figure 4.5 B).

In wild type spines, MEKi dosing was also found increase bone volume independent of the *Nf1<sup>null</sup>* genotype (+301%,  $P<0.001$ ). Bone mineral density was also increased (+13%,  $P<0.05$ ) (Figure 4.5 B).

The number of TRAP+ cells in the tissue surrounding the collagen sponge remnant was assessed for both treatments. MEKi significantly reduced the number of TRAP+ cells found within the fibrous tissue adjacent to the collagen sponge remnant in wild type mice (-62%,  $P<0.03$ ), with an identical decrease noted in *Nf1<sup>null</sup>* spines (-62%,  $P=0.001$ ) (Figure 6). Similarly, ZA reduced the number of TRAP+ cells surrounding the collagen sponge remnant (-43%,  $P=0.054$ ) (Figure 4.6).

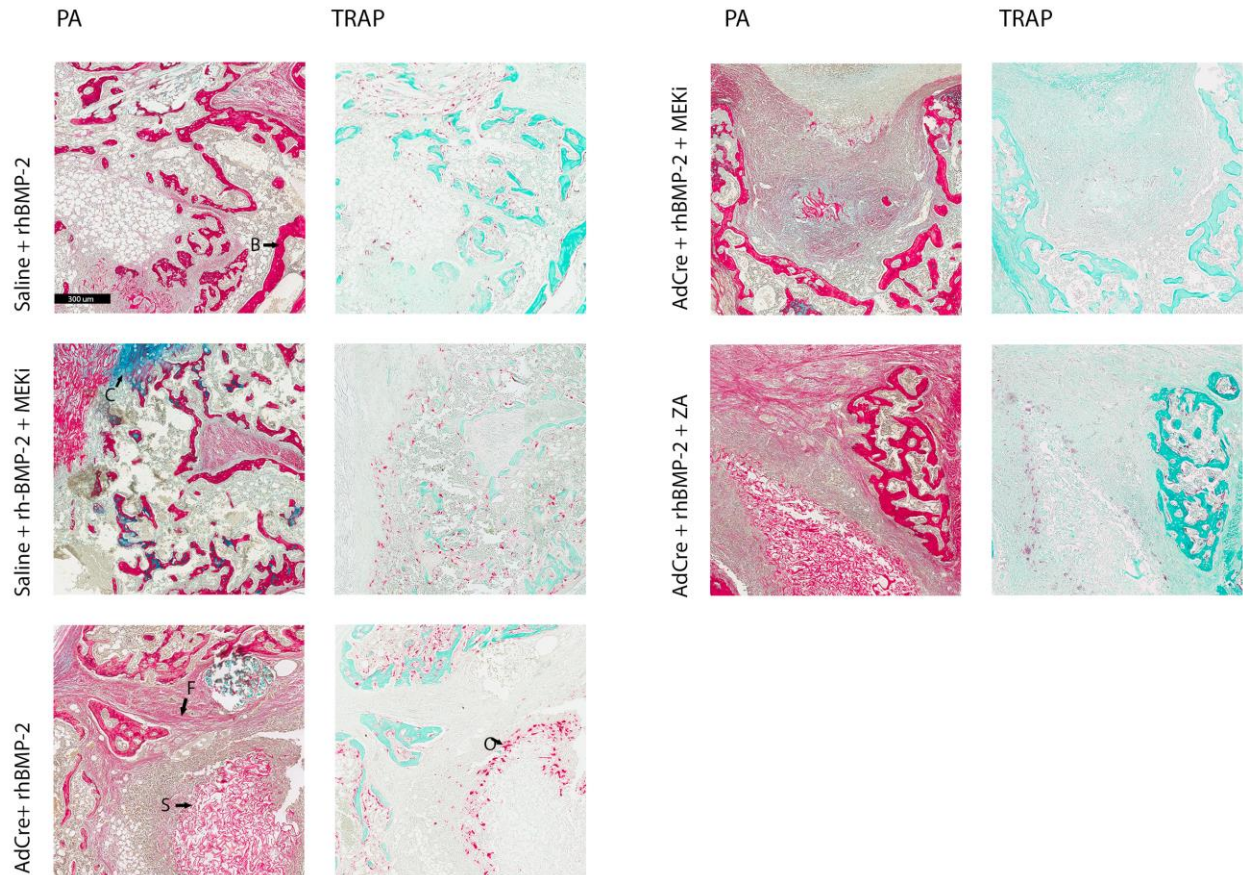


**Figure 4. 5** Histological sections were stained with a Picro Sirius Red and Alcian Blue protocol which stains bone (red) and cartilage (blue) and TRAP stain with Light Green counterstain. The bony fusion mass is seen to be more robust in animals that received saline/BMP-2 co-dosing at the time of surgery. These spines demonstrate a large bony fusion mass with uninterrupted cellular marrow space. In contrast, animals that received AdCre-BMP-2 co-dosing at the time of surgery have fusion masses that are less robust and show a varying degrees of marrow infiltration with a fibrous material (F). In mice which received AdCre treatment, a rim of TRAP positive cells (O) is seen between the remnant of the collagen sponge (S) and the fibrous tissue. Treatment with MEK inhibitor in the saline/BMP-2 group shows a large volume of cartilaginous tissue (C) in the fusion mass. This finding was not found to be significant nor was it reliably reproduced in the AdCre-BMP-2 group treated with MEK inhibitor.

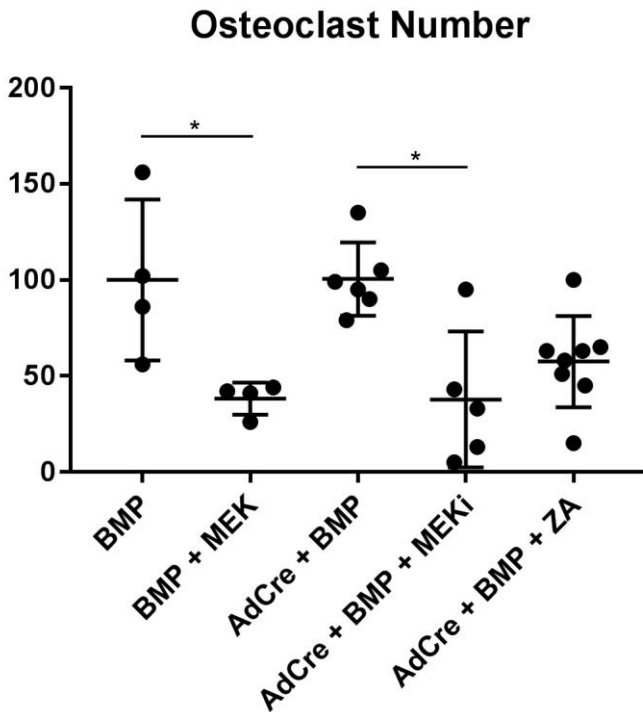


**Figure 4. 46** Quantification of the number of osteoclasts located at the perimeter of collagen sponge revealed that the MEK inhibitor PD0325901 and the bisphosphonate ZA led to an 81% and 43% reduction respectively. Animal groups which did not receive AdCre delivery did not generate a fusion mass with infiltration of marrow space by fibrous tissue and did not exhibit a significant volume of collagen sponge remaining at the 21 day cull. There was, therefore, no population of osteoclasts located remote from bone to be quantified.

### **MEKi and bisphosphonate treatments did not reduce fibrosis in *Nf1<sup>null</sup>* spines**

Neither MEKi nor bisphosphonate treatment had any significant effect on the amount of fibrous tissue (n.s.) (Figure 4.3 B).

In wild type spines, a considerable increase was seen in the relative proportion of cartilage in the fusion mass (23-fold) (Figure 4.3 D). This is consistent with prior reports

of retained cartilage with PD0325901 in mouse tibial fracture healing [240] . Notably, no change was seen in cartilage in the *Nf1<sup>null</sup>* spines.

## DISCUSSION

A variety of approaches have used to model the manifestations of NF1, and in this paper we describe a combination of genetic manipulation and surgery. Historically, conditional knockout mice have been used for several purposes: to model features of the NF1 heterozygous state that are not recapitulated in mice, and to model clinical manifestations associated with *NF1* double inactivation. In the case of bone, the traditional *Nf1<sup>+/-</sup>* mouse [241] was found to have normal systemic bone density [242], which contrasted with clinical findings of low bone mineral density in adults and children with NF1 [11,12]. However, there is no evidence that NF1 osteopenia is associated with double inactivation of the *NF1* gene. In contrast, tibial pseudarthrosis has been linked to localized double inactivation of NF1 [227]. This led to murine genetic models of bone-targeted conditional *Nf1* deletion, including osteocytes [243] and mesenchymal stem cells and osteoblasts [228, 229, 244, 245]. Notably, the first of these studies [244] produced mice with a scoliotic deformity, albeit not as severe as seen clinically. The differences in the models may be due to either genetics or differing biomechanical forces in quadrupeds [246].

While there have been unpublished accounts of NF1-/- tissue in dystrophic scoliosis (David A Stevenson, personal communications) there is no consensus data on the prevalence of double inactivation of the NF1 allele in dystrophic scoliosis. Nevertheless,

other groups have employed tissue specific double knockout models in order to recapitulate spinal deformity. [227] In this study, we used a cre-expressing adenovirus to drive deletion of *Nf1-flox* alleles in the spine. This is analogous to the technique we used to delete *Nf1* in fracture healing to model a clinical pseudarthrosis [240]. It has been previously validated by PCR and by fluorescent reporter that AdCre drives recombination in local tissues. Moreover, this method produced reduced bone healing, increased fibrous tissue at the fracture site, and aberrant multinucleated TRAP+ cells within the fibrous tissues. Notably, increased fibrous tissue and associated TRAP+ cells were recapitulated in this spine model. In particular, the fibrous tissue proliferation was a major complication in the spine model, with 47% of the mean fusion mass identified as mesenchymal or fibrous.

Treatment with AdCre virus yielded an insignificant difference in bone volume when compared to non-virus groups. Similar results were previously reported with this surgical approach in the *Nf1<sup>+/-</sup>* heterozygous line [226]. Unlike *Nf1<sup>+/-</sup>* and *Nf1<sup>null</sup>* fracture models [240], the spine fusion procedure employs a substantive dose of rhBMP-2 that stimulates considerable bone formation. We hypothesize that this dose of rhBMP-2 is sufficient to overcome the limited bone anabolism associated with NF1. However, in a clinical setting, rhBMP-2 doses may be insufficient to yield a robust bony fusion mass, and the high degree of fibrosis seen in this model may similarly impede successful union. Consequent to the strength of rhBMP-2, this model does not reliably produce failure of fusion, which is an intrinsic limitation of the system.

Considering the role of the Ras-MEK-ERK cascade in bone homeostasis, interruption of this pathway was expected to shift the equilibrium in favor of bone formation. In tibial

fracture models, MEK inhibitor PD0325901 increased the volume of mineralized bone in a fracture callus in wild type and *Nf1<sup>null</sup>* fractures [240]. In the spine, PD0325901 increased the bone volume in both wild type and *Nf1<sup>null</sup>* fusion masses, and by a similar amount. Due to the robust response to rhBMP-2 alone this increased bone with MEKi treatment did not impact on fusion rate, which was complete in all groups. In the case of wild type fractures, PD0325901 led to cartilage retention at the fracture site, possibly due to suppression of matrix metalloproteinase activity [159]. In the context of spine fusion, this was hypothesized to be of lesser importance, as the rhBMP-2 induced fusion mass was speculated to form with minimal cartilage. However, some increased cartilage retention was nonetheless seen in wild type spine fusions, indicating the rhBMP-2 stimulates both cartilage and bone formation at the spine. This was not a complication seen in the *Nf1<sup>null</sup>* fusion setting.

PD0325901 was found to decrease the number of osteoclasts (TRAP+) cells in the fusion mass of all mice. Prior reports have shown that *Nf1* deficiency can produce upregulations in osteopontin, Rankl, and Tgf $\beta$ , [235] which may be exploited by dosing with PD0325901. However, MEK inhibition yielded a global reduction in osteoclast number which was independent of *Nf1* activity which suggest it has anti-resorptive effects. The bisphosphonate ZA was used as a positive control in this system as it has reliably increased rhBMP-2 bone masses in *Nf1*-deficient fracture [15, 225] and spine fusion [226] models. The effect of ZA was chiefly to increase bone mineral density, rather than bone volume; this was the inverse of that seen with PD0325901 treatment. This suggests that the bisphosphonate produces more highly mineralized bone rather than augmenting the zone of effective rhBMP-2 action.

In terms of clinical translation, both PD0325901 and ZA both have potential utility in augmenting rhBMP-2 induced spine fusion. ZA is an established and well tolerated therapy for improving bone mineral density that has been used off-label for improving BMP-induced NF1 pseudarthrosis repair [203]. PD0325901 is currently undergoing clinical trials for treating NF1 tumors, however has not been applied in an orthopedic scenario. The use of MEK inhibitors in humans is reasonably new, but has been shown to be well tolerated in a cancer setting [247]. However, their side effect profile is significant with many patients exhibiting hematological dyscrasias (leucopenia, thrombocytopenia, and anemia) and symptoms such as rash, fatigue, diarrhea, epistaxis, and blurred vision.

## **CONCLUSIONS**

In this paper we describe a new model for spine fusion in individuals with NF1. While this model has a number of significant limitations, such as a lack of an initial scoliosis and an inability to produce a failure of fusion, key features such as extensive fibrotic and osteoclastic infiltration were recapitulated. Treatment with both ZA and the MEK inhibitor PD0325901 produced positive effects on the model, indicating that symptomatic and pathway-focused approaches both have potential as therapeutic modalities.

## **ACKNOWLEDGEMENTS**

This research was supported by funding from the National Health and Medical Research Council APP1003478, including salary support for Dr. Schindeler. Zoledronic acid used in the study was provided by Novartis AG. Prof Little has previously received research funding from Novartis AG for projects unrelated to this study.



#### (iv) Lineage tracking of mesenchymal and endothelial progenitors in BMP-induced bone formation

Mille Kolind <sup>1†</sup>, Justin D Bobyn <sup>1,2†</sup>, Brya G Matthews <sup>3</sup>, Kathy Mikulec <sup>1</sup>, Alastair Aiken <sup>1</sup>, David G Little <sup>1,2</sup>, Ivo Kalajzic <sup>3</sup>, Aaron Schindeler<sup>1,2§</sup>

<sup>1</sup> Centre for Children's Bone Health, The Children's Hospital at Westmead, Westmead, NSW, Australia

<sup>2</sup> Discipline of Paediatrics and Child Health, Faculty of Medicine, University of Sydney, Sydney, NSW, Australia

<sup>3</sup> Department of Reconstructive Sciences, School of Dental Medicine, UConn Health, Farmington, CT, USA

Published in *Bone*, December 2015

#### Abstract

To better understand the relative contributions of mesenchymal and endothelial progenitor cells to rhBMP-2 induced bone formation, we examined the distribution of lineage-labelled cells in *Tie2-Cre: Ai9* and  *$\alpha$ SMA-creERT2: Col2.3-GFP: Ai9* reporter mice. Established orthopedic models of ectopic bone formation in the hind limb and spine fusion were employed. *Tie2*-lineage cells were found extensively in the ectopic bone and spine fusion masses, but co-staining was only seen with tartrate-resistant acid phosphatase (TRAP) activity (osteoclasts) and CD31 immunohistochemistry (vascular endothelial cells), and not alkaline phosphatase (AP) activity (osteoblasts). To further confirm the lack of a functional contribution of *Tie2*-lineage cells to BMP-induced bone, we developed conditional knockout mice where *Tie2*-lineage cells are rendered null for

key bone transcription factor *osterix* (*Tie2-cre:Osx<sup>fx/fx</sup>* mice). Conditional knockout mice showed no difference in BMP-induced bone formation compared to littermate controls. Pulse labelling of mesenchymal cells with Tamoxifen in mice undergoing spine fusion revealed that  $\alpha$ SMA-lineage cells contributed to the osteoblastic lineage (*Col2.3-GFP*), but not to endothelial cells or osteoclast populations. These data indicate that the  $\alpha$ SMA<sup>+</sup> and *Tie2*<sup>+</sup> progenitor lineages make distinct cellular contributions to bone formation, angiogenesis, and resorption/remodeling.

## Research Highlights

- *Tie2*-lineage cells were tracked in BMP-2 induced bone using fluorescent report mice
- *Tie2*-lineage cells contributed to vessels and osteoclasts but not osteoblasts
- $\alpha$ SMA-lineage (mesenchymal) cells contributed to osteoblasts
- Conditional deletion of *Osx* in *Tie2*-lineage cells did not affect BMP-2 induced bone

## Introduction

Bone is a tissue that developmentally arises from the mesoderm. This is regulated by a variety of signals, however expression of the bone morphogenetic proteins (BMPs) are key factors that modulate this process [248]. Recombinant human BMPs (rhBMPs) are utilized in orthopedic medicine as potent inducers of new bone formation and are approved for the treatment of open fractures and non-unions [249]. When used clinically, cells are exposed to super-physiological concentrations of these factors, which has the potential to transform cells beyond those of the mesenchymal lineages.

In 2009 a study by Lounev *et al.* examined the contribution of different cell lineages to bone in a model of rhBMP-2 induced ectopic bone formation and in the Nse-BMP4 transgenic mouse [250]. A variety of transgenic mouse strains employing the Rosa26R (R26R) reporter were used to assess the relative input of *MyoD*-lineage, *Tie2*-lineage, and *SMMHC*-lineage cells. These were intended to reflect the contributions of myogenic, endothelial and mesenchymal progenitors respectively. Ectopic bone formed readily in muscle, a tissue that is often adjacent to bone and has been speculated to contain numerous types of cellular progenitors that could contribute to bone formation and repair [185, 251]

Lounev *et al.* reported that *MyoD*-lineage cells made a negligible contribution to rhBMP-2 induced ectopic bone formation [248]. This was later contrasted by studies showing greater *MyoD*-lineage contribution in a variant of the ectopic bone formation model featuring rhBMP-7 as well as increased tissue trauma [252]. Intriguingly, Lounev *et al.*

found that up to 50% of cells in the ectopic bone were of the *Tie2*-lineage. In a subsequent study, the group described a mechanism by which *Tie2*-lineage cells could undergo an endothelial-mesenchymal transition (EMT) to form osteoblasts [253]. While this study focused on describing the genetic disease *fibrodysplasia ossificans progressiva*, it was unclear whether EMT could also occur when endothelial cells were exposed to high concentrations of rhBMPs.

The potential of endothelial *Tie2*-lineage cells to contribute to bone repair has been further implied by a range of cell transplantation studies. Purified endothelial progenitor cells (EPCs) have been repeatedly demonstrated to enhance orthopedic repair [254-258], although the precise mechanism for this is unclear. EPCs have been shown to enhance angiogenesis, potentially by secretion of pro-angiogenic growth factors [259], or by direct contribution to new vessels. Transplanted EPCs have also been shown to enhance tissue mineralization [253], raising the possibility of a direct contribution of these cells to bone repair.

In 2012 Wosczyzna *et al.* published a report indicating that the *Tie2*-lineage cells included multiple sub-populations of cells, some capable and some incapable of contributing to rhBMP-2 induced cartilage and bone formation [260]. The populations that formed cartilage and bone were not of endothelial origin, suggesting that EMT was not the underlying mechanism in this model. Both the Lounev and Wosczyzna studies utilized a *Tie2*-cre line that demarks endothelial and hematopoietic, progenitors as well as a subset of mesenchymal-like progenitors [261].

In this study we report the contribution of endothelial cells to rhBMP-2 induced ectopic bone formation and spine fusion using an alternative *Tie2*-cre mouse, which shows

greater specificity for the endothelial lineages [262, 263]. These cell tracking studies employ a Cre-dependent fluorescent tdTomato reporter that allows for co-labeling with chondrocyte, osteoblastic, osteoclastic, and vascular markers [264]. Conditional knockout mouse models were also employed where *Tie2*-lineage cells selectively inactivated the key osteogenic transcription factor *osterix*. This approach allowed for the functional assessment of the contribution of cells of the *Tie2*-lineage to new bone formation. To complement these experiments we examined the contribution of mesenchymal progenitors using mice with an inducible  $\alpha$ SMA-creERT2 transgene. Prior studies have shown that this cell lineage directly contributes to bone formation and repair [169, 265-267].

## **Materials & Methods**

### ***Mouse lines and Genotyping***

The *Ai9* reporter line (B6.Cg-Gt(ROSA)26Sortm9(CAG-tdTomato)Hze/J) was purchased from Jackson Laboratories[262]. The *Tie2-cre* line (B6.Cg-Tg(Tek-cre)12Flv/J) was sourced from the Garvan Institute for Medical Research with permission from the original laboratory [268]. The *Osx*<sup>fx/fx</sup> line was sourced from Benoit de Crombrugge (MD Anderson Cancer Center, Houston, TX, USA) [258]. The *Tie2-cre* × *Ai9* line was generated in-house by cross breeding and showed no adverse phenotype; the line specifically labels *Tie2*-lineage with a fluorescent tdTomato reporter. The *Tie2-cre* × *Osx*<sup>fx/fx</sup> line was generated by crossing for two generations to create homozygous conditional double knockout mice; in this line there is targeted disruption of the key

osteoblastic gene *osterix* (*Osx*) in all cells of the *Tie2*-lineage. Mice were genotyped from ear biopsies using real time PCR with specific probes designed for each gene (Transnetyx, Cordova, TN, USA). Experiments using the *Tie2-cre* cross strains were approved by the CHW/CMRI Animal Ethics Committee (Protocol K248, K303). All strains were on the C57BL6/J background, and hemizygous strains were maintained on wild type mice purchased from the Animal Resources Centre (ARC, Perth, Australia).

*αSMA-creERT2* (smooth muscle  $\alpha$ -actin promoter)  $\times$  *Ai9* mice, which enable labeling of mesenchymal progenitors [169, 265] that also incorporated a GFP transgene under the control of the upstream 2.3kb region of the *Col1a1* promoter (*Col2.3-GFP* transgene) to label osteoblasts [269] were sourced from in-house colonies at the University of Connecticut (Farmington, CT, USA). Experiments using these mice were approved by the UConn animal ethics committees.

### ***Surgical models***

Implants were manufactured by adding 20  $\mu$ l sterile saline containing 5 $\mu$ g recombinant human BMP-2 (Medronic Australasia, North Ryde, Australia) onto collagen-hydroxyapatite sponge prior to surgery. For the ectopic bone formation model, uniform discs manufactured using a surgical tissue punch were surgically implanted into the hind limbs of mice using published methods [202]. For the spine fusion model, twin porous collagen sponges (Medronic Australasia) were inserted parallel to the vertebrae as previously described [204]. All mice were aged 8-12 weeks. Anesthesia was induced with inhaled isoflurane (hind limb model) or using Ketamine/Xylazine (35mg/kg; 5mg/kg) (spine fusion model). Buprenorphine (0.05–0.1 mg/kg) was administered

subcutaneously (s.c.) preoperatively and every 12 hours as required for pain management. Post-surgery saline was given s.c. to prevent dehydration. Mice of the  *$\alpha$ SMA-creERT2  $\times$  Ai9* cross received tamoxifen at a dose of 75 mg/kg on the day of surgery to induce lineage labelling. Mice were euthanized at 7, 14, or 21 days (ectopic bone) or 2, 10, or 17 days (spine fusion) for radiological and/or histological analyses.

### ***Radiological imaging***

The formation of rhBMP-2 induced bone was confirmed and visualized by digital X-ray (25 kV, 2x magnification; Faxitron X-ray Corp, Illinois, USA). For studies where ectopic bone was quantified, samples were scanned by micro-computed tomography (microCT) using a SkyScan 1174 compact microCT scanner (Kontich, Belgium) at a pixel resolution of 14.8  $\mu$ m. All samples were scanned in 70% ethanol, using a 0.5 mm aluminum filter, 50 kV X-ray tube voltage, and 800  $\mu$ A tube electric current. A global threshold to define bone tissue in pellets was set at a mineral density of 0.3 g/cm<sup>3</sup>. Images were reconstructed using NRecon, version 1.6.1.7 (SkyScan), and analyzed using CTAnalyser software, version 1.11.8.0 (SkyScan).

### ***Immunofluorescence and Microscopy***

The endogenous fluorescent signal from the tdTomato reporter strain was captured using either an epi-fluorescent microscope or a Leica TCS SP5 confocal laser scanning microscope. The sections were cover-slipped and the intrinsic fluorescent signal imaged directly. ELF97 Phosphatase Substrate (Molecular Probes) was used to detect alkaline

phosphatase (AP) and tartrate-resistant acidic phosphatase (TRAP). AP assay was done according to the manufactures instructions. For TRAP: The classical TRAP buffer (110 mM acetate buffer, pH 5.2, 1.1 mM sodium nitrite, 7.4 mM tartrate) was used followed by 200 $\mu$ M concentration of ELF97 incubation for 5-min. Slides were washed with an EDTA containing wash buffer. The fluorescence was visualized with a DAPI/Hoechst longpass filter set.

For examining co-labelling between endogenous tdTomato signal and immunofluorescent staining for lineage markers, the following methods were used. Slides were rehydrated in PBS for 20 min and treated with 0.5% Triton X-100 for 20 min. The sections were blocked in 10% goat serum PBS for 1 h at room temperature prior to incubation with a primary antibody (SOX9, Millipore AB5535; CD31, BD Pharmigen MEC13.3) in blocking buffer overnight at 4°C. After washing the sections were incubated with Alexa-Fluor-647 conjugated secondary antibody (Molecular Probes diluted in PBS. Tissue was counter stained with 200 ng/ml 4',6-diamidino-2-phenylindole (DAPI, molecular probes) for 1 min and washed in PBS and mounted in Aqueous Mounting Medium (DAKO). Images were captured using an epi-fluorescent microscope with appropriate filters or using the Leica TCS SP5 confocal laser scanning microscope

### ***Statistical analyses***

Statistical analysis of microCT data was conducted with non-parametric testing as amount of bone formed by these assays has not been determined to follow a normal distribution. Significance differences in bone volume were determined using a Mann Whitney U test with a cutoff of  $\alpha < 0.05$  (Graphpad Prism, La Jolla, CA, USA).



## Results

### ***Tie2*-lineage cells localize to rhBMP-2 induced bone**

To assess the contribution of *Tie2*-lineage cells to newly formed bone we performed a model of rhBMP-2 induced ectopic bone formation in *Tie2-cre: Ai9* reporter mice. Ectopic bone was present at 2 weeks by X-ray and specimens were analyzed by fluorescent imaging. The muscle adjacent to the ectopic bone had labelling with the appearance of microvessels, and labelling was absent from the muscle fibers (Figure 5.1 A). The ectopic bone showed abundant staining suggestive of a significant involvement of *Tie2*-lineage cells in the bone formation process. Closer examination revealed an abundance of *Tie2*-lineage cells on the bone surfaces (Figure 5.1 B).

Examination of native long bones revealed negligible staining in the cortical bone, although again vessel-like staining was seen in the bone marrow space (Figure 5.1 C).

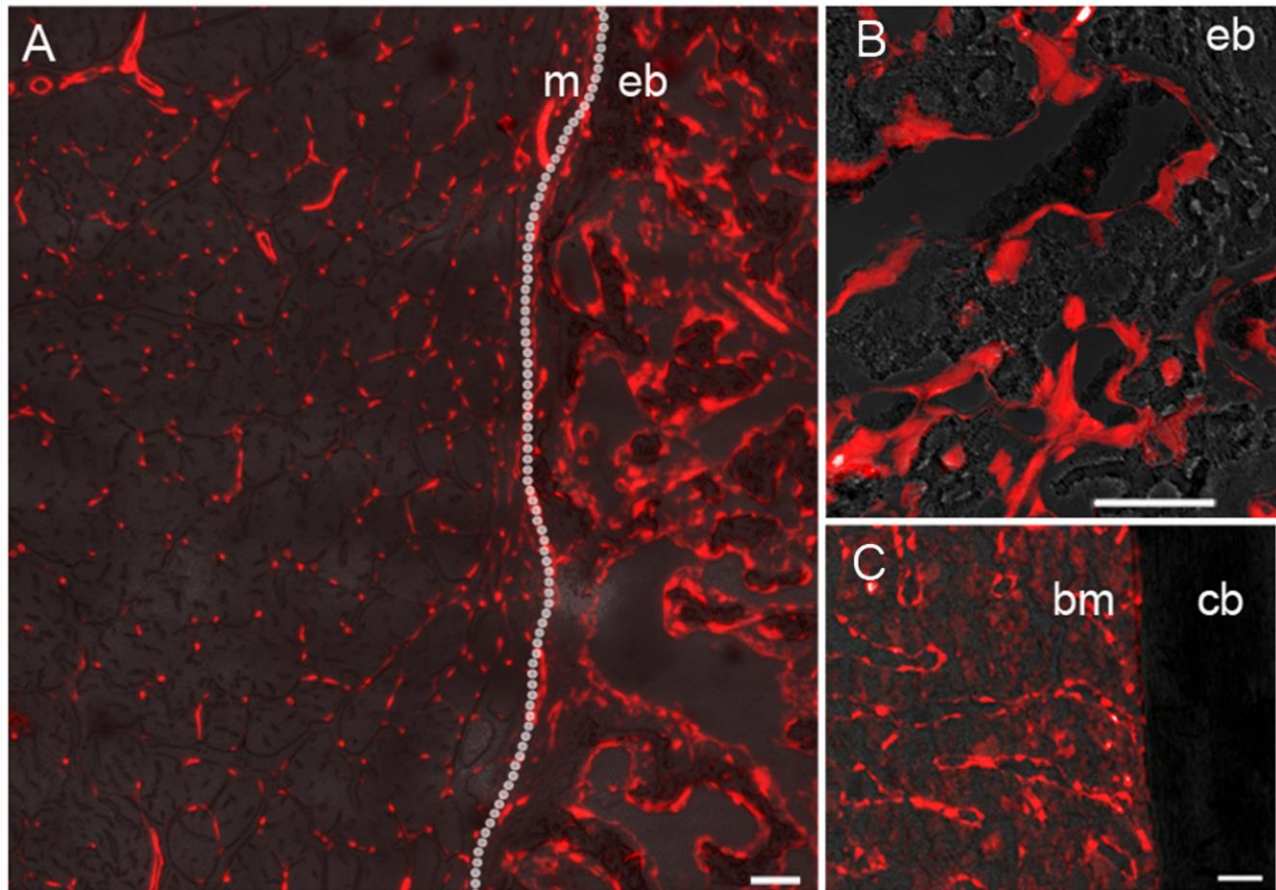


**Figure 5. 1** Confocal fluorescent images of Tie2-lineage cells (tdTomato, red) in rhBMP-2 induced muscle, native bone, bone marrow, and rhBMP-2 induced ectopic bone. Images are shown at the muscle/ectopic bone interface (A) within an ectopic bone nodule (B), and within the native bone of the femur (C). Text labels, m = muscle, eb = ectopic bone, bm = bone marrow, cb = cortical bone. Scale bar = 50  $\mu$ m.

***Tie2*-lineage cells contribute to the vasculature and to resorbing osteoclasts in native and rhBMP-2 induced bone**

Specimens from d7 were analyzed to look at the contribution of *Tie2*-lineage cells to early progenitors. Co-staining for endothelial cell marker CD31 revealed that all new vessels were derived from *Tie2*-lineage cells (Figure 5.2A). Some cells that were of the *Tie2*-lineage that did not co-express CD31 were present, often near or adjacent to

vessels. Co-staining for cartilage marker Sox9 showed no overlap between or co-staining between chondrocytes and *Tie2*-lineage cells (Figure 5.2 B).

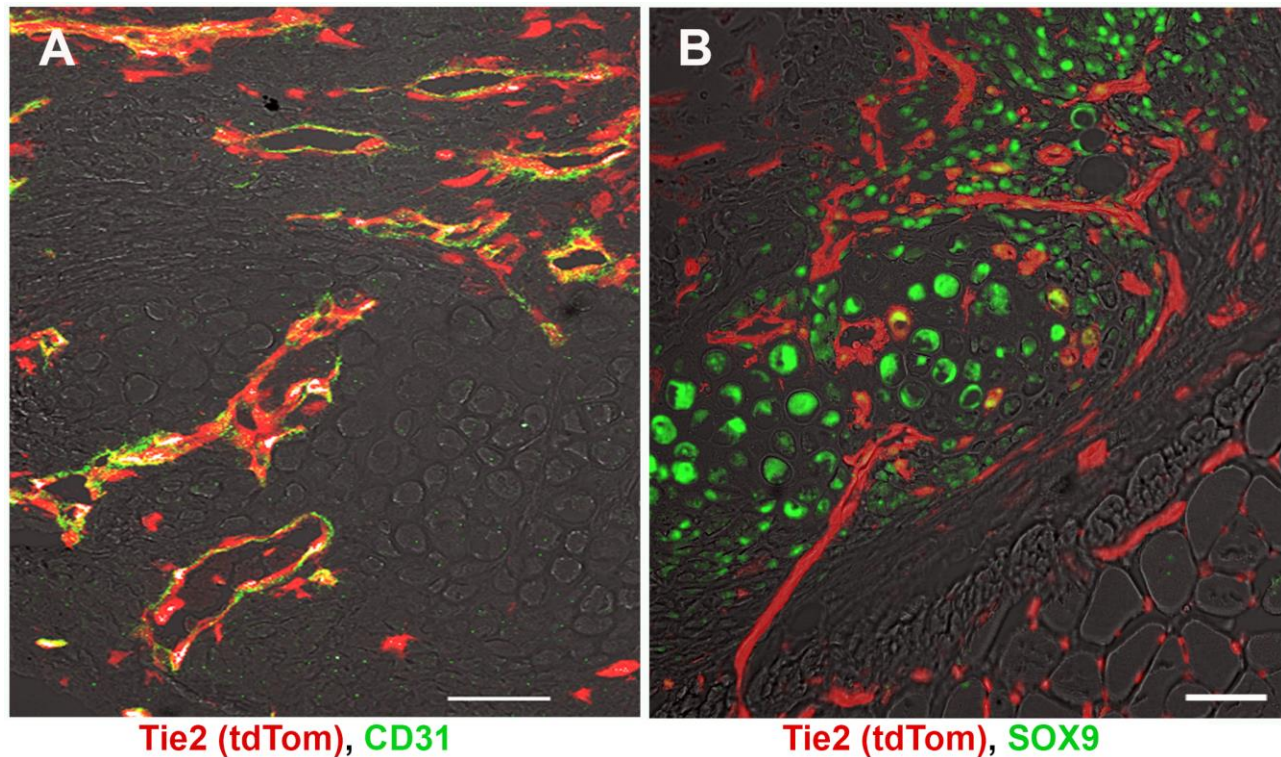


**Figure 5. 2** Fluorescent images of ectopic bone showing *Tie2*-lineage cells (tdTomato) overlaid with vascular marker CD31 (A) or chondrocyte marker SOX9 (B). *Tie2*-lineage cells were found to demark the new blood vessels in the ectopic bone but not cartilage islands. Scale bar = 50  $\mu\text{m}$

Fluorescent histochemical staining was performed on d14 sections for the osteoclast marker TRAP and the osteoblast marker AP. TRAP<sup>+</sup> cells co-labelled with tdTomato, indicating they originated from the *Tie2*-lineage (Figure 5.3 A-B). In contrast, there was no overlap between tdTomato and AP (Figure 5.3 C-D).



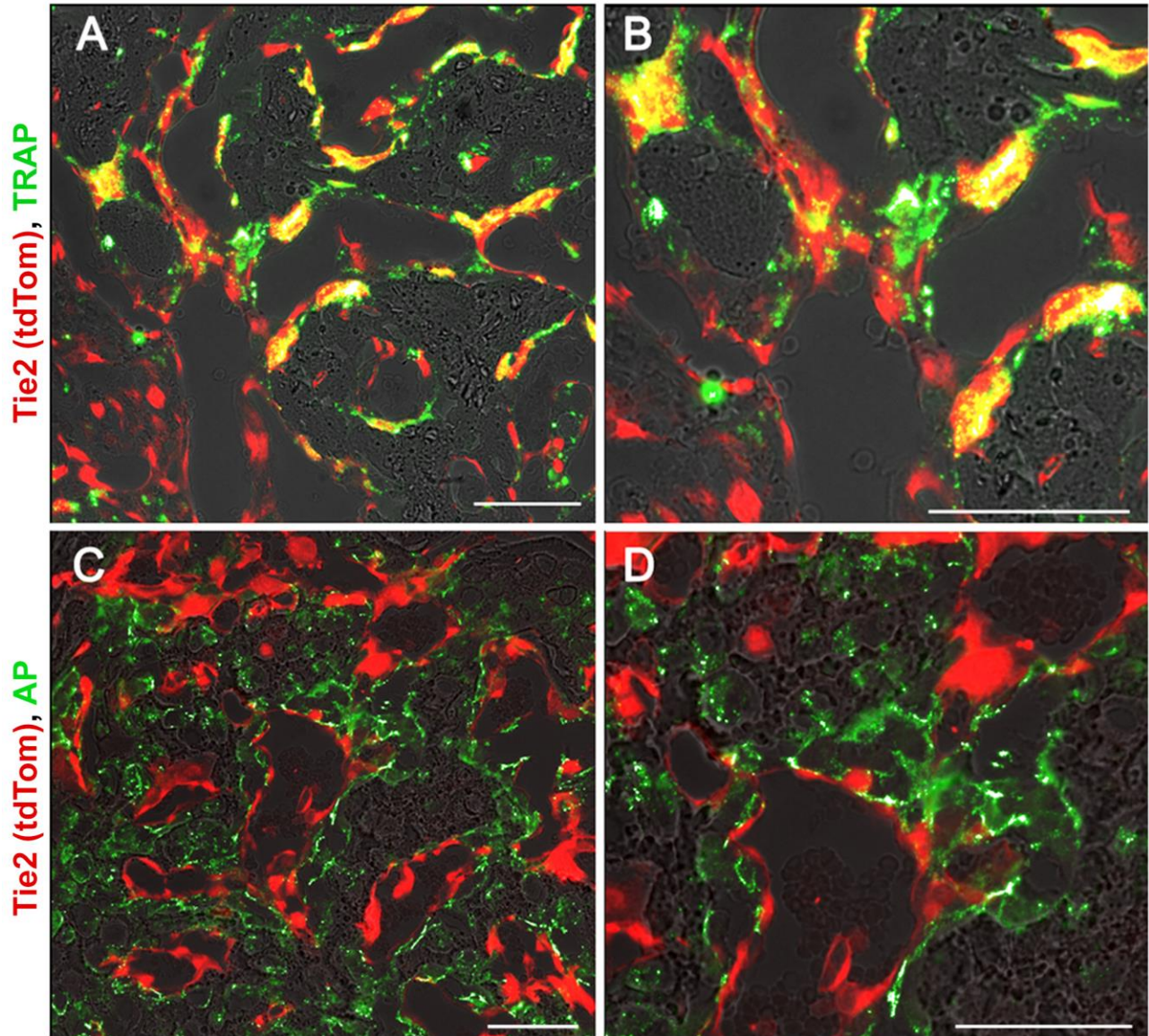


**Figure 5. 3** Fluorescent images of ectopic bone showing *Tie2*-lineage cells (tdTomato) overlaid with tartrate-resistant acid phosphatase/TRAP activity stain (ELF97, green) to label osteoclasts (A, zoom in B). No overlap was seen between *Tie2*-lineage cells with an alkaline phosphatase/AP activity stain (ELF97) to label osteoblasts (C, zoom in D). Scale bar = 50  $\mu\text{m}$ .

## **Targeted deletion of *osterix* in *Tie2*-lineage cells does not affect rhBMP-2 induced bone formation**

To further examine the functional importance of *Tie2*-lineage cells in this model, experiments were performed in *Tie2-cre:Osx<sup>fx/fx</sup>* mice. *Osx* has been previously shown to be essential for the osteogenic differentiation of osteochondral progenitors [270] and thus this line could be used to assess whether *Tie2*-lineage cells make a significant contribution to osteoblastic bone formation. *Tie2-cre:Osx<sup>fx/fx</sup>* mice underwent 12 weeks of assessment for health and welfare and no adverse phenotype was found. This included no defects in skeletogenesis or skeletal health (data not shown), implying that the contribution *Tie2*-lineage cells to osteoblasts is not developmentally important.

Next, rhBMP-2 induced bone nodules at 21d were imaged by X-ray (Figure 5.4A-B) and microCT reconstruction (Figure 5.4C-D) from control littermates lacking the *Tie2-cre* transgene (*Tie2-cre<sup>-/-</sup>*; *Osx<sup>fx/fx</sup>*, *Osx<sup>fx/+</sup>*). Ectopic nodules had a standard appearance by tissue histology, with a cortical-like shell and an interior marrow-like space with trabecular-like bony elements (Figure 5.4E). Quantification by microCT confirmed that there was no significant difference in bone formation between the genotypes (Figure 5.4F).

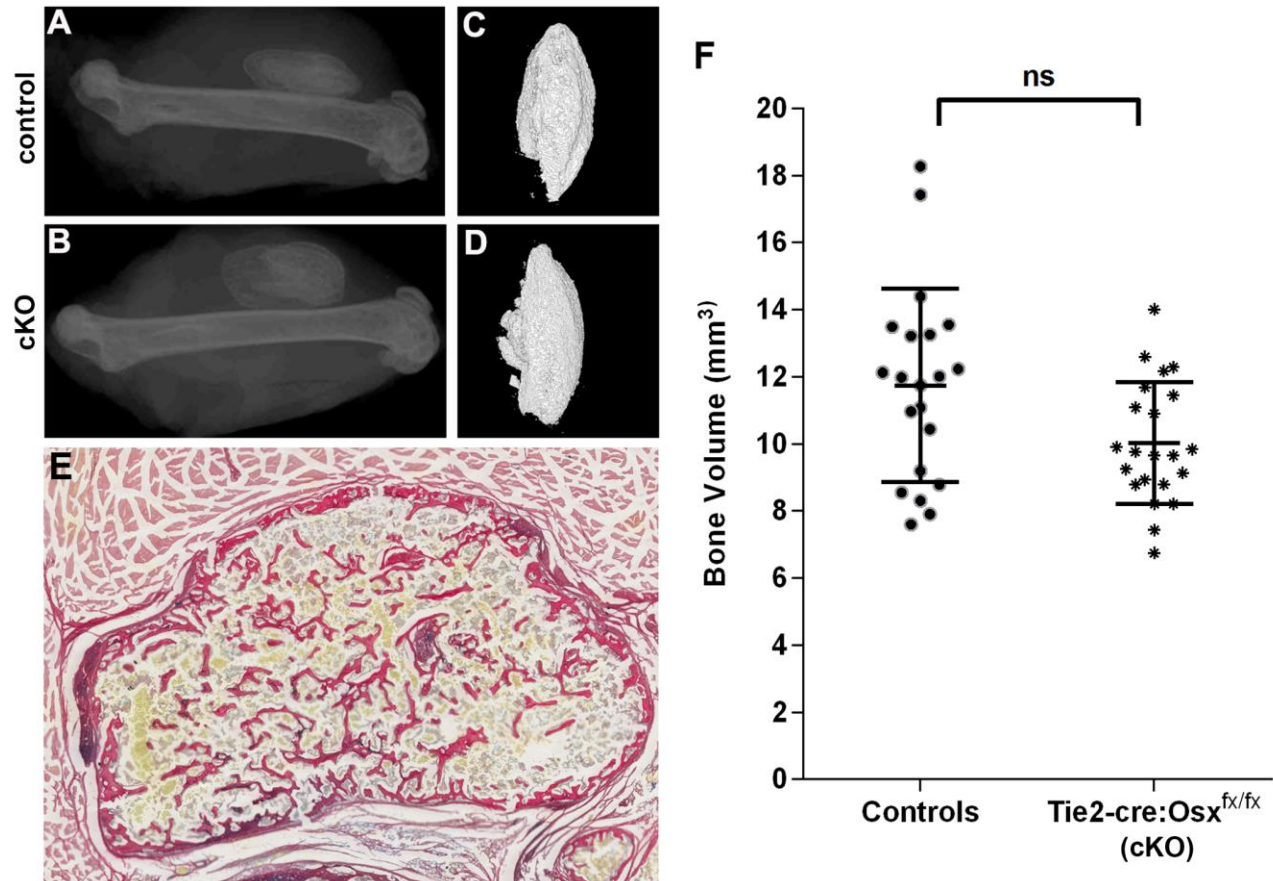


**Figure 5.4** rhBMP-2 induced ectopic bone formation in *Tie2-cre-Osx<sup>fx/fx</sup>* mice and littermate controls. Representative XRs (A, B) and microCT reconstructions (C, D) are shown for the specimens corresponding to the median bone volume for each group (A, C = littermate controls, B, D = *Tie2-cre-Osx<sup>fx/fx</sup>* mice). The bone formed in all cases showed a cortical shell with some trabecular-like elements visualized using Picro Sirius Red/Alcian Blue staining (E). MicroCT quantification revealed no significant difference in bone volume of ectopic rhBMP-2 induced bone with deletion of the *Osx* gene in *Tie2*-lineage cells (F).

### Contribution of *Tie2*-lineage cells and $\alpha$ SMA-lineage cells in an rhBMP-2 induced spine fusion model

As an alternative model of rhBMP-2 induced bone formation, fusion was induced in the mouse spine as a location that would have a capacity for contribution by soft tissue progenitors and endogenous osteoprogenitors. Fusion occurred rapidly after the

surgical procedure, with new bone bridging the vertebral processes apparent within 10 days (Figure 5.5).

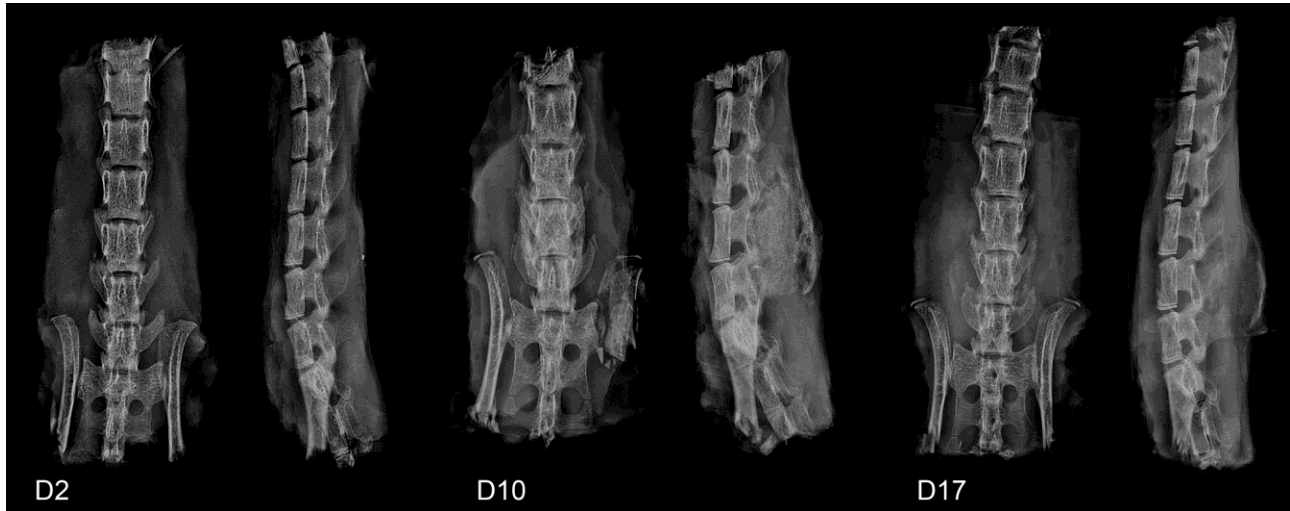


**Figure 5. 5** X-ray (XR) images showing the progression of rhBMP-2 induced spine fusion. After implantation of collagen sponges loaded with rhBMP-2, no mineralized bone was seen at D2, but a fusion mass was apparent in all specimens by D10 and D17. Anterior-posterior and lateral views are shown for all time points.

In the *Tie2-cre: Ai9* reporter mice, comparable results were seen to the hind limb rhBMP-2 implantation model. Samples obtained from mice culled at day 2 post-operatively had not yet formed any new bone overlying the vertebrae and no significant tdTomato staining was noted in these areas. However, specimens from this time point showed a pattern of co-localization of tdTomato and TRAP<sup>+</sup> cells in the original cortical bone of the lumbar spinous process (Supp Figure 5.1). Abundant staining tdTomato was noted in the vertebral fusion masses of *Tie2-cre: Ai9* mice by day 10. Co-staining with TRAP revealed that all TRAP<sup>+</sup> cells co-labelled with endogenous tdTomato (Supp Figure 5.1). Additionally, it was noted that the majority of cells that expressed tdTomato were co-labelled with TRAP<sup>+</sup> cells, suggesting that the majority of cells in the fusion of a *Tie-2-*

lineage contribute to the cellular milieu by way of osteoclastogenesis. CD31 staining was also found to significantly overlap with tdTomato expression (Supp Figure 5.2).

The spine fusion model was also performed in the  *$\alpha$ SMA-creERT2:Col2.3-GFP:Ai9* mouse line to allow for the tracking of mesenchymal progenitors after tamoxifen induction (tdTomato) while co-labeling osteoblasts (GFP). Tamoxifen injection was administered at the time of surgery and the contribution of  *$\alpha$ SMA*-lineage progenitors was assessed at day 2, 10 and 17 (Figure 5.6). As with the *Tie2-cre:Ai9* reporter mice, at the 2 day time point, no contribution by tdTomato cells was seen. However by day 10 and day 17, a robust fluorescent signal was present throughout the fusion mass. All osteoblastic cells expressing *Col2.3-GFP* were found to be tdTomato+ and thus originate from the  *$\alpha$ SMA*-lineage. A greater proportion of the tdTomato+ expressed the *Col2.3-GFP* marker over time, and by day 17 a significant proportion of the  *$\alpha$ SMA* cells labelled at surgery expressed the osteoblastic marker (Figure 5.6). In contrast,  *$\alpha$ SMA*-lineage cells were found to not co-localize with the TRAP activity stain. Control animals not receiving tamoxifen showed no leakiness of the tdTomato reporter at any time point (example at d17, Supp Fig 3).



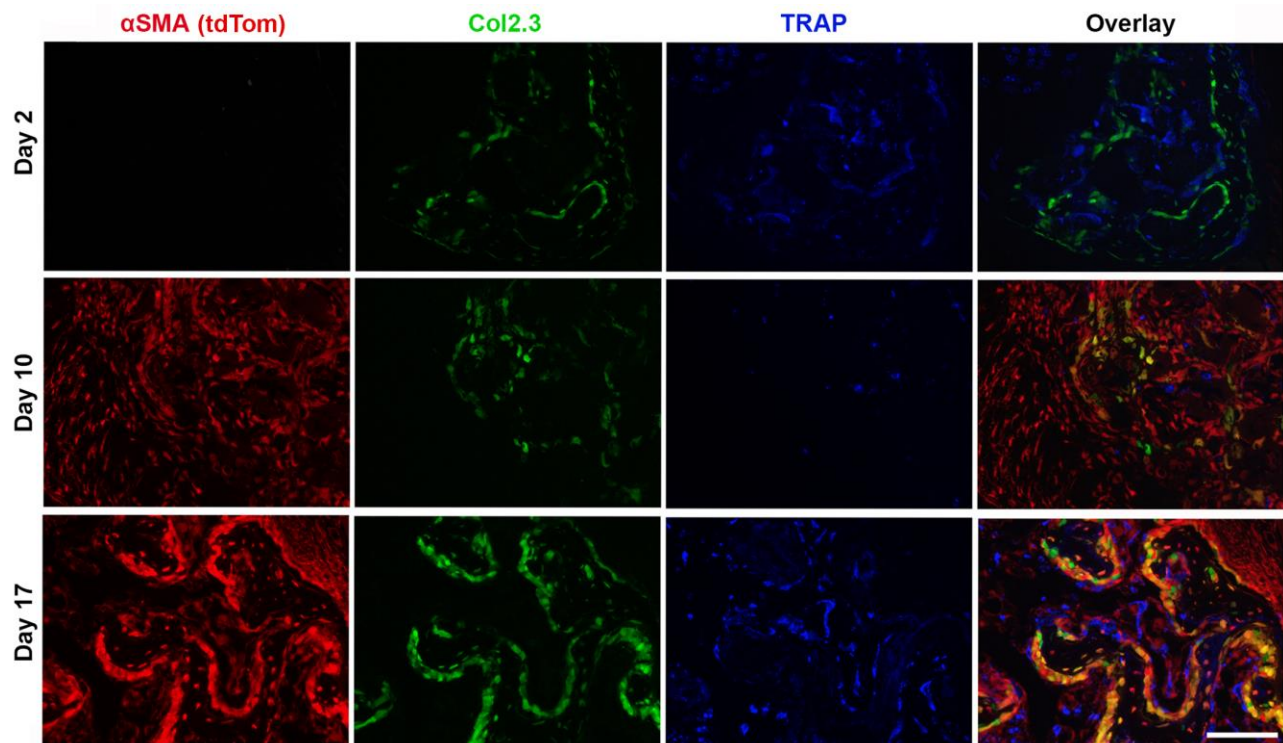


**Figure 5. 6** Fluorescent images of spine fusion bone masses with co-labeling for  $\alpha$ SMA-lineage cells expressing tdTomato (red), Col2.3-GFP (green), and a TRAP activity stain (blue). Based on the image overlays, Col2.3-GFP+ cells are demonstrated to originate from  $\alpha$ SMA-lineage progenitors. In contrast, no overlap was seen with TRAP+ cells previously shown to originate from the *Tie2*-lineage. Scale bar = 50  $\mu$ m.

## Discussion

In orthopedic medicine, the cell populations that give rise to osteoblasts that generate new bone remain poorly defined. It is generally accepted that cells from the periosteum can play a major role in fracture repair, particularly in closed fractures where the periosteum is largely intact [271]. Conversely, in animal models and clinical practice periosteal stripping is associated with impairment of bone repair [272]. Mesenchymal

cells from the marrow compartment have been shown to readily differentiate into an osteogenic lineage *in vitro*, but the importance of these cells in bone repair is less well defined [204, 273, 274]. However, even in fractures with intramedullary nailing, poor marrow availability and significant periosteal stripping, healing can still eventuate. This indirectly evidences a potential contribution by progenitors from non-osseous tissues to new bone formation.

In this study we have aimed to address the potential transdifferentiation of vascular endothelial progenitors under conditions featuring high concentrations of exogenously supplied rhBMP-2. Endothelial to mesenchymal transitions have emerged as a occurring in range of tissue processes, particularly in development and in tissue fibrosis [275]. It has also been linked to genetic disease, specifically the abnormal ossification seen in *fibrodysplasia ossificans progressiva* and mutations in the BMP-receptor *ACVR1* [253]. This led us to speculate that even if *Tie2*-lineage cells did not make a significant contribution to normal bone formation or repair, excessive BMP signaling could lead to transition of endothelial progenitors into osteoblasts.

Nevertheless, these data comprehensively demonstrate that *Tie2*-lineage cells contribute to the developing vascular network and not osteoblasts. Prior studies showing extensive *Tie2*-lineage reporter staining in the bone are likely to be confounded by two issues. Firstly, *Tie2* is expressed by hematopoietic lineages as well as endothelial cells, which give rise to osteoclasts. The co-staining of the osteoclastic marker TRAP with tdTomato+ cells reinforces the concept that the cells seen within the bone in prior studies may have been osteoclasts. Prior studies using histochemical markers such as LacZ did not allow for co-staining with other lineage markers [191].

Secondly, other studies demarking cells of the *Tie2*-lineage in bone utilized an alternative transgenic mouse line that showed a wider pattern of distribution including mesenchymal cells [261]. In contrast, our *Tie2-cre: Ai9* mouse line demonstrates a more restrictive pattern of expression [262, 263], which may explain the lack of contribution to mesenchymal elements. This highlights a challenge associated with lineage tracking studies, which can be the non-specificity and/or leakiness of Cre mouse models [276]. Thus caution must be made with the interpretation of all tracking studies.

The findings of a lack of contribution of *Tie2*-lineage cells to osteoblasts was found in both the hind limb rhBMP-2 induced ectopic bone formation model and in the rhBMP-2 induced spine fusion model. In the latter model, all osteoblasts (marked with the *Col2.3-GFP* transgene) were observed to originate from  $\alpha$ SMA-lineage lineage progenitors. This mouse, which enables the inducible labelling of progenitors just prior to intervention, has proven a valuable tool for identifying physiological processes where the primary cellular contribution is mesenchymal [169, 265, 267].

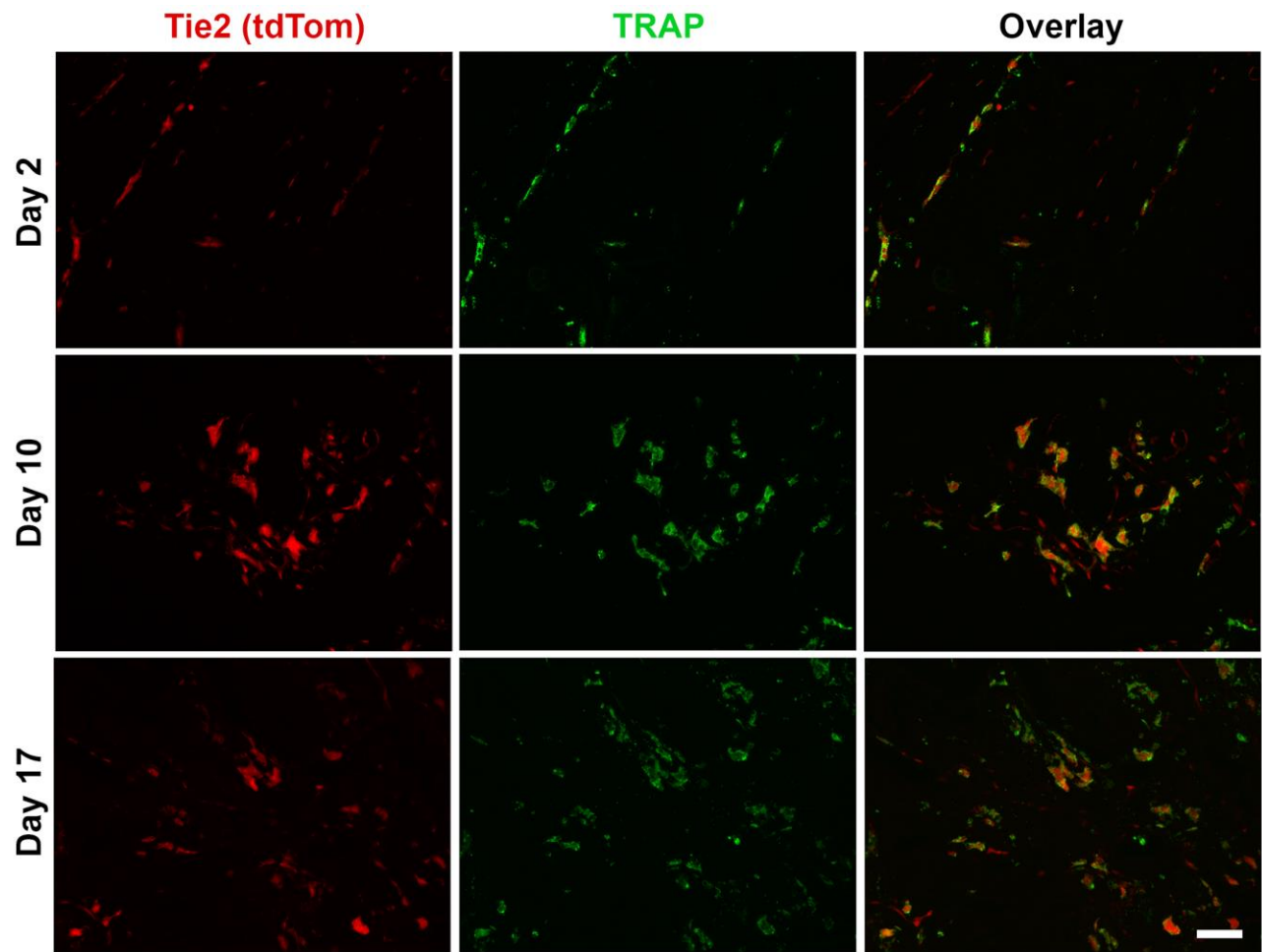
Finally, confirmation of the lack of a functional importance for *Tie2*-lineage cells in the direct formation of bone was seen using the novel *Tie2-cre: Osx<sup>fx/fx</sup>* mouse line. Loss of the osterix gene in cells of the chondrogenic lineage has been previously reported to disrupt global bone formation [259]. In contrast the *Tie2-cre: Osx<sup>fx/fx</sup>* were viable with no adverse phenotype, suggesting no significant contribution of *Tie2*-lineage cells to bone formation. Moreover, in parallel with the findings of the *Tie2-cre: Ai9* mouse line showing no reporter expression in osteoblasts, the *Tie2-cre: Osx<sup>fx/fx</sup>* line showed no deficit in rhBMP-2 induced ectopic bone formation.

In summary, this study uses rigorous methodology to demonstrate that *Tie2*-lineage and  $\alpha$ SMA-lineage cells make distinct contributions to rhBMP-2 induced bone formation. Moreover, despite evidence that BMPs and in particular high doses of rhBMPs may be able to induce endothelial to mesenchymal transitions, we have found no evidence for this in our *in vivo* bone formation models. We conclude that while this process may be problematic in certain disease states, it does not feature under normal physiological conditions. These data further suggest that the advantages of endothelial progenitor transplantation in orthopedics and bone tissue engineering are likely due to increases in angiogenesis rather than by these cells contributing directly to the local osteoblastic populations.

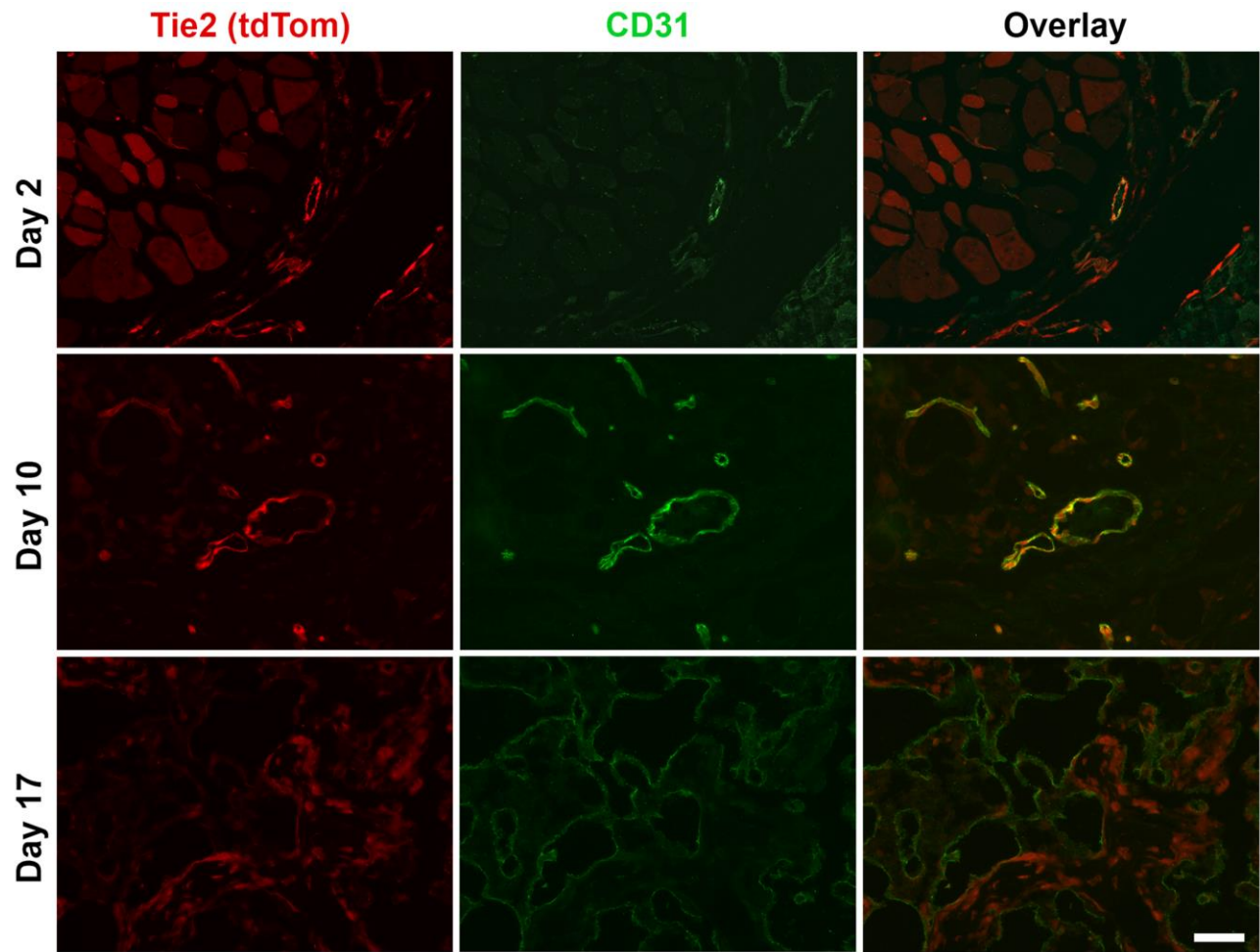
## **Acknowledgments**

This study was directly supported by NHMRC project grant APP1003480 and A Schindeler received salary support from NHMRC project grant APP1003478. I Kalajzic receives salary support from NIH/NIAMS grant AR055607. The Leica SP5 in the CLEM Suite at KRI was supported by the following grants: Cancer Institute New South Wales Research Equipment [10/REG/1-23], Australian National Health and Medical Research Council [2009-02759], the Ian Potter Foundation [20100508], the Perpetual Foundation [730], Ramaciotti Foundation [3037/2010], and the Sydney Medical School Research Infrastructure Major Equipment Scheme.

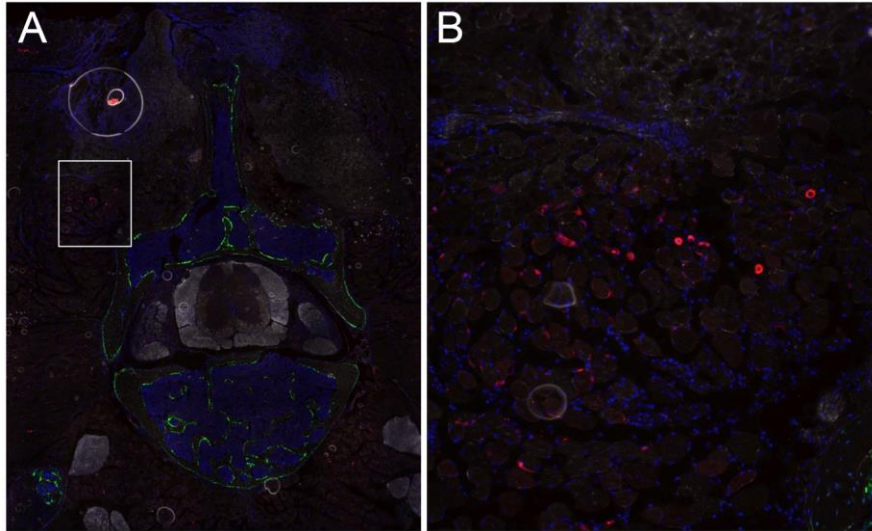
## Supplemental Figures



**Supplementary Figure 5. 1** Fluorescent images of Tie2-lineage cells (tdTomato) with TRAP activity (ELF97) in spine fusion masses showing recapitulates the findings seen in ectopic bone nodules (Figure 3). Osteoclasts were observed in the fusion mass from D10 onwards. Scale bar = 50  $\mu\text{m}$



**Supplementary Figure 5. 2** Fluorescent images of Tie2-lineage cells (tdTomato) with CD31 immunohistochemistry in spine fusion masses showing recapitulates the findings seen in ectopic bone nodules (Figure 2A). Scale bar = 50  $\mu$ m



**Supplementary Figure 5.3** Control fluorescent images of rhBMP-2 induced spine fusion masses in Tamoxifen untreated  $\alpha$ SMA-CreERT2Col2.3-GFP: Ai9 mice at d17. (A) DAPI staining (blue) of nuclei, (B) tdTomato (red) is not seen without Tamoxifen treatment, (C) Col2.3-GFP+ expression (green) is seen in the new bone, and (D) an overlay with light microscopy to visualize the bone. Scale bar = 50

## **(v) DISCUSSION**

### **Animal Models of NF1 and Clinical Translation**

Despite the apparent limitations of animal (particularly mouse) models, they can be an invaluable tool for bridging the gap between in vitro research and clinical trials. Appropriate planning and selection of an animal model is critical for translating to human clinical applications. [277] Our research relied upon a capacity to reproduce an NF1 phenotype in a physiologically complex system enabled by an in vivo model. Appropriate outcomes measures and study design were employed to increase translational power. The development of our model was informed by prior research which employed similar models to achieve translational results. In particular, genetic models of NF1 have been successful is reproducing the cellular picture observed in the bone healing deficiencies in humans [159, 278]. Successful pharmacological intervention in these models, such as with BMPs and bisphosphonates, has informed current clinical standard of care for treating these complications. [232]

Murine models of NF1 have proven to be of great utility for screening pharmacological treatments for the learning deficits, cognitive impairment, and neurobehavioral deficits reported in children with NF1. Nf1<sup>+/-</sup> mice have been shown to display features that mimic the cognitive phenotype of humans with NF1. [279, 280] The observed learning difficulties likely result from increased GABA release, which is normally regulated by Ras activity. Lovastatin, a drug that targets Ras phosphorylation, is able to reverse GABA release as well as the learning impairments in mice. When lovastatin was given



to children with NF1, it was observed to improve verbal and nonverbal memory. [280, 281].

A genetically modified mouse that featuring double inactivation of NF1 in GFAP expressing glial cells (Nf1 OPG mouse) has been generated that develops optic gliomas. Optic gliomas are lesions that present in 15% of children with NF1. [282]. The Nf1 OPG mouse exhibits deficits in selective and non-selective attention [128] and are noted to have decreased levels of dopamine. Treatment with an agent that increases dopamine signalling, Methylphenidate (MPH), normalizes the attention system abnormality in these mice. [128, 283]. When Methylphenidate is given to children with NF1, a similar effect is noted. [284] It can therefore be appreciated that genetic modelling of NF1 in mice has significant relevance to treatment options in humans.

Since the publication of our research, there have been contributions to the field that may represent novel directions to guide future research. With respect to NF1 pseudarthrosis, Ghadakzadeh et al, employed the AdCre virus transduction to generate a model of tibial pseudarthrosis [285]. This group demonstrated significant amounts of fibrous tissue in the fracture site, supporting both our research with this mouse when applied to tibial pseudarthrosis [159] and spine fusion. Elevated levels of  $\beta$ -catenin were found in the pseudarthrotic tissue. By crossing *Catnbtm2*Kem mice with Nf1 conditional knockout (KO) mice, they were able to conditionally express a null  $\beta$ -catenin protein. By inhibiting  $\beta$ -catenin, they were able to rescue the pseudarthrotic phenotype. This result was reproduced when mice were injected with an adenovirus that expressed Dkk-1, a negative regulator of the canonical Wnt pathway, which is implicated in  $\beta$ -catenin signalling . Baht et al [278] were able to improve healing and reduce fibrous tissue in the

same model by treating the mice with Nefopam, a non-narcotic analgesic known to reduce  $\beta$ -catenin signalling.

The AdCre-virus induced knockout model of NF1 has proven to be reproducible and reliable by our team and others. It has been shown to be able to reproduce the poor healing and fibroproliferation seen in humans. However, the effectiveness of this technique is limited to the tissue population that is exposed to the virus. Recent mouse models have been developed which conditionally result in double inactivation of the Nf1 gene in osteocytes [243], mesenchymal stem cells and osteoblasts [228, 229, 244, 245]. Conditional deletion of Nf1 in osteoblasts produced a scoliotic deformity with similarities to human dystrophic scoliosis. A tibial fracture model in this mouse [244] demonstrated impaired healing. We predict that this mouse would also exhibit an impaired response to spine fusion surgery. Wang et al found that treatment with lovastatin improved fracture healing. Notably, this model did not show an abundance of fibrous tissue in the fracture site. This suggests that the cell lineages contributing to the healing deficiencies in Nf1 are multiple and not limited to the mesenchymal/osteoblast line.

To date, there is no consensus on which approach to modelling NF1 deficiency in mice is ideal. Each model has benefits and weaknesses that must be considered when constructing a study. Systemic Nf1<sup>+/-</sup> mice perhaps most accurately model the genetics of the human deficiency, but this produces variable and often weaker phenotypes than humans. Despite this they have proven very useful in NF1 cognitive research. [128] In the context of bone, lineage specific homozygous knock-out models mimic the morphology of the NF1 skeletal dysplasia, but lack some important cellular features with great clinical relevance, such as the presence of fibrous tissue in fracture non-unions

and paraspinal tumours [229]. Homozygous deletion of the Nf1 gene with an AdCre virus provides the most accurate picture of pseudarthrosis in the tibia [159], but does not recapitulate the dystrophic developmental abnormalities of the NF1 skeleton, such as tibial bowing, scoliosis and dural ectasia. Considered together, these techniques represent a piecemeal approach to modelling the human phenotype of NF1.

### **Models of NF1 Spine Fusion**

In order to effectively investigate spine fusion in NF1 and the effect of interventions, we undertook the creation of a reproducible and reliable preclinical model. Prior to our research, there is a body of literature involving animal models of scoliotic deformity that we were able to draw upon. The majority were considered to be mechanical models and typically relied upon larger animals so that vertebrae and ribs could be manipulated to induce scoliosis. [246] [173]. Such models are useful for investigating corrective techniques. However, in the context of NF1 – specifically dystrophic type curves – the deformity is often driven by an identifiable anatomic abnormality such as vertebral dystrophy or parivertebral soft tissue masses. [286]. In these patients, the primary problem is not one of intraoperative correction, but one of postoperative failure of fusion [93]. For this reason, we sought to create a model of spine fusion that would allow us to study the factors that limited the success of these procedures in NF1. Building upon this model, we aimed to examine interventions which may be able to rescue the non-healing phenotype of NF1.

We designed a surgical approach with the intention of applying it to a model of NF1. At the time of our formulation, mice were the only animal available in which an Nf1

deficient state could be established. Additionally, the small size of the mouse, low cost of housing, and large breeding litters were advantageous for the purpose of study [237]. The anatomy of the mouse spine differs from that of the human with respect to orientation, vertebral number and morphology. The horizontal orientation of the spine has been cited as a limitation of quadrupedal models in reproducing the mechanical conditions present in human scoliosis. This represents a significant limitation in the context of reproducing deformity. Considering our intention was to reproduce the cellular picture of NF1 rather than the biomechanical environment surrounding scoliosis, we did not suspect this would overly limit our results. In the rodent lumbar spine, the transverse processes, one of the osseous targets for a posterolateral intertransverse fusion, is orientated more anteriorly than in the human in which it projects directly laterally. The result of this is that in our model, in which we reproduced the surgical approach used in humans, the transverse processes are excluded from the fusion and the articular processes provide the bony bed for the fusion. Our model involved the decortication of the fusion bed with consequent stripping of the overlying periosteum. The removal of the periosteum was performed to reproduce the surgical approach utilized in humans, rather than to isolate the fusion process from periosteal contribution.

In wild type mice, our model was able to reproducibly and reliably produce a robust fusion of the lumbar spine when a dose of 10  $\mu$ g of rhBMP-2 was delivered bilaterally via implanted collagen sponge. 10  $\mu$ g was chosen as this was a proportionate dose to that delivered in rabbit models and is the dose that our lab has utilized reliably in murine fracture models. [287] This yielded a very large fusion mass in all animals, larger than

what is seen in humans at recommended doses. This is a predictable finding as rodent fracture models have repeatedly shown that they heal more readily than their human counterparts. So called 'critical defect' models in rodents have been shown to heal without intervention at a rate that exceeds humans. [288] This is particularly relevant to mice, whose size and ability to heal does not reflect the clinical outcomes in human patients. For this reason we did not rely upon fusion rate as an outcome measure in our work. Instead, we looked at the cellular response at the site of fusion and compared the osteogenic response between animals and intervention groups. In the future, it may be possible to apply our model to larger rodents as genetic models become available. The recent presentation of a rat NF1 knockout model may represent a viable subject for this research.

When we applied the spine fusion to a mouse strain that was systemically Nf1+/-, we noted a decrease in bone volume and density, reflecting a decreased osteogenic activity and excessive resorption. This finding reflects the results seen in fracture and ectopic bone models in this genotype.[50, 200] Although this model of NF1 apparently reproduces the genotype seen in individuals with the disease, it fails to recapitulate the severity of the human phenotype. When subjected to a midshaft tibial fracture, which often results in non-unions in humans with NF1, Nf1+/- mice were not shown to have any deficiency of healing compared to wild type mice. Additionally, in the human patient, the non-united fractures are infiltrated with fibrous tissue. This was only replicated to a small degree in mice receiving fractures of the distal tibia and did not sufficiently mirror the non-unions seen in humans. The reason for this discrepancy may be genetic. There is evidence that NF1 tumorigenesis is associated with a double inactivation of the NF1

gene, in which one allele is constitutionally inactivated and the other is lost to somatic mutation. Such a process is referred to as the 'two-hit' hypothesis. [289] Garcia et al found that 25% of dermal neurofibromas showed loss of heterozygosity (LOH) for the Nf1 gene [290], while Upadhyaya et al found LOH in 36% of excised spinal neurofibromas. [291]. Samples of fibrotic tissue retrieved from tibial pseudarthrosis at the time of surgery showed double inactivation of the NF1 gene, suggesting that the second hit occurred in the mesenchymal progenitors from the periosteum. [292] LOH, therefore, may contribute to the severity of the human phenotype.

In order to recreate the conditions found in NF1 LOH, fracture studies have utilised a location specific condition knockout model of NF1. In this model, injection of a cre expressing adenovirus induces local double inactivation of the Nf1 gene in Nf1<sup>flox/flox</sup> mice. When injected at the site of tibial fractures, these mice showed an increased non-union rate relative to controls with significant amounts of fibrous tissue in the fracture site. [159] Encouraged by the apparent similarity to the clinical results seen in humans, we applied our spine fusion model to this mouse model of NF1. As was seen in the Nf1<sup>+/-</sup> mouse, all spines fused and thus intervertebral union rate was not an acceptable outcome measure. The aggressive osteogenic response to BMPs by mice was noted earlier and seemingly overwhelms the Nf1<sup>-/-</sup> phenotype. Mice receiving paraspinal delivery of the AdCre virus demonstrated significant volumes of fibrous tissue and increased number of TRAP<sup>+</sup> cells surrounding the delivery sponge. This provided a more suitable model for investigating the conditions associated with spine fusion failure in NF1 than the previous model which used Nf1<sup>+/-</sup> mice. With the AdCre virus

generated Nf1<sup>-/-</sup> tissue in the spine, we produced a model of spine fusion in NF1. This exhibited more abundant fibrosis than seen in the Nf1<sup>+/-</sup> model.

Animal models of human disease have been burdened at times by poor translatability. This is particularly true of mouse models. It has been suggested that the efficacy of novel therapies has been overestimated by as much as 30% due to poor translation from animal models. [293]. Despite their advantages in size and cost, a trend of moving away from mouse models is developing as they may not accurately model human disease processes. Seok et al demonstrated that mice do not mimic their human counterparts with respect to inflammatory diseases [294] and that this is due to different genomic responses to inflammatory stresses. Due to the significant role of inflammation in the process of bone healing, mice are a problematic subject. This has been explored earlier with respect to the augmented healing abilities of mice relative to humans and the exaggerated response to BMPs.

### **Pharmaceutical interventions to rescue poor NF1 spine fusion**

We hypothesized that by addressing the osteogenic deficiency and increased resorption seen in NF1 with targeted interventions, we would improve the fusion outcomes. Loss of activity of neurofibromin results in the unopposed activity of Ras. The MEK inhibitor PD0325901 was chosen to interfere with the Ras-MEK-ERK pathway. This agent had been shown to be effective in reducing NF1 tumour growth [295, 296]. Zoledronic acid, a bisphosphonate, is well tolerated and is an effective anti-resorptive agent which has shown efficacy in preserving bone in patients with Nf1. [203] We found that dosing with PD0325901 resulted in increased volume of bone in both wild type and Nf1<sup>-/-</sup> spines

and to decrease the number of local TRAP+ cells observed in the fibrous tissue of Nf1<sup>-/-</sup> spines. It did not, however, reduce the volume of fibrous tissue in the fusion masses. The similar osteogenic activity of PD0325901 in both wild type and Nf1<sup>-/-</sup> spines suggests that its primary activity in bone is anabolic, but it may have a small anti-resorptive capacity in light of its effect on TRAP+ cells.

## **BMPS**

BMPs are strongly osteogenic, and have long been used to augment bone anabolism clinically. RhBMP-2 and rhBMP-7 are both approved for use in lumbar spine fusion and recalcitrant long bone unions. [297] Various doses of rhBMP-2 were investigated during the development of our murine spine fusion model. [237] We found that the development of a reliable fusion mass depended upon treatment with rhBMP-2. Those mice that received saline delivered locally via collagen sponge instead of rhBMP-2 did not yield any evidence of fusion. With respect to clinical translation, this may represent a limitation. The use of BMPs for augmenting lumbar fusion has been a source of controversy. The osteogenic and pro-inflammatory properties of BMPs may result in compression of nearby anatomy via the formation of ectopic bone and inflamed soft tissues respectively. [298-300] This has predominantly been a problem when used off-label for cervical fusion. Additionally, published clinical guidelines for treatment of NF1 pseudarthrosis [232] suggest that the use of growth factors in the context of NF1 is poorly understood. There is anecdotal evidence that in addition to increasing bone anabolism in these patients BMPs may also increase the risk of malignancy [301] or worsen the patients existing tumour burden. [302] Current recommended practice for



promoting fusion in humans is to use autogenous bone graft harvested from the iliac crest. Bone graft is osteogenic, osteoinductive and osteoconductive and may behave more predictably in patients with NF1. Future research may modify the established surgical model to investigate the use of bone graft, rather than BMPs, to induce a reliable fusion.

Bisphosphonates are a recognized class which exert their anti-resorptive activity by inhibiting osteoclast activity. They are well tolerated in the elderly population where they are used to maintain bone mineral density. They are less frequently used in the paediatric population, but have been used with success in treating children with hypercalcaemia [303] [304], osteopathy [305] and calcinosis [306, 307]. A systematic review of the literature [308] has found that oral and intravenous use of bisphosphonates in a paediatric Osteogenesis Imperfecta population increases bone mineral density and reduces fracture incidence. Adverse effects are uncommon and when present include gastrointestinal upset, fever and muscle soreness. As mentioned previously, it has proven to be advantageous in treatment of NF1 related pseudarthrosis of the tibia. [203, 232] For this reason, it is likely to be a safe and effective candidate for adjuvant treatment of spine fusion in NF1. Consistent with this theoretic basis, zoledronic acid increased bone mineral density of fusion masses. Moreover, in the context of bone repair, long term bisphosphonates could maintain any new bone formed by pre-treatment or co-treatment with a pro-anabolic agent.

MEK inhibitors are a newer class of drug that have found popularity in several trials attempting to target and slow cancer growth. MEK inhibition represents an attractive

approach as the Ras-MEK-ERK pathway is implicated in the mitogenic signalling activated by known oncogenes. [309] Although the drug has been shown to well tolerated at active doses in cancer trials, it is associated with a number of side effects including rash, diarrhoea, nausea, fatigue and blurred vision. [310]. It has also been associated with increased incidence of blood dyscrasias (anaemia, thrombocytopenia, leucopenia) [247]. Clinically, the MEK inhibitor AZD644 has been trialled as a therapy for refractory low-grade gliomas in a paediatric cohort [311]. The side effect profile was similar to that observed in adults. MEK inhibition in mice with Trametinib has been shown to improve strength and size of callus in *Nf1*-deficient mice. [312] Our research suggests that while they may show non-specific anabolic activity in bone which augments BMP mediated fusion, they do not reduce the amount of fibrous tissue in the fusion mass (or fracture callus) and as such do not represent a sufficiently targeted approach to treating the orthopaedic dysplasia of NF1. While the use of MEK inhibitors is associated with unpleasant side effects, these are limited to the duration of treatment and resolve once therapy is ceased.

We have shown that the anabolic deficiency and increased resorption in NF1 can be targeted and improved with a combination therapy of osteogenic agents such as BMPs and antiresorptive agents such as bisphosphonates. These have been used to great effect in humans and well as mice. Our recent research suggests that the osteogenic activity of BMPs can be further augmented with adjuvant therapies, such as a MEK inhibitor. Despite this, we have not been able to reduce the volume of fibrous tissue in the fusion mass of the lumbar spine. We expect that clinically, this will continue to be a challenge that limits the success of corrective procedures. We are interested in

investigating novel adjuvant therapies which may rescue the fibrous proliferative phenotype. By targeting  $\beta$ -catenin expression, Nefopam has been shown to reduce the presence of fibrous tissue in tibial pseudarthrosis. [278]. This may prove beneficial in improving outcomes in spine fusion. Like MEK inhibitors, Lovastatin targets the unopposed activity of Ras that occurs secondary to neurofibromin deficiency. This drug is effective at reversing the cognitive phenotype in Nf1+/- mice and humans, and improves tibial fracture healing in osteoblast double-knockout models. The later model did not show evidence of fibrous tissue at the fracture site, and thus lovastatin was not tested against a fibroproliferative non-union. Future research may utilise our established AdCre virus model, which reliably produces a fibrous tibial non-union and lumbar fusion mass, and treat with lovastatin in order to investigate its ability to rescue this process.

We were unable to demonstrate reduction of fibrous proliferation by antagonism of the Ras-MEK-ERK cascade with the MEK inhibitor PD0325901. An alternative method for interfering with this process is via inhibition of the c-Jun NH2-terminal kinase (JNK) pathway. JNK signalling is required for the Ras to exert its oncogenic activity. [313] Increased JNK activity in bone marrow stromal cells (BMSCs) has been observed in vitro, and inhibition of this signalling resulted in increased osteoblastogenesis. [238] Our lab, in a currently unpublished study, has investigated the effect of JNK inhibition on open tibial fracture healing using the drug CC-930 in the AdCre virus model of NF1. Treatment with CC-930 significantly reduced the amount of fibrous tissue within the fracture site. This agent may demonstrate utility in reducing the fibrous proliferation we observed in BMP induced spine fusion surgery in our murine model of NF1. It would be expected that the short-term use of this drug during the post-operative healing phase, in

conjunction with bisphosphonates would yield a robust fusion mass with less fibrous tissue. The anabolic activity of our intervention may be further strengthened with the addition of PD0325901. The translational power of this agent is unclear at this moment as it is a novel drug. CC-930 has recently undergone phase 1 clinical trial and has shown to be generally well tolerated with limited adverse effects. [314]

### **Cellular contributors to the bony fusion mass**

It has been a long held assumption [315] that vascular endothelial cells contributed to bone healing as osteoblastic progenitors. Early investigations used bright-field and electron microscopy without using lineage tracking techniques. Sequential histological sections from time points throughout the fracture healing period seemed to suggest that endothelial cells migrated from vascular lumens and differentiated into osteoblast progenitors. This early research was rudimentary and modern lineage tracking techniques have improved the resolution of this field of study. The limitations of early, non-genetic, cell labelling studies has been previously discussed. An optimal lineage tracing technique selectively and permanently labels a cell type permitting the observation of its contribution to differentiated cell populations. Transgenic subject that have been bred to express fluorescence under a cell specific promoter following Cre recombination are frequently used for this research. When the promoter is stable, labelling is specific and permanent. These are classified as 'knock-in' models, and allow the observation of cellular mechanisms without interfering with their function. When these techniques are used to delete a gene, they are 'knock-out' models. By altering cell physiology and deleting genes responsible for promoting differentiation,

knock-out models are also able to provide valuable information about cellular contribution to various processes. Targeted interventions can be developed and tested if the cellular contributors to a physiological or pathological process are known.

In an attempt to identify the cellular contributors to spine fusion, Tie-2 and  $\alpha$ -smooth muscle actinin ( $\alpha$ -SMA) expressing cells were labelled and their contributions observed.

In contrast to our hypothesis, Tie-2 expressing cells did not contribute to the osteoblast population within the fusion mass. These cells were noted to co-label with CD31 expressing cells and TRAP+ cells, suggesting a contribution to angiogenesis and to the osteoclast population respectively. Tie-2 is used as a marker of vascular endothelial cells but is also expressed by haematopoietic stem cells, which give rise to osteoclasts.

Although we cannot demonstrate contribution of endothelial cells to osteoblastogenesis, evidence suggest that increasing availability of endothelial cells to a fracture site improves healing. Critical defect models involving sheep tibia [316] and rat femora [317] demonstrated improved union rates after transplantation of blood derived endothelial progenitor cells (EPCs). This is likely a primary consequence of increased angiogenesis and neovascularization. Seebach et al propose that that while transplanted EPCs contribute to early vascularization, they exert their effect primarily by recruiting host EPCs via the cytokine VEGF [318]. Considering our results, it is unlikely that endothelial cells contribute directly to the process of osteogenesis.

Tie-2 expressing cells were found not to contribute to the osteoblast population of the fusion mass, nevertheless all osteoblastic cells expressing Col2.3-GFP were found to co-label with tdTomato+ cells, indicating that they derive from the  $\alpha$ -SMA lineage. Mobilisation of  $\alpha$ -SMA expressing mesenchymal stem cells (MSC) may present a

clinical benefit where healing or bone formation is impaired. AMD3100 is an antagonist of CXCR4, which regulates release of MSC from the bone marrow. Kumar et al found that treatment with AMD3100 and the growth factor IGF1 increased the proportion of circulating MSC and improved healing in a murine tibial defect model. [319] In a study investigating kidney fibrosis, treatment with AMD3100 increased expression of  $\alpha$ -SMA in kidney biopsies. [320] Similar results were found in the liver of mice receiving AMD3100 [321] Under the trade name Plerixafor, AMD3100 has been demonstrated to be well tolerated and effective at mobilising haematopoietic cells in human patients. [322, 323]. MSCs contributed to osteogenesis in our model, however the relationship between MSCs and fibrosis may limit its effectiveness as a target for therapy in NF1.

Cho et al [324] found that fibrous tissue retrieved from tibial pseudarthrosis from patients with NF1 showed evidence that the hamartoma cells were arrested at a certain stage of osteoblastic differentiation. This was supported by the work of Lee et al, which demonstrated that human fibrous hamartoma showed signs of failed osteoblastic differentiation [242]. Our recent work with JNK inhibitors in the AdCre model of NF1 showed that when a tdTomato fluorescent transgene was included, the fibrous cells were labelled as being Nf1<sup>-/-</sup>. Together, this suggests that the cells implicated in fibrous proliferation are a subset of otherwise normal osteogenic cells (likely of mesenchymal origin) that fail to differentiate fully secondary to the aberrant signalling observed in NF1. Ghadakzadeh et al reported that antagonism of  $\beta$ -catenin expression with Dickkopf-related protein 1 (DKK1) rescued the fibroproliferative phenotype in Nf1<sup>-/-</sup> tibial pseudarthrosis. Similarly, conditional knockout of  $\beta$ -catenin expression using a Nf1<sup>flox/flox</sup>;Catnb<sup>tm2Kem</sup> mouse showed improved healing with decreased fibrous

tissue at 21 days post fracture. [284]. Future research might investigate the effect of deletion of  $\beta$ -catenin alleles on cellular contribution to a fusion mass in Nf1<sup>-/-</sup> spines. Inclusion of a fluorescent transgene would permit the tracing of cells contributing to the fusion mass that were transduced by the virus, though this would certainly compound the time and cost required to generate the transgenic mouse line.

Lineage tracing using an  $\alpha$ -SMA promoter yielded valuable insights into mesenchymal stem cell contribution to the fusion mass in wild type mice. Though labour intensive and costly, this transgenic mouse could be crossed with an Nf1<sup>flox/flox</sup> mouse to generate a mouse that is Nf1<sup>-/-</sup> in cells expressing  $\alpha$ -SMA. These cells would be traceable due to labelling by the TdTomato transgene. This model could, by itself, generate quantitative data regarding the contribution of  $\alpha$ -SMA expressing cells to the spine fusion process in NF1. Moreover, it would provide a compelling foundation upon which to investigate signalling modulation, as with  $\beta$ -catenin blockade, and mesenchymal cell mobilisation, as with AMD3100.

Future in vitro research may investigate the altered gene expression witnessed in MSCs in Nf1 deficient states. The loci of aberrant expression could be used as targets for future investigation and therapeutic intervention. To achieve this, MSCs would be harvested from the marrow of Nf1<sup>+/-</sup> and Nf1<sup>flox/flox</sup> and exposed to Cre-expressing adenovirus. RNA sequencing (RNA-seq) would be performed to profile the gene expression in these cells and identify differences between the groups.

## **Future approaches to NF1 modelling and treatment**

### **Advanced Genetic Models of NF1 deficiency**

Conditional mutagenesis via the Cre-LoxP system has proven to be a powerful tool for generating new models of gene modified mice. This system permits the lineage-specific genetic recombination with high specificity. Changes to a parent cell are maintained in its progeny, allowing the descendent cells to be tracked after division or transdifferentiation. Moreover, tissue-specific cre-expressing strains can be crossed with a variety of reporter or conditional knockout strains allowing substantive versatility in new model generation.

Despite its wide adoption and utility for generating new genetic models of disease, Cre-loxP mice possesses significant limitations. Traditionally, this technique has been limited to use in mice due in part to early mapping of the mouse genome and generation of reliable lines of mouse clones. However, recent advancements in the mapping of the rat genome and development of rat clones has enabled the use of Cre-LoxP systems in rats. [325]. In addition, the generation of a transgenic line requires multiple generations of breeding and cross-breeding. [326] This process is lengthy and costly, even in animals such as mice which are small and have a relatively short gestation period. Should the technology be applicable to larger animals, the issues of cost are proportional to animal size and gestation time, rendering it increasingly prohibitive as animal size increases. This process must be repeated for every gene that is investigated. Finally, any leakiness of Cre-recombinase leads to decreased specificity of recombination and mosaicism.

The CRISPR/Cas9 system has been established as a simple tool for genome editing in plants and animals. [327] It has been used successfully to generate double allelic knockouts of targeted genes in one step in a single generation by injecting of sgRNA



and CAS9 mRNA into the pronuclear stage zygotes. This method yields systemic knockout of the targeted gene. [328, 329] For the purposes of the modelling of genetic disease, this technique may prove to be a more convenient alternative to the Cre-LoxP system as it avoids the processes of gene floxing and selective breeding. In the face of CRISPR/Cas9 technology, one of the strengths of Cre/LoxP system has been that it permits tissue specific recombination. Carroll et al [330] have described a technique for generating a cardiac-specific Cas9 transgenic mouse by targeting cardiomyocytes of post-natal mice with an Adeno-Associated Virus 9 (AAV9). They targeted the Myh6 locus, which would be embryonically lethal if edited at the zygote stage. Bi-allelic deletion of Nf1 is similarly embryonically lethal. The AAV9 delivery system may represent a promising technique for inducing tissue specific knockout of the Nf1 gene.

Yang et al [331] have proposed a technique for conditional gene editing that bridges the CRISPR/Cas9 and Cre/LoxP systems. They demonstrated that it was possible to flox targeted alleles by injecting Cas9 mRNA, sgRNAs and single-stranded DNA oligos into mouse zygotes. This was a one-step process and successful editing was confirmed by PCR. Subsequent gene editing could then be initiated by Cre-driven recombination. This technique was limited by low efficiency and off-target insertion. As this technology improves, it may provide an alternative to the labour-intensive generation of transgenic mice.

Far from being a silver bullet, the technology is in its infancy and must overcome some limitations including issues of specificity and delivery. CRISPR/Cas9 achieves its effect by inducing cleavage of the genome at a targeted location. Lack of specificity of the system would result in cleavage at off target sites, which may result in either an

impaired effect or an unpredicted phenotype. Fu et al found that in human genome editing, off-target cleavage may occur between 5.6% and 125% as often as on-target. These off-target cleavages may be up to 5 nucleotides away from the target location. [332] Recent work suggests that the error in Cas9 targeting can be anticipated and minimized with careful design. [333, 334] The efficiency of the CRISPR/Cas9 system is also complicated by issues of delivery. In order to effect alterations to the genome, the system must enter the nucleus of the target cell. In vitro, this may be achieved by physical intracellular implantation. In vivo delivery of the system, to date, remains a challenge. Viral and non-viral delivery systems have been explored for use in mammals. [335] Viral delivery, while the most common, is associated with limited packing size and longer exposure of the Cas9 system with consequent increases in off-target cleavage and acquired immunogenicity. These limitations may be overcome with non-viral delivery systems, in particular nanoparticle delivery. [336]

It is unlikely that the CRISPR/Cas9 technology will represent a therapy or cure for patient with NF1 in the near future. It is more likely that its prime utility will be to create genetic models of the disease in animals to investigate interventions. The orthopaedic manifestations of NF1 present with deformity and pathology that must be addressed surgically, often in tandem with pharmacological therapy. Generation of NF1 models using larger animals would provide a useful foundation upon which to investigate surgical intervention, as larger animals experience biomechanical forces more similar to humans. CRISPR/Cas9 has been proven to be effective at initiating gene deletion in larger animals such as rabbits [337], goats [338], sheep [339] and chickens [340]

amongst others. Recently, 3 groups have produced swine models of NF1 using this technology, though the results have not yet been published.

### **Non-Pharmaceutical Therapeutic Approaches**

For orthopaedic NF1 patients, surgery has remained the mainstay of treatment for correcting spinal deformity and non-union despite the potential benefits of adjuvant pharmacological therapies. In the context of spine fusion, the primary complication facing NF1 spines is the development of non-union. However, this is only a failure with respect to the intentions of early work in the field, which depended upon intervertebral fusion to maintain correction. This fusion came at the cost of high incidences of revision and growth arrest in the spines of patients. A modification to the expected outcomes of surgery, namely to initiate correction without establishing fusion, may decrease the rate of morbidity observed with the procedures.

Intervertebral spinal fusion alone can have a high utility in maintaining correction of a scoliotic deformity of the spine. Early experience in the field advocated early and aggressive fusion [93, 148]. These patients were often younger than 12 years old with up to a quarter of them requiring reoperation for failed fusion. The difficulty in achieving successful fusion in patients with NF1 has prompted investigation into correction of deformity without fusion. Growing rods are a type of spinal instrumentation that are used to correct deformity without fusion, thereby permitting continued growth of the immature spine. A recent retrospective analysis of 14 patients suggests that this is a safe and effective option for correcting early onset scoliosis (EOS) in patients with NF1. Complications were primarily that of implant failure. [341]

Currently, the literature regarding growing rods without fusion, as an alternative to early fusion, is limited. This is a fertile topic for exploration with preclinical models in which deformity may be induced. The conditional osteoblast murine model described by Wang et al [229] would be ideally suited to such modelling were it not for the small size of the animal which prohibits instrumentation. Induction of deformity in the spines of larger animals, either CRISPR/cas9 deletion of the Nf1 gene in cells of osteoblast lineage or by means of mechanical tethering are options for investigating outcomes between treatment modalities.

## **Conclusion**

The unifying aim of this research has been to contribute to the understanding of NF1 bone phenotype and the challenges it imposes upon spine fusion for the correction of scoliosis. In order to achieve this, we initially created a rodent model for posterolateral lumbar spine fusion. This built a foundation upon which would could test investigate cellular contributions to spine fusion as well as interventions in the context of NF1. This surgical model has since been used by other teams [342-344], and is testament to its reproducibility and reliability. We consider this to be a significant contribution to the field.

Using this surgical approach we were able to incorporate genetic models of NF1 affecting the spine, comparing both heterozygosity and loss of heterozygosity for the Nf1 gene. These models recapitulated the bone healing phenotype seen in humans with varying degrees of severity. We were able to use this model to investigate anabolic (BMP) and anti-catabolic (bisphosphonate) pharmacological interventions, as well as

targeted therapies that are specific to the NF1 disease process (MEK inhibitor). This research has yielded significant data which suggests a possible utility for these agents in humans.

The spine fusion model also allowed us to perform in vivo lineage cell tracing experiments. This research has provided insightful data that counters prior assumptions about the contribution of Tie-2 expressing cells to the process of bone repair. We have shown that these cells co-label with osteoclasts, and hence may play a resorptive role in bone homeostasis. Additionally, we were able to show that  $\alpha$ -SMA expressing cells, which represent a population of cells of mesenchymal origin, strongly co-label with osteoblasts and may therefore be exploited to improve bony union.

Treatment of scoliosis in NF1 remains a challenge as the success of fusion is impeded by deficiencies of anabolism, excessive resorption, and fibroproliferation. The molecular and cellular pathways responsible are likely multifactorial and therefore will require a multimodal approach to therapy consisting of surgical techniques and adjuvant pharmacological interventions. Genome editing via the CRISPR/Cas9 system may present with therapeutic options in the future, but in the short term this technique will provide the most utility in expanding the pre-clinical models of NF1 at the disposal of researchers. Such models have been and will continue to be valuable in the screening of novel pharmacological and surgical interventions that are targeted at the deficiencies specific to the NF1 disease process.

## References

1. Ruggieri, M. and A. Polizzi, *From Aldrovandi's "Homuncio" (1592) to Buffon's girl (1749) and the "Wart Man" of Tilesius (1793): Antique illustrations of mosaicism in neurofibromatosis? [8]*. Vol. 40. 2003. 227-32.
2. Moore, K.L., Dalley, A. F., *Skeletal System*, in *Clinically Oriented Anatomy*, P.J. Kelley, Editor. 1999, Lippincott Williams & Wilkins. p. 14-26.
3. Tortora G. J., D.B., *The Skeletal System: Bone Tissue*, in *Principles of Anatomy and Physiology*, R. B, Editor. 2006, John Wiley & Sons. p. 171-289.
4. Dickson, R., *THE AETIOLOGY OF SPINAL DEFORMITIES*. The Lancet, 1988. **331**(8595): p. 1151-1155.
5. Steele, D.G. and C.A. Bramblett, *The anatomy and biology of the human skeleton*. 1988: Texas A&M University Press.
6. Boyle, W.J., W.S. Simonet, and D.L. Lacey, *Osteoclast differentiation and activation*. Nature, 2003. **423**(6937): p. 337-42.
7. Caetano-Lopes, J., H. Canhao, and J.E. Fonseca, *Osteoblasts and bone formation*. Acta Reumatol Port, 2007. **32**(2): p. 103-10.
8. Teitelbaum, S.L., *Bone Resorption by Osteoclasts*. Science, 2000. **289**(5484): p. 1504-1508.
9. Raisz, L.G., *Physiology and pathophysiology of bone remodeling*. Clin Chem, 1999. **45**(8 Pt 2): p. 1353-8.
10. Dunning, D., *Basic mammalian bone anatomy and healing*. Veterinary Clinics of North America: Exotic Animal Practice, 2002. **5**(1): p. 115-128.
11. Provot, S. and E. Schipani, *Molecular mechanisms of endochondral bone development*. Biochemical and Biophysical Research Communications, 2005. **328**(3): p. 658-665.
12. Hulth, A., *Current Concepts of Fracture Healing*. Clinical Orthopaedics and Related Research, 1989. **249**: p. 265-284.
13. Dimitriou, R., E. Tsiridis, and P.V. Giannoudis, *Current concepts of molecular aspects of bone healing*. Injury, 2005. **36**(12): p. 1392-1404.
14. Einhorn, T.A.M.D., *The Cell and Molecular Biology of Fracture Healing*. [Miscellaneous Article]. 1999.
15. Schindeler, A., et al., *Bone remodeling during fracture repair: The cellular picture*. Seminars in Cell & Developmental Biology, 2008. **19**(5): p. 459-466.
16. McKibbin, B., *The biology of fracture healing in long bones*. J Bone Joint Surg Br, 1978. **60-B**(2): p. 150-62.
17. Panagiotis, M., *Classification of non-union*. Injury, 2005. **36**(4, Supplement 1): p. S30-S37.
18. Carano, R.A.D. and E.H. Filvaroff, *Angiogenesis and bone repair*. Drug Discovery Today, 2003. **8**(21): p. 980-989.
19. Pacicca, D.M., et al., *Expression of angiogenic factors during distraction osteogenesis*. Bone, 2003. **33**(6): p. 889-898.
20. Street, J., et al., *Is human fracture hematoma inherently angiogenic?* Clin Orthop Relat Res, 2000(378): p. 224-37.

21. Trueta, J., *Blood supply and the rate of healing of tibial fractures*. Clin Orthop Relat Res, 1974(105): p. 11-26.
22. Hausman, M.R., M.B. Schaffler, and R.J. Majeska, *Prevention of fracture healing in rats by an inhibitor of angiogenesis*. Bone, 2001. **29**(6): p. 560-564.
23. Minamide, A., et al., *Evaluation of carriers of bone morphogenetic protein for spinal fusion*. Spine (Phila Pa 1976), 2001. **26**(8): p. 933-9.
24. RHINELANDER, F.W., *The Normal Microcirculation of Diaphyseal Cortex and Its Response to Fracture*. J Bone Joint Surg Am, 1968. **50**(4): p. 784-800.
25. Trueta, J. and A. Trias, *THE VASCULAR CONTRIBUTION TO OSTEOGENESIS: IV. The Effect of Pressure upon the Epiphysial Cartilage of the Rabbit*. J Bone Joint Surg Br, 1961. **43-B**(4): p. 800-813.
26. Arnold, M., et al., *Radiation-induced impairment of bone healing in the rat femur: effects of radiation dose, sequence and interval between surgery and irradiation*. Radiotherapy and Oncology, 1998. **48**(3): p. 259-265.
27. Eilber, F.R., et al., *Limb salvage for skeletal and soft tissue sarcomas multidisciplinary preoperative therapy*. Cancer, 1984. **53**(12): p. 2579-2584.
28. Pelker, R.R., et al., *Radiation-induced alterations of fracture healing biomechanics*. Journal of Orthopaedic Research, 1984. **2**(1): p. 90-96.
29. Macey, L.R., et al., *Defects of early fracture-healing in experimental diabetes*. J Bone Joint Surg Am, 1989. **71**(5): p. 722-33.
30. Daftari, T.K., et al., *Nicotine on the Revascularization of Bone Graft: An Experimental Study in Rabbits*. Spine, 1994. **19**(8): p. 904-911.
31. Hankemeier, S., et al., *Alteration of fracture stability influences chondrogenesis, osteogenesis and immigration of macrophages*. Journal of Orthopaedic Research, 2001. **19**(4): p. 531-538.
32. PARK, S.-H., et al., *The Influence of Active Shear or Compressive Motion on Fracture-Healing*. J Bone Joint Surg Am, 1998. **80**(6): p. 868-78.
33. COUTTS, R.D., et al., *The Effect of Delayed Internal Fixation on Healing of the Osteotomized Dog Radius*. Clinical Orthopaedics and Related Research, 1982. **163**: p. 254-260.
34. Piekarski, K., A.M. Wiley, and J.E. Bartels, *The Effect of Delayed Internal Fixation on Fracture Healing: An Experimental Study*. Acta Orthopaedica Scandinavica, 1969. **40**(5): p. 543 - 551.
35. Sarmiento, A., L.L. Latta, and R.R. Tarr, *The effects of function in fracture healing and stability*. Instr Course Lect, 1984. **33**: p. 83-106.
36. S. CHAO, E.Y., et al., *The Effect of Rigidity on Fracture Healing in External Fixation*. Clinical Orthopaedics and Related Research, 1989. **241**: p. 24-35.
37. CORNELL, C.N. and J.M. LANE, *Newest Factors in Fracture Healing*. Clinical Orthopaedics and Related Research, 1992. **277**: p. 297-311.
38. FROST, H.M., *The Biology of Fracture Healing: An Overview for Clinicians. Part II*. Clinical Orthopaedics and Related Research, 1989. **248**: p. 294-309.
39. Kalfas, I.H., *Principles of bone healing*. Neurosurg Focus, 2001. **10**(4): p. E1.
40. AHRENGART, L., *Periarticular Heterotopic Ossification After Total Hip Arthroplasty: Risk Factors and Consequences*. Clinical Orthopaedics and Related Research, 1991. **263**: p. 49-58.

41. Sawyer, J.R., et al., *Heterotopic ossification: clinical and cellular aspects*. Calcif Tissue Int, 1991. **49**(3): p. 208-15.
42. McCarthy, E.F. and M. Sundaram, *Heterotopic ossification: a review*. Skeletal Radiol, 2005. **34**(10): p. 609-19.
43. Hakim, M. and E.F. McCarthy, *Heterotopic Mesenteric Ossification*. Am. J. Roentgenol., 2001. **176**(1): p. 260-261.
44. Mohler, E.R., III, et al., *Bone Formation and Inflammation in Cardiac Valves*. Circulation, 2001. **103**(11): p. 1522-1528.
45. Vattikuti, R. and D.A. Towler, *Osteogenic regulation of vascular calcification: an early perspective*. Am J Physiol Endocrinol Metab, 2004. **286**(5): p. E686-696.
46. Urist, M.R., *Bone: Formation by Autoinduction*. Science, 1965. **150**(3698): p. 893-899.
47. Boden, S.D., et al., *Use of recombinant human bone morphogenetic protein-2 to achieve posterolateral lumbar spine fusion in humans: a prospective, randomized clinical pilot trial 2002 volvo award in clinical studies*. Spine, 2002. **27**(23): p. 2662-2673.
48. YAMAZAKI, Y., et al., *Response of the Mouse Femoral Muscle to an Implant of a Composite of Bone Morphogenetic Protein and Plaster of Paris*. Clinical Orthopaedics and Related Research, 1988. **234**: p. 240-249.
49. Gersbach, C.A., R.E. Guldberg, and A.J. García, *In vitro and in vivo osteoblastic differentiation of BMP-2- and Runx2-engineered skeletal myoblasts*. Journal of Cellular Biochemistry, 2007. **100**(5): p. 1324-1336.
50. Schindeler, A. and D.G. Little, *Recent insights into bone development, homeostasis, and repair in type 1 neurofibromatosis (NF1)*. Bone, 2008. **42**(4): p. 616-622.
51. Schindeler, A., et al., *Models of tibial fracture healing in normal and Nf1-deficient mice*. Journal of Orthopaedic Research, 2008. **26**(8): p. 1053-1060.
52. Wang, E.A., et al., *Recombinant human bone morphogenetic protein induces bone formation*. Proceedings of the National Academy of Sciences, 1990. **87**(6): p. 2220-2224.
53. Katagiri, T., et al., *Bone morphogenetic protein-2 converts the differentiation pathway of C2C12 myoblasts into the osteoblast lineage*. J Cell Biol, 1994. **127**(6 Pt 1): p. 1755-66.
54. Okubo, Y., et al., *In Vitro and in Vivo Studies of a Bone Morphogenetic Protein-2 Expressing Adenoviral Vector*. J Bone Joint Surg Am, 2001. **83**(1\_suppl\_2): p. S99-104.
55. Yamaguchi, A., et al., *Recombinant human bone morphogenetic protein-2 stimulates osteoblastic maturation and inhibits myogenic differentiation in vitro*. J Cell Biol, 1991. **113**(3): p. 681-7.
56. Kaplan, F., et al., *The histopathology of fibrodysplasia ossificans progressiva. An endochondral process*. J Bone Joint Surg Am, 1993. **75**(2): p. 220-230.
57. Gannon, F.H., et al., *Bone morphogenetic protein 2/4 in early fibromatous lesions of fibrodysplasia ossificans progressiva*. Human Pathology, 1997. **28**(3): p. 339-343.
58. Olmsted, E.A., F.S. Kaplan, and E.M. Shore, *Bone Morphogenetic Protein-4 Regulation in Fibrodysplasia Ossificans Progressiva*. Clinical Orthopaedics and Related Research, 2003. **408**: p. 331-343.
59. Feldman, G., et al., *Fibrodysplasia Ossificans Progressiva, a Heritable Disorder of Severe Heterotopic Ossification, Maps to Human Chromosome 4q27-31*. The American Journal of Human Genetics, 2000. **66**(1): p. 128-135.
60. Shore, E.M., et al., *A recurrent mutation in the BMP type I receptor ACVR1 causes inherited and sporadic fibrodysplasia ossificans progressiva*. Nat Genet, 2006. **38**(5): p. 525-7.



61. Boström, K., *Insights into the mechanism of vascular calcification*. The American Journal of Cardiology, 2001. **88**(2, Supplement 1): p. 20-22.
62. Bostrom, K., et al., *Bone morphogenetic protein expression in human atherosclerotic lesions*. J Clin Invest, 1993. **91**(4): p. 1800-9.
63. Serbedzija, G.N., M. Bronner-Fraser, and S.E. Fraser, *A vital dye analysis of the timing and pathways of avian trunk neural crest cell migration*. Development, 1989. **106**(4): p. 809-816.
64. Bronner-Fraser, M. and S.E. Fraser, *Cell lineage analysis reveals multipotency of some avian neural crest cells*. Nature, 1988. **335**: p. 161.
65. Progzatzky, F., M.J. Dallman, and C.L. Celso, *From seeing to believing: labelling strategies for in vivo cell-tracking experiments*. Interface focus, 2013. **3**(3): p. 20130001.
66. Kretzschmar, K. and Fiona M. Watt, *Lineage Tracing*. Cell, 2012. **148**(1): p. 33-45.
67. Sato, M., et al., *New approach to cell lineage analysis in mammals using the cre-loxP system*. Molecular Reproduction and Development, 2000. **56**(1): p. 34-44.
68. Lobe, C.G., et al., *Z/AP, a double reporter for cre-mediated recombination*. Dev Biol, 1999. **208**(2): p. 281-92.
69. Hollinshead, W.H., *Anatomy of the Spine: Points of Interest to Orthopaedic Surgeons*. J Bone Joint Surg Am, 1965. **47**: p. 209-15.
70. Risser, J.C., *Scoliosis: Past and Present*. J Bone Joint Surg Am, 1964. **46**: p. 167-99.
71. Rogala, E.J., D.S. Drummond, and J. Gurr, *Scoliosis: incidence and natural history. A prospective epidemiological study*. The Journal of bone and joint surgery. American volume, 1978. **60**(2): p. 173-176.
72. McMaster, M.J. and K. Ohtsuka, *The natural history of congenital scoliosis. A study of two hundred and fifty-one patients*. J Bone Joint Surg Am, 1982. **64**(8): p. 1128-47.
73. Berven, S. and D.S. Bradford, *Neuromuscular scoliosis: causes of deformity and principles for evaluation and management*. Semin Neurol, 2002. **22**(2): p. 167-78.
74. Cheung, K.C., et al., *Recent advances in the aetiology of adolescent idiopathic scoliosis*. International Orthopaedics, 2008. **32**(6): p. 729-734.
75. Veldhuizen, A.G., D.J. Wever, and P.J. Webb, *The aetiology of idiopathic scoliosis: biomechanical and neuromuscular factors*. European Spine Journal, 2000. **9**(3): p. 178-184.
76. Yong-Hing, K. and G.D. MACEWEN, *Scoliosis associated with osteogenesis imperfecta*. Journal of Bone & Joint Surgery, British Volume, 1982. **64**(1): p. 36-43.
77. Rideau, Y., et al., *The treatment of scoliosis in Duchenne muscular dystrophy*. Muscle & nerve, 1984. **7**(4): p. 281-286.
78. Pyeritz, R.E. and V.A. McKusick, *The Marfan syndrome: diagnosis and management*. New England Journal of Medicine, 1979. **300**(14): p. 772-777.
79. Hensinger, R. and G. MacEwen, *Spinal deformity associated with heritable neurological conditions: spinal muscular atrophy, Friedreich's ataxia, familial dysautonomia, and Charcot-Marie-Tooth disease*. The Journal of bone and joint surgery. American volume, 1976. **58**(1): p. 13.
80. Holm, V.A. and E.L. Larnen, *Prader - Willi Syndrome and Scoliosis*. Developmental Medicine & Child Neurology, 1981. **23**(2): p. 192-201.
81. Beighton, P. and F. Horan, *Orthopaedic aspects of the Ehlers-Danlos syndrome*. J Bone Joint Surg Br, 1969. **51**(3): p. 444-453.

82. Hanley, E.N., Jr., *The indications for lumbar spinal fusion with and without instrumentation*. Spine (Phila Pa 1976), 1995. **20**(24 Suppl): p. 143S-153S.
83. Risser, J.C., Q.M. Iqbal, and K. Nagata, *SCOLIOSIS AFTER TERMINATION OF VERTEBRAL GROWTH*. Annals of the Royal College of Surgeons of England, 1977. **59**(2): p. 119-123.
84. Marketos, S.G. and P.K. Skiadas, *Galen: a pioneer of spine research*. Spine (Phila Pa 1976), 1999. **24**(22): p. 2358-62.
85. Heary, R.F. and K. Madhavan, *The history of spinal deformity*. Neurosurgery, 2008. **63**(3 Suppl): p. 5-15.
86. Hadra, B., *WIRING THE SPINOUS PROCESSES IN POTT'S DISEASE*. JBJS, 1891. **1**(1): p. 206-210.
87. Howorth, M., *Evolution of spinal fusion*. Annals of surgery, 1943. **117**(2): p. 278.
88. Albee, F.H., *The classic. Transplantation of a portion of the tibia into the spine for Pott's disease. A preliminary report*. Jama, 57: 885, 1911. Clin Orthop Relat Res, 1972. **87**: p. 5-8.
89. Allan, F.G., *Scoliosis: operative correction of fixed curves*. J Bone Joint Surg Br, 1955. **37-B**(1): p. 92-6.
90. HARRINGTON, P.R., *The History and Development of Harrington Instrumentation*. Clinical Orthopaedics and Related Research, 1988. **227**: p. 3-5.
91. Finkemeier, C.G., *Bone-Grafting and Bone-Graft Substitutes*. J Bone Joint Surg Am, 2002. **84**(3): p. 454-464.
92. Carlisle, E. and J.S. Fischgrund, *Bone morphogenetic proteins for spinal fusion*. The Spine Journal. **5**(6, Supplement 1): p. S240-S249.
93. CRAWFORD, A.H., *Pitfalls of Spinal Deformities Associated With Neurofibromatosis in Children*. Clinical Orthopaedics and Related Research, 1989. **245**: p. 29-42.
94. BROWN, L.T., *BEEF BONE IN STABILIZING OPERATIONS OF THE SPINE*. J Bone Joint Surg Am, 1922. **4**(4): p. 711-750.
95. Shields, L.B.E., et al., *Adverse Effects Associated With High-Dose Recombinant Human Bone Morphogenetic Protein-2 Use in Anterior Cervical Spine Fusion*. Spine, 2006. **31**(5): p. 542-547 10.1097/01.brs.0000201424.27509.72.
96. Rigo, M., C. Reiter, and H.-R. Weiss, *Effect of conservative management on the prevalence of surgery in patients with adolescent idiopathic scoliosis*. Developmental Neurorehabilitation, 2003. **6**(3-4): p. 209-214.
97. Shandsjr, A.R., et al., *END-RESULT STUDY OF THE TREATMENT OF IDIOPATHIC SCOLIOSIS Report of the Research Committee of The American Orthopaedic Association*. The Journal of Bone & Joint Surgery, 1941. **23**(4): p. 963-977.
98. Tsirikos, A., A. Saifuddin, and M. Noordeen, *Spinal deformity in neurofibromatosis type-1: diagnosis and treatment*. European Spine Journal, 2005. **14**(5): p. 427-439.
99. Crawford, A.H.J. and N. Bagamery, *Osseous Manifestations of Neurofibromatosis in Childhood*. Journal of Pediatric Orthopaedics, 1986. **6**(1): p. 72-88.
100. Young, H., S. Hyman, and K. North, *Review Article : Neurofibromatosis I: Clinical Review and Exceptions to the Rules*. Journal of Child Neurology, 2002. **17**(8): p. 613-621.
101. Vitale, M.G., A. Guha, and D.L. Skaggs, *Orthopaedic Manifestations of Neurofibromatosis in Children: An Update*. Clinical Orthopaedics and Related Research, 2002. **401**: p. 107-118.

102. Fidler, M. and R. Jowett, *Muscle imbalance in the aetiology of scoliosis*. Journal of Bone & Joint Surgery, British Volume, 1976. **58-B(2)**: p. 200-201.
103. Moen, K.Y. and A.L. Nachemson, *Treatment of scoliosis. An historical perspective*. Spine, 1976. **24(24)**: p. 2570-5.
104. Bridwell, K.H., *Surgical Treatment of Idiopathic Adolescent Scoliosis*. Spine, 1999. **24(24)**: p. 2607.
105. Elefteriou, F., et al., *Skeletal abnormalities in neurofibromatosis type 1: Approaches to therapeutic options*. American Journal of Medical Genetics Part A, 2009. **149A(10)**: p. 2327-2338.
106. Burwell, R.G., *Aetiology of idiopathic scoliosis: current concepts*. Developmental Neurorehabilitation, 2003. **6(3-4)**: p. 137-170.
107. Hibbs, R.A., J.C. Risser, and A.B. Ferguson, *Scoliosis treated by the fusion operation an end-result study of three hundred and sixty cases*. Journal of Bone and Joint Surgery, 1931. **13**: p. 91-104.
108. DePalma, A.F. and R.H. Rothman, *The nature of pseudarthrosis*. Clin Orthop Relat Res, 1968. **59**: p. 113-8.
109. Closkey, R.F., et al., *Mechanics of Interbody Spinal Fusion: xsAnalysis of Critical Bone Graft Area*. Spine, 1993. **18(8)**: p. 1011-1015.
110. Delecrin, J., et al., *Influence of local environment on incorporation of ceramic for lumbar fusion. Comparison of laminar and intertransverse sites in a canine model*. Spine (Phila Pa 1976), 1997. **22(15)**: p. 1683-9.
111. Laroche, M., *Intraosseous circulation from physiology to disease*. Joint Bone Spine, 2002. **69(3)**: p. 262-269.
112. Laroche, M., et al., *[Lower limb arteriopathy and male osteoporosis]*. Rev Rhum Mal Osteoartic, 1992. **59(2)**: p. 95-101.
113. Laroche, M., et al., *Fractures of the femoral neck and arterial disease of the lower limbs*. Osteoporos Int, 1994. **4(5)**: p. 285.
114. Whitecloud, T.S.I., J.M. Davis, and P.M. Olive, *Operative Treatment of the Degenerated Segment Adjacent to a Lumbar Fusion*. Spine, 1994. **19(5)**: p. 531-536.
115. Yone, K., et al., *Indication of Fusion for Lumbar Spinal Stenosis in Elderly Patients and Its Significance*. Spine, 1996. **21(2)**: p. 242-248.
116. Gajraj, N.M., *The effect of cyclooxygenase-2 inhibitors on bone healing*. Reg Anesth Pain Med, 2003. **28(5)**: p. 456-65.
117. Glassman, S.D., et al., *The Effect of Postoperative Nonsteroidal Anti-inflammatory Drug Administration on Spinal Fusion*. Spine, 1998. **23(7)**: p. 834-838.
118. Martin, G.J.J., S.D. Boden, and L. Titus, *Recombinant Human Bone Morphogenetic Protein-2 Overcomes the Inhibitory Effect of Ketorolac, a Nonsteroidal Anti-inflammatory Drug (NSAID), on Posterolateral Lumbar Intertransverse Process Spine Fusion*. Spine, 1999. **24(21)**: p. 2188.
119. Reuben, S., D. Ablett, and R. Kaye, *High dose nonsteroidal anti-inflammatory drugs compromise spinal fusion*. Canadian Journal of Anesthesia / Journal canadien d'anesthésie, 2005. **52(5)**: p. 506-512.
120. Jones, M.K., et al., *Inhibition of angiogenesis by nonsteroidal anti-inflammatory drugs: insight into mechanisms and implications for cancer growth and ulcer healing*. Nat Med, 1999. **5(12)**: p. 1418-23.

121. Dormond, O., et al., *NSAIDs inhibit alpha V beta 3 integrin-mediated and Cdc42/Rac-dependent endothelial-cell spreading, migration and angiogenesis*. *Nat Med*, 2001. **7**(9): p. 1041-7.
122. Ho, M.-L., et al., *Effects of nonsteroidal anti-inflammatory drugs and prostaglandins on osteoblastic functions*. *Biochemical Pharmacology*, 1999. **58**(6): p. 983-990.
123. Krischak, G., et al., *The non-steroidal anti-inflammatory drug diclofenac reduces appearance of osteoblasts in bone defect healing in rats*. *Archives of Orthopaedic and Trauma Surgery*, 2007. **127**(6): p. 453-458.
124. Chang, J.-K., et al., *Nonsteroidal Anti-Inflammatory Drug Effects on Osteoblastic Cell Cycle, Cytotoxicity, and Cell Death*. *Connective Tissue Research*, 2005. **46**(4): p. 200 - 210.
125. Hadley, M.N. and S.V. Reddy, *Smoking and the Human Vertebral Column: A Review of the Impact of Cigarette Use on Vertebral Bone Metabolism and Spinal Fusion*. *Neurosurgery*, 1997. **41**(1): p. 116-124.
126. Andersen, T.M.S., et al., *Smoking as a Predictor of Negative Outcome in Lumbar Spinal Fusion. [Miscellaneous]*.
127. Silcox, D.H.I., et al., *The Effect of Nicotine on Spinal Fusion*. *Spine*, 1995. **20**(14): p. 1549-1553.
128. Brown, J.A., et al., *Reduced striatal dopamine underlies the attention system dysfunction in neurofibromatosis-1 mutant mice*. *Human Molecular Genetics*, 2010. **19**(22): p. 4515-4528.
129. Glassman, S.D.M.D., et al., *The Effect of Cigarette Smoking and Smoking Cessation on Spinal Fusion. [Article]*.
130. Emery, S.E., et al., *The biological and biomechanical effects of irradiation on anterior spinal bone grafts in a canine model*. *J Bone Joint Surg Am*, 1994. **76**(4): p. 540-8.
131. Nagel, D.A., et al., *A PARADIGM OF DELAYED UNION AND NONUNION IN THE LUMBOSACRAL JOINT - A STUDY OF MOTION AND BONE-GRAFTING OF THE LUMBOSACRAL SPINE IN SHEEP*. *Spine*, 1991. **16**(5): p. 553-559.
132. Hurley, L.A., et al., *The role of soft tissues in osteogenesis. An experimental study of canine spine fusions*. *J Bone Joint Surg Am*, 1959. **41-A**: p. 1243-54.
133. Muschler, G.F., et al., *Evaluation of bone-grafting materials in a new canine segmental spinal fusion model*. *Journal of Orthopaedic Research*, 1993. **11**(4): p. 514-524.
134. Feiertag, M.A., et al., *A rabbit model for nonunion of lumbar intertransverse process spine arthrodesis*. *Spine (Phila Pa 1976)*, 1996. **21**(1): p. 27-31.
135. Gurr, K.R., et al., *Roentgenographic and biomechanical analysis of lumbar fusions: A canine model*. *Journal of Orthopaedic Research*, 1989. **7**(6): p. 838-848.
136. McAfee, P.C., et al., *The Effect of Spinal Implant Rigidity on Vertebral Bone Density A Canine Mode*. *Spine*, 1991. **16**(6S): p. S190-S197.
137. Fuller, D.A., S. Stevenson, and S.E. Emery, *The Effects of Internal Fixation on Calcium Carbonate: Ceramic Anterior Spinal Fusion in Dogs*. *Spine*, 1996. **21**(18): p. 2131-2136.
138. Boden, S.D., *The biology of posterolateral lumbar spinal fusion*. *Orthopedic Clinics of North America*, 1998. **29**(4): p. 603-+.
139. Steinmann, J.C. and H.N. Herkowitz, *Pseudarthrosis of the spine*. *Clin Orthop Relat Res*, 1992(284): p. 80-90.

140. Castelein, R.M., J.H.v. Dieën, and T.H. Smit, *The role of dorsal shear forces in the pathogenesis of adolescent idiopathic scoliosis – A hypothesis*. Medical hypotheses, 2005. **65**(3): p. 501-508.
141. Brosius, S., *A History of von Recklinghausen's NF1*. Journal of the History of the Neurosciences, 2010. **19**(4): p. 333-348.
142. Akenside, M., *Observations on cancers*. Med Trans Coll Phys Lond, 1768. **1**(64): p. 1255-1266.
143. Smith, R.W., *A treatise on the pathology, diagnosis and treatment of neuroma*. 1898: New Sydenham Society.
144. Virchow, R., *Die krankhaften Geschwülste; dreissig Vorlesungen: gehalten während des Wintersemesters 1862-1863 an der Universität zu Berlin*. Vol. 2. 1864: Hirschwald.
145. Von Recklinghausen, F., *Ueber die multiplen Fibrome der Haut und ihre Beziehung zu den multiplen Neuomen: Festschrift zur Feier des fünfundzwanzigjährigen Bestehens des pathologischen Instituts zu Berlin Herrn Rudolf Virchow*. 1882: Hirschwald.
146. Hyman, S.L., A. Shores, and K.N. North, *The nature and frequency of cognitive deficits in children with neurofibromatosis type 1*. Neurology, 2005. **65**(7): p. 1037-1044.
147. Braun, J.T. and E. Akyuz, *Prediction of Curve Progression in a Goat Scoliosis Model*. Journal of Spinal Disorders & Techniques, 2005. **18**(3): p. 272-276.
148. Calvert, P., M. Edgar, and P. Webb, *Scoliosis in neurofibromatosis. The natural history with and without operation*. J Bone Joint Surg Br, 1989. **71-B**(2): p. 246-251.
149. Kallemeier, P., et al., *Validation, reliability, and complications of a tethering scoliosis model in the rabbit*. European Spine Journal, 2006. **15**(4): p. 449-456.
150. Wang, X., et al., *Changes in Serum Melatonin Levels in Response to Pinealectomy in the Chicken and Its Correlation With Development of Scoliosis*. Spine, 1998. **23**(22): p. 2377-2381.
151. Fagan, A., D. Kennaway, and A. Oakley, *Pinealectomy in the chicken: a good model of scoliosis?* European Spine Journal, 2009. **18**(8): p. 1154-1159.
152. Cheung, K.M.C., et al., *The Effect of Pinealectomy on Scoliosis Development in Young Nonhuman Primates*. Spine, 2005. **30**(18): p. 2009-2013.
153. Gorman, K.F. and F. Breden, *Idiopathic-type scoliosis is not exclusive to bipedalism*. Med Hypotheses, 2009. **72**(3): p. 348-52.
154. Burwell, R.G., et al., *Pathogenesis of idiopathic scoliosis. The Nottingham concept*. Acta orthopaedica Belgica, 1992. **58 Suppl 1**: p. 33-58.
155. Akel, I., et al., *The Effect of Calmodulin Antagonists on Experimental Scoliosis: A Pinealectomized Chicken Model*. Spine, 2009. **34**(6): p. 533-538  
10.1097/BRS.0b013e31818be0b1.
156. Schwab, F., et al., *A Porcine Model for Progressive Thoracic Scoliosis*. Spine, 2009. **34**(11): p. E397-E404 10.1097/BRS.0b013e3181a27156.
157. Moreau, A., et al., *Melatonin Signaling Dysfunction in Adolescent Idiopathic Scoliosis*. Spine, 2004. **29**(16): p. 1772-1781.
158. Wang, X., et al., *Characterization of the Scoliosis That Develops After Pinealectomy in the Chicken and Comparison With Adolescent Idiopathic Scoliosis in Humans*. Spine, 1997. **22**(22): p. 2626-2635.
159. El-Hoss, J., et al., *A murine model of neurofibromatosis type 1 tibial pseudarthrosis featuring proliferative fibrous tissue and osteoclast-like cells*. J Bone Miner Res, 2012. **27**(1): p. 68-78.

160. Kühnisch, J., et al., *Multiscale, converging defects of macro-porosity, microstructure and matrix mineralization impact long bone fragility in NF1*. PloS one, 2014. **9**(1): p. e86115.
161. AURORI, B.F., et al., *Pseudarthrosis After Spinal Fusion for Scoliosis: A Comparison of Autogeneic and Allogeneic Bone Grafts*. Clinical Orthopaedics and Related Research, 1985. **199**: p. 153-158.
162. BETZ, R.R., et al., *Scoliosis Surgery in Neurofibromatosis*. Clinical Orthopaedics and Related Research, 1989. **245**: p. 53-56.
163. McMaster, M.J. and J.I. James, *Pseudoarthrosis after spinal fusion for scoliosis*. J Bone Joint Surg Br, 1976. **58**(3): p. 305-12.
164. Li, H., et al., *Ras dependent paracrine secretion of osteopontin by Nf1 +/- osteoblasts promote osteoclast activation in a neurofibromatosis type I murine model*. Pediatr Res, 2009. **65**(6): p. 613-8.
165. Yu, X., et al., *Neurofibromin and its inactivation of Ras are prerequisites for osteoblast functioning*. Bone, 2005. **36**(5): p. 793-802.
166. Bosch, P., et al., *Osteoprogenitor cells within skeletal muscle*. J Orthop Res, 2000. **18**(6): p. 933-44.
167. DIAZ-FLORES, L., et al., *Pericytes as a Supplementary Source of Osteoblasts in Periosteal Osteogenesis*. Clinical Orthopaedics and Related Research, 1992. **275**: p. 280-286.
168. Levy, M.M., et al., *Osteoprogenitor cells of mature human skeletal muscle tissue: an in vitro study*. Bone, 2001. **29**(4): p. 317-322.
169. Grcevic, D., et al., *In vivo fate mapping identifies mesenchymal progenitor cells*. Stem cells, 2012. **30**(2): p. 187-196.
170. Lewinson, D., et al., *Expression of vascular antigens by bone cells during bone regeneration in a membranous bone distraction system*. Histochemistry and cell biology, 2001. **116**(5): p. 381-388.
171. Hibbs, R.A., *A Further Consideration of an Operation for Pott's Disease of the Spine: With Report of Cases from the Service of the New York Orthopaedic Hospital*. Ann Surg, 1912. **55**(5): p. 682-8.
172. Sandhu, H.S., et al., *Evaluation of rhBMP-2 with an OPLA carrier in a canine posterolateral (transverse process) spinal fusion model*. Spine (Phila Pa 1976), 1995. **20**(24): p. 2669-82.
173. Drespe, I.H., et al., *Animal models for spinal fusion*. Spine J, 2005. **5**(6 Suppl): p. 209S-216S.
174. Bouchard, J.A., et al., *Effects of Irradiation on Posterior Spinal Fusions A Rabbit Model*. Spine, 1994. **19**(16): p. 1836-1841.
175. Palumbo, M., et al., *Posterolateral intertransverse lumbar arthrodesis in the New Zealand White rabbit model: I. Surgical anatomy*. Spine J, 2004. **4**(3): p. 287-92.
176. Valdes, M., et al., *Posterolateral intertransverse lumbar arthrodesis in the New Zealand White rabbit model: II. Operative technique*. Spine J, 2004. **4**(3): p. 293-9.
177. Wing, K.J., et al., *Stopping Nicotine Exposure Before Surgery: The Effect on Spinal Fusion in a Rabbit Model*. Spine, 2000. **25**(1): p. 30.
178. Salamon, M.L., et al., *The effects of BMP-7 in a rat posterolateral intertransverse process fusion model*. J Spinal Disord Tech, 2003. **16**(1): p. 90-5.
179. Schimandle, J.H. and S.D. Boden, *Spine update. The use of animal models to study spinal fusion*. Spine (Phila Pa 1976), 1994. **19**(17): p. 1998-2006.

180. Wang, J.C., et al., *Effect of regional gene therapy with bone morphogenetic protein-2-producing bone marrow cells on spinal fusion in rats*. J Bone Joint Surg Am, 2003. **85-A**(5): p. 905-11.
181. Hasharoni, A., et al., *Murine spinal fusion induced by engineered mesenchymal stem cells that conditionally express bone morphogenetic protein—2*. Journal of Neurosurgery: Spine, 2005. **3**(1): p. 47-52.
182. Alden, T.D., et al., *Percutaneous spinal fusion using bone morphogenetic protein-2 gene therapy*. Journal of Neurosurgery: Spine, 1999. **90**(1): p. 109-114.
183. Rao, R.D., V.B. Bagaria, and B.C. Cooley, *Posterolateral intertransverse lumbar fusion in a mouse model: surgical anatomy and operative technique*. Spine J, 2007. **7**(1): p. 61-7.
184. Wiltse, L.L., et al., *The paraspinal sacrospinalis-splitting approach to the lumbar spine*. J Bone Joint Surg Am, 1968. **50**(5): p. 919-26.
185. Schindeler, A., R. Liu, and D.G. Little, *The contribution of different cell lineages to bone repair: Exploring a role for muscle stem cells*. Differentiation, 2009. **77**(1): p. 12-18.
186. Gao, X., et al., *CHD7 Gene Polymorphisms Are Associated with Susceptibility to Idiopathic Scoliosis*. The American Journal of Human Genetics, 2007. **80**(5): p. 957-965.
187. Tonsgard, J.H., *Clinical Manifestations and Management of Neurofibromatosis Type 1*. Seminars in Pediatric Neurology, 2006. **13**(1): p. 2-7.
188. Hinrichs, S., et al., *A transgenic mouse model for human neurofibromatosis*. Science, 1987. **237**(4820): p. 1340-1343.
189. Bostrom, K.I., *Cell differentiation in vascular calcification*. Z Kardiol, 2000. **89 Suppl 2**: p. 69-74.
190. Chen, J.C., et al., *MyoD-cre transgenic mice: a model for conditional mutagenesis and lineage tracing of skeletal muscle*. Genesis, 2005. **41**(3): p. 116-21.
191. Lounev, V.Y., et al., *Identification of Progenitor Cells That Contribute to Heterotopic Skeletogenesis*. J Bone Joint Surg Am, 2009. **91**(3): p. 652-663.
192. Willette, R.N., et al., *BMP-2 Gene Expression and Effects on Human Vascular Smooth Muscle Cells*. Journal of Vascular Research, 1999. **36**(2): p. 120-125.
193. Trueta, J. and V.P. Amato, *THE VASCULAR CONTRIBUTION TO OSTEOGENESIS: III. Changes in the Growth Cartilage Caused by Experimentally Induced Ischaemia*. J Bone Joint Surg Br, 1960. **42-B**(3): p. 571-587.
194. Wallace, M., et al., *Type 1 neurofibromatosis gene: identification of a large transcript disrupted in three NF1 patients*. Science, 1990. **249**(4965): p. 181-186.
195. Fienman, N.L. and W.C. Yakovac, *Neurofibromatosis in childhood*. The Journal of pediatrics, 1970. **76**(3): p. 339-346.
196. Young, H., S. Hyman, and K. North, *Neurofibromatosis 1: clinical review and exceptions to the rules*. Journal of child neurology, 2002. **17**(8): p. 613-621.
197. Crawford, A.H., et al., *The immature spine in type-1 neurofibromatosis*. J Bone Joint Surg Am, 2007. **89 Suppl 1**: p. 123-42.
198. Lammert, M., et al., *Decreased bone mineral density in patients with neurofibromatosis 1*. Osteoporos Int, 2005. **16**(9): p. 1161-6.
199. Dulai, S., et al., *Decreased Bone Mineral Density in Neurofibromatosis Type 1: Results From a Pediatric Cohort*. Journal of Pediatric Orthopaedics, 2007. **27**(4): p. 472-475  
10.1097/01.bpb.0000271310.87997.ae.
200. Schindeler, A., et al., *Models of tibial fracture healing in normal and Nf1-deficient mice*. J Orthop Res, 2008. **26**(8): p. 1053-60.

201. Schindeler, A., et al., *Distal tibial fracture repair in a neurofibromatosis type 1-deficient mouse treated with recombinant bone morphogenetic protein and a bisphosphonate*. J Bone Joint Surg Br, 2011. **93**(8): p. 1134-1139.
202. Schindeler, A., et al., *Modeling bone morphogenetic protein and bisphosphonate combination therapy in wild-type and Nf1 haploinsufficient mice*. Journal of Orthopaedic Research, 2008. **26**(1): p. 65-74.
203. Birke, O., et al., *Preliminary experience with the combined use of recombinant bone morphogenetic protein and bisphosphonates in the treatment of congenital pseudarthrosis of the tibia*. J Child Orthop, 2010. **4**(6): p. 507-17.
204. Bobyn, J., et al., *Posterolateral inter-transverse lumbar fusion in a mouse model*. Journal of Orthopaedic Surgery and Research, 2013. **8**.
205. Brannan, C.I., et al., *Targeted disruption of the neurofibromatosis type-1 gene leads to developmental abnormalities in heart and various neural crest-derived tissues*. Genes Dev, 1994. **8**(9): p. 1019-29.
206. Carragee, E.J., E.L. Hurwitz, and B.K. Weiner, *A critical review of recombinant human bone morphogenetic protein-2 trials in spinal surgery: emerging safety concerns and lessons learned*. The Spine Journal, 2011. **11**(6): p. 471-491.
207. Elefteriou, F., et al., *Skeletal abnormalities in neurofibromatosis type 1: approaches to therapeutic options*. American Journal of Medical Genetics Part A, 2009. **149**(10): p. 2327-2338.
208. Little, D.G., M. Ramachandran, and A. Schindeler, *The anabolic and catabolic responses in bone repair*. Journal of Bone & Joint Surgery, British Volume, 2007. **89-B**(4): p. 425-433.
209. Lee, S.M., et al., *Is double inactivation of the Nf1 gene responsible for the development of congenital pseudarthrosis of the tibia associated with NF1?* Journal of Orthopaedic Research, 2012. **30**(10): p. 1535-1540.
210. Boyan, B., et al., *Potential of porous poly - D, L - lactide - co - glycolide particles as a carrier for recombinant human bone morphogenetic protein - 2 during osteoinduction in vivo*. Journal of Biomedical Materials Research Part A, 1999. **46**(1): p. 51-59.
211. Yamamoto, M., Y. Ikada, and Y. Tabata, *Controlled release of growth factors based on biodegradation of gelatin hydrogel*. Journal of Biomaterials Science, Polymer Edition, 2001. **12**(1): p. 77-88.
212. Mori, S., et al., *Antiangiogenic agent (TNP-470) inhibition of ectopic bone formation induced by bone morphogenetic protein-2*. Bone, 1998. **22**(2): p. 99-105.
213. Ferner, R.E., *Neurofibromatosis 1 and neurofibromatosis 2: a twenty first century perspective*. Lancet Neurol, 2007. **6**(4): p. 340-51.
214. Korf, B.R., *Diagnostic outcome in children with multiple cafe au lait spots*. Pediatrics, 1992. **90**(6): p. 924-7.
215. Rosenbaum, T. and K. Wimmer, *Neurofibromatosis type 1 (NF1) and associated tumors*. Klin Padiatr, 2014. **226**(6-7): p. 309-15.
216. Akbarnia, B.A., et al., *Prevalence of scoliosis in neurofibromatosis*. Spine (Phila Pa 1976), 1992. **17**(8 Suppl): p. S244-8.
217. Crawford, A.H., *Pitfalls of spinal deformities associated with neurofibromatosis in children*. Clin Orthop Relat Res, 1989(245): p. 29-42.
218. D L Burk, J., et al., *Spinal and paraspinal neurofibromatosis: surface coil MR imaging at 1.5 T1*. Radiology, 1987. **162**(3): p. 797-801.



219. Koptan, W. and Y. ElMiligui, *Surgical correction of severe dystrophic neurofibromatosis scoliosis: an experience of 32 cases*. European Spine Journal, 2010. **19**(9): p. 1569-1575.
220. Hu, Z., et al., *Morphological Differences in the Vertebrae of Scoliosis Secondary to Neurofibromatosis Type 1 With and Without Paraspinal Neurofibromas*. Spine (Phila Pa 1976), 2016. **41**(7): p. 598-602.
221. Tsirikos, A.I., A. Saifuddin, and M.H. Noordeen, *Spinal deformity in neurofibromatosis type-1: diagnosis and treatment*. European Spine Journal, 2005. **14**(5): p. 427-439.
222. Khong, P.L., et al., *MR imaging of spinal tumors in children with neurofibromatosis 1*. AJR Am J Roentgenol, 2003. **180**(2): p. 413-7.
223. Egelhoff, J.C., et al., *Spinal MR findings in neurofibromatosis types 1 and 2*. American Journal of Neuroradiology, 1992. **13**(4): p. 1071-1077.
224. Thakkar, S.D., U. Feigen, and V.F. Mautner, *Spinal tumours in neurofibromatosis type 1: an MRI study of frequency, multiplicity and variety*. Neuroradiology, 1999. **41**(9): p. 625-9.
225. Deo, N., et al., *Improved union and bone strength in a mouse model of NF1 pseudarthrosis treated with recombinant human bone morphogenetic protein-2 and zoledronic acid*. J Orthop Res, 2017.
226. Bobyn, J., et al., *Maximizing bone formation in posterior spine fusion using rhBMP-2 and zoledronic acid in wild type and NF1 deficient mice*. J Orthop Res, 2014. **32**(8): p. 1090-4.
227. Stevenson, D.A., et al., *Bone Mineral Density in Children and Adolescents with Neurofibromatosis Type 1*. The Journal of Pediatrics, 2007. **150**(1): p. 83-88.
228. Rhodes, S.D., et al., *Dystrophic spinal deformities in a neurofibromatosis type 1 murine model*. PLoS One, 2015. **10**(3): p. e0119093.
229. Wang, W., et al., *Mice lacking Nf1 in osteochondroprogenitor cells display skeletal dysplasia similar to patients with neurofibromatosis type 1*. Hum Mol Genet, 2011. **20**(20): p. 3910-24.
230. Sweeney, E.E., et al., *Photothermal therapy improves the efficacy of a MEK inhibitor in neurofibromatosis type 1-associated malignant peripheral nerve sheath tumors*. Sci Rep, 2016. **6**: p. 37035.
231. Farassati, F., et al., *Ras signaling influences permissiveness of malignant peripheral nerve sheath tumor cells to oncolytic herpes*. Am J Pathol, 2008. **173**(6): p. 1861-72.
232. Stevenson, D.A., et al., *Approaches to treating NF1 tibial pseudarthrosis: consensus from the Children's Tumor Foundation NF1 Bone Abnormalities Consortium*. Journal of Pediatric Orthopaedics, 2013. **33**(3): p. 269-275.
233. Huynh, H., P.K. Chow, and K.C. Soo, *AZD6244 and doxorubicin induce growth suppression and apoptosis in mouse models of hepatocellular carcinoma*. Mol Cancer Ther, 2007. **6**(9): p. 2468-76.
234. Henderson, Y.C., et al., *MEK inhibitor PD0325901 significantly reduces the growth of papillary thyroid carcinoma cells in vitro and in vivo*. Mol Cancer Ther, 2010. **9**(7): p. 1968-76.
235. Lorusso, P., et al., *A phase 1-2 clinical study of a second generation oral MEK inhibitor, PD 0325901 in patients with advanced cancer*. Journal of Clinical Oncology, 2005. **23**(16\_suppl): p. 3011-3011.
236. Zha, Y., et al., *Use of Cre-adenovirus and CAR transgenic mice for efficient deletion of genes in post-thymic T cells*. Journal of Immunological Methods, 2008. **331**(1): p. 94-102.

237. Bobyn, J., et al., *Posterolateral inter-transverse lumbar fusion in a mouse model*. J Orthop Surg Res, 2013. **8**: p. 2.
238. Sullivan, K., et al., *JNK inhibitors increase osteogenesis in Nf1-deficient cells*. Bone, 2011. **49**(6): p. 1311-6.
239. Heervä, E., et al., *Osteoclasts in neurofibromatosis type 1 display enhanced resorption capacity, aberrant morphology, and resistance to serum deprivation*. Bone, 2010. **47**(3): p. 583-590.
240. El-Hoss, J., et al., *Modulation of endochondral ossification by MEK inhibitors PD0325901 and AZD6244 (Selumetinib)*. Bone, 2014. **59**: p. 151-61.
241. Jacks, T., et al., *Tumour predisposition in mice heterozygous for a targeted mutation in Nf1*. Nat Genet, 1994. **7**(3): p. 353-61.
242. Lee, D.Y., et al., *Disturbed osteoblastic differentiation of fibrous hamartoma cell from congenital pseudarthrosis of the tibia associated with neurofibromatosis type I*. Clinics in orthopedic surgery, 2011. **3**(3): p. 230-237.
243. Kamiya, N., et al., *Targeted Disruption of NF1 in Osteocytes Increases FGF23 and Osteoid With Osteomalacia-like Bone Phenotype*. Journal of Bone and Mineral Research, 2017. **32**(8): p. 1716-1726.
244. Wang, W., et al., *Local low-dose lovastatin delivery improves the bone-healing defect caused by Nf1 loss of function in osteoblasts*. Journal of Bone and Mineral Research, 2010. **25**(7): p. 1658-1667.
245. El Khassawna, T., et al., *Deterioration of fracture healing in the mouse model of NF1 long bone dysplasia*. Bone, 2012. **51**(4): p. 651-660.
246. Bobyn, J.D., et al., *Animal models of scoliosis*. Journal of Orthopaedic Research, 2015. **33**(4): p. 458-467.
247. Shapiro, G.I., et al., *Abstract CT046: Phase I dose escalation study of the CDK4/6 inhibitor palbociclib in combination with the MEK inhibitor PD-0325901 in patients with <em>RAS</em> mutant solid tumors*. Cancer Research, 2017. **77**(13 Supplement): p. CT046-CT046.
248. Wan, M. and X. Cao, *BMP signaling in skeletal development*. Biochemical and Biophysical Research Communications, 2005. **328**(3): p. 651-657.
249. Axelrad, T.W. and T.A. Einhorn, *Bone morphogenetic proteins in orthopaedic surgery*. Cytokine & Growth Factor Reviews, 2009. **20**(5-6): p. 481-488.
250. Lounev, V.Y., et al., *Identification of progenitor cells that contribute to heterotopic skeletogenesis*. J Bone Joint Surg Am, 2009. **91**(3): p. 652-63.
251. Liu, R., A. Schindeler, and D.G. Little, *The potential role of muscle in bone repair*. Journal of Musculoskeletal & Neuronal Interactions, 2010. **10**(1): p. 71-76.
252. Liu, R., et al., *Myogenic progenitors contribute to open but not closed fracture repair*. BMC Musculoskeletal Disorders, 2011. **12**.
253. Medici, D., et al., *Conversion of vascular endothelial cells into multipotent stem-like cells*. Nature Medicine, 2010. **16**(12): p. 1400-U80.
254. Lee, D.Y., et al., *Mobilization of endothelial progenitor cells in fracture healing and distraction osteogenesis*. Bone, 2008. **42**(5): p. 932-941.
255. Preininger, B., et al., *CD133: Enhancement of Bone Healing by Local Transplantation of Peripheral Blood Cells in a Biologically Delayed Rat Osteotomy Model*. Plos One, 2013. **8**(2).

256. He, X., et al., *BMP2 Genetically Engineered MSCs and EPCs Promote Vascularized Bone Regeneration in Rat Critical-Sized Calvarial Bone Defects*. Plos One, 2013. **8**(4).
257. Atesok, K., et al., *Endothelial Progenitor Cells Promote Fracture Healing in a Segmental Bone Defect Model*. Journal of Orthopaedic Research, 2010. **28**(8): p. 1007-1014.
258. Li, R., et al., *Endothelial Progenitor Cells for Fracture Healing: A Microcomputed Tomography and Biomechanical Analysis*. Journal of Orthopaedic Trauma, 2011. **25**(8): p. 467-471.
259. Li, R., et al., *Expression of VEGF Gene Isoforms in a Rat Segmental Bone Defect Model Treated With EPCs*. Journal of Orthopaedic Trauma, 2012. **26**(12): p. 689-692.
260. Wosczyzna, M.N., et al., *Multipotent progenitors resident in the skeletal muscle interstitium exhibit robust BMP-dependent osteogenic activity and mediate heterotopic ossification*. Journal of Bone and Mineral Research, 2012. **27**(5): p. 1004-1017.
261. Kisanuki, Y.Y., et al., *Tie2-Cre transgenic mice: a new model for endothelial cell-lineage analysis in vivo*. Dev Biol, 2001. **230**(2): p. 230-42.
262. Koni, P.A., et al., *Conditional vascular cell adhesion molecule 1 deletion in mice: Impaired lymphocyte migration to bone marrow*. Journal of Experimental Medicine, 2001. **193**(6): p. 741-753.
263. Schlaeger, T.M., et al., *Uniform vascular-endothelial-cell-specific gene expression in both embryonic and adult transgenic mice*. Proceedings of the National Academy of Sciences of the United States of America, 1997. **94**(7): p. 3058-3063.
264. Madisen, L., et al., *A robust and high-throughput Cre reporting and characterization system for the whole mouse brain*. Nature Neuroscience, 2010. **13**(1): p. 133-U311.
265. Roguljic, H., et al., *In vivo Identification of Periodontal Progenitor Cells*. Journal of Dental Research, 2013. **92**(8): p. 709-715.
266. Matthews, B.G., et al., *Analysis of aSMA- Labeled Progenitor Cell Commitment Identifies Notch Signaling as an Important Pathway in Fracture Healing*. Journal of Bone and Mineral Research, 2014. **29**(5): p. 1283-1294.
267. Dymont, N.A., et al., *Lineage Tracing of Resident Tendon Progenitor Cells during Growth and Natural Healing*. Plos One, 2014. **9**(4).
268. Akiyama, H., et al., *Osteo-chondroprogenitor cells are derived from Sox9 expressing precursors*. Proceedings of the National Academy of Sciences of the United States of America, 2005. **102**(41): p. 14665-14670.
269. Kalajzic, I., et al., *Use of type I collagen green fluorescent protein transgenes to identify subpopulations of cells at different stages of the osteoblast lineage*. Journal of Bone and Mineral Research, 2002. **17**(1): p. 15-25.
270. Matsubara, T., et al., *BMP2 Regulates Osterix through Msx2 and Runx2 during Osteoblast Differentiation*. Journal of Biological Chemistry, 2008. **283**(43): p. 29119-29125.
271. Colnot, C., *Skeletal Cell Fate Decisions Within Periosteum and Bone Marrow During Bone Regeneration*. Journal of Bone and Mineral Research, 2009. **24**(2): p. 274-282.
272. Oni, O.O.A., H. Stafford, and P.J. Gregg, *A STUDY OF DIAPHYSEAL FRACTURE REPAIR USING TISSUE-ISOLATION TECHNIQUES*. Injury-International Journal of the Care of the Injured, 1992. **23**(7): p. 467-470.

273. Colnot, C., S. Huang, and J. Helms, *Analyzing the cellular contribution of bone marrow to fracture healing using bone marrow transplantation in mice*. Biochemical and Biophysical Research Communications, 2006. **350**(3): p. 557-561.
274. Lu, C., et al., *Recombinant Human Bone Morphogenetic Protein-7 Enhances Fracture Healing in an Ischemic Environment*. Journal of Orthopaedic Research, 2010. **28**(5): p. 687-696.
275. Schindeler, A., M. Kolind, and D.G. Little, *Cellular transitions and tissue engineering*. Cellular reprogramming, 2013. **15**(2): p. 101-106.
276. Seime, T., et al., *Inducible cell labeling and lineage tracking during fracture repair*. Development Growth & Differentiation, 2015. **57**(1): p. 10-23.
277. Denayer, T., T. Stöhr, and M. Van Roy, *Animal models in translational medicine: Validation and prediction*. New Horizons in Translational Medicine, 2014. **2**(1): p. 5-11.
278. Baht, G.S., et al., *Pharmacologically targeting beta-catenin for NF1 associated deficiencies in fracture repair*. Bone, 2017. **98**: p. 31-36.
279. Li, W., et al., *The HMG-CoA reductase inhibitor lovastatin reverses the learning and attention deficits in a mouse model of neurofibromatosis type 1*. Current Biology, 2005. **15**(21): p. 1961-1967.
280. Acosta, M.T., et al., *The Learning Disabilities Network (LeaDNet): Using neurofibromatosis type 1 (NF1) as a paradigm for translational research*. American Journal of Medical Genetics Part A, 2012. **158A**(9): p. 2225-2232.
281. Acosta, M.T., et al., *Lovastatin as treatment for neurocognitive deficits in neurofibromatosis type 1: phase I study*. Pediatric neurology, 2011. **45**(4): p. 241-245.
282. Listerick, R., et al., *Optic pathway gliomas in children with neurofibromatosis 1: consensus statement from the NF1 Optic Pathway Glioma Task Force*. Annals of neurology, 1997. **41**(2): p. 143-149.
283. Diggs-Andrews, K.A., et al., *Dopamine deficiency underlies learning deficits in neurofibromatosis-1 mice*. Annals of Neurology, 2013. **73**(2): p. 309-315.
284. Lion-François, L., et al., *The effect of methylphenidate on neurofibromatosis type 1: a randomised, double-blind, placebo-controlled, crossover trial*. Orphanet journal of rare diseases, 2014. **9**: p. 142-142.
285. Ghadakhzadeh, S., et al.,  *$\beta$ -Catenin modulation in neurofibromatosis type 1 bone repair: therapeutic implications*. The FASEB Journal, 2016. **30**(9): p. 3227-3237.
286. Sirois III, J.L. and J.C. Drennan, *Dystrophic spinal deformity in neurofibromatosis*. Journal of Pediatric Orthopaedics, 1990. **10**(4): p. 522-526.
287. Cheng, T.L., A. Schindeler, and D.G. Little, *BMP-2 delivered via sucrose acetate isobutyrate (SAIB) improves bone repair in a rat open fracture model*. Journal of Orthopaedic Research, 2016. **34**(7): p. 1168-1176.
288. Wu, Y., et al., *Enhanced healing of rabbit segmental radius defects with surface-coated calcium phosphate cement/bone morphogenetic protein-2 scaffolds*. Materials Science and Engineering: C, 2014. **44**: p. 326-335.
289. Serra, E., et al., *Confirmation of a Double-Hit Model for the NF1 Gene in Benign Neurofibromas*. The American Journal of Human Genetics, 1997. **61**(3): p. 512-519.
290. Garcia - Linares, C., et al., *Dissecting loss of heterozygosity (LOH) in neurofibromatosis type 1 - associated neurofibromas: Importance of copy neutral LOH*. Human mutation, 2011. **32**(1): p. 78-90.

291. Upadhyaya, M., et al., *The spectrum of somatic and germline NF1 mutations in NF1 patients with spinal neurofibromas*. Neurogenetics, 2009. **10**(3): p. 251-263.
292. Sant, D.W., et al., *Evaluation of somatic mutations in tibial pseudarthrosis samples in neurofibromatosis type 1*. Journal of medical genetics, 2015. **52**(4): p. 256-261.
293. Mak, I.W., N. Evaniw, and M. Ghert, *Lost in translation: animal models and clinical trials in cancer treatment*. American journal of translational research, 2014. **6**(2): p. 114.
294. Seok, J., et al., *Genomic responses in mouse models poorly mimic human inflammatory diseases*. Proceedings of the National Academy of Sciences, 2013. **110**(9): p. 3507-3512.
295. Jessen, W.J., et al., *MEK inhibition exhibits efficacy in human and mouse neurofibromatosis tumors*. The Journal of Clinical Investigation, 2013. **123**(1): p. 340-347.
296. Jousma, E., et al., *Preclinical assessments of the MEK inhibitor PD - 0325901 in a mouse model of neurofibromatosis type 1*. Pediatric blood & cancer, 2015. **62**(10): p. 1709-1716.
297. Ong, K.L., et al., *Off-label use of bone morphogenetic proteins in the United States using administrative data*. Spine, 2010. **35**(19): p. 1794-1800.
298. Cahill, K.S., et al., *Prevalence, complications, and hospital charges associated with use of bone-morphogenetic proteins in spinal fusion procedures*. Jama, 2009. **302**(1): p. 58-66.
299. Wong, D.A., et al., *Neurologic impairment from ectopic bone in the lumbar canal: a potential complication of off-label PLIF/TLIF use of bone morphogenetic protein-2 (BMP-2)*. The Spine Journal, 2008. **8**(6): p. 1011-1018.
300. Vaidya, R., et al., *Complications in the use of rhBMP-2 in PEEK cages for interbody spinal fusions*. Clinical Spine Surgery, 2008. **21**(8): p. 557-562.
301. Jean-Paul, S., et al., *Could an osteoinductor result in degeneration of a neurofibroma in NF1?* European Spine Journal, 2010. **19**(2): p. 220-225.
302. Oetgen, M.E. and B.S. Richards, *Complications associated with the use of bone morphogenetic protein in pediatric patients*. Journal of Pediatric Orthopaedics, 2010. **30**(2): p. 192-198.
303. Shoemaker, L.R., *Expanding role of bisphosphonate therapy in children*. The Journal of pediatrics, 1999. **134**(3): p. 264-267.
304. Lteif, A.N. and D. Zimmerman, *Bisphosphonates for treatment of childhood hypercalcemia*. Pediatrics, 1998. **102**(4): p. 990-993.
305. Glorieux, F.H., et al., *Cyclic administration of pamidronate in children with severe osteogenesis imperfecta*. New England Journal of Medicine, 1998. **339**(14): p. 947-952.
306. Ambler, G.R., et al., *Rapid improvement of calcinosis in juvenile dermatomyositis with alendronate therapy*. The Journal of rheumatology, 2005. **32**(9): p. 1837-1839.
307. Van der Sluis, I.M., et al., *Idiopathic infantile arterial calcification: clinical presentation, therapy and long-term follow-up*. European journal of pediatrics, 2006. **165**(9): p. 590-593.
308. Rijks, E.B., et al., *Efficacy and safety of bisphosphonate therapy in children with osteogenesis imperfecta: a systematic review*. Hormone research in paediatrics, 2015. **84**(1): p. 26-42.
309. LoRusso, P.M., et al., *Phase I pharmacokinetic and pharmacodynamic study of the oral MAPK/ERK kinase inhibitor PD-0325901 in patients with advanced cancers*. Clinical Cancer Research, 2010: p. 1078-0432. CCR-09-1883.

310. Haura, E.B., et al., *A phase II study of PD-0325901, an oral MEK inhibitor, in previously treated patients with advanced non-small cell lung cancer*. *Clinical Cancer Research*, 2010. **16**(8): p. 2450-2457.
311. Banerjee, A., et al., *A phase I study of AZD6244 in children with recurrent or refractory low-grade gliomas: A Pediatric Brain Tumor Consortium report*. 2014, American Society of Clinical Oncology.
312. de la Croix Ndong, J., et al., *Combined MEK inhibition and BMP2 treatment promotes osteoblast differentiation and bone healing in Nf1Osx<sup>-/-</sup> mice*. *Journal of Bone and Mineral Research*, 2015. **30**(1): p. 55-63.
313. Kraniak, J.M., et al., *The role of neurofibromin in N-Ras mediated AP-1 regulation in malignant peripheral nerve sheath tumors*. *Molecular and cellular biochemistry*, 2010. **344**(1-2): p. 267-276.
314. Ye, Y., et al., *Safety, Tolerability, And Pharmacokinetics Of Ascending Single Oral Doses Of Cc-930, A Novel Jnk Inhibitor, In Healthy Subjects*. *Clinical Pharmacology & Therapeutics*, 2011. **89**: p. S31.
315. Brighton, C.T. and R.M. Hunt, *Early histological and ultrastructural changes in medullary fracture callus*. *JBJS*, 1991. **73**(6): p. 832-847.
316. Rozen, N., et al., *Transplanted blood-derived endothelial progenitor cells (EPC) enhance bridging of sheep tibia critical size defects*. *Bone*, 2009. **45**(5): p. 918-924.
317. Matsumoto, T., et al., *Therapeutic potential of vasculogenesis and osteogenesis promoted by peripheral blood CD34-positive cells for functional bone healing*. *The American journal of pathology*, 2006. **169**(4): p. 1440-1457.
318. Seebach, C., et al., *Endothelial progenitor cells improve directly and indirectly early vascularization of mesenchymal stem cell-driven bone regeneration in a critical bone defect in rats*. *Cell transplantation*, 2012. **21**(8): p. 1667-1677.
319. Kumar, S. and S. Ponnazhagan, *Mobilization of bone marrow mesenchymal stem cells in vivo augments bone healing in a mouse model of segmental bone defect*. *Bone*, 2012. **50**(4): p. 1012-1018.
320. Yang, J., et al., *Continuous AMD3100 treatment worsens renal fibrosis through regulation of bone marrow derived pro-angiogenic cells homing and T-cell-related inflammation*. *PloS one*, 2016. **11**(2): p. e0149926.
321. Saiman, Y., et al., *Inhibition of the CXCL12/CXCR4 chemokine axis with AMD3100, a CXCR4 small molecule inhibitor, worsens murine hepatic injury*. *Hepatology Research*, 2015. **45**(7): p. 794-803.
322. McDermott, D.H., et al., *A phase I clinical trial of long-term, low-dose treatment of WHIM syndrome with the CXCR4 antagonist plerixafor*. *Blood*, 2014. **123**(15): p. 2308-2316.
323. Liles, W.C., et al., *Mobilization of hematopoietic progenitor cells in healthy volunteers by AMD3100, a CXCR4 antagonist*. *Blood*, 2003. **102**(8): p. 2728-2730.
324. Cho, T.-J., et al., *Biologic characteristics of fibrous hamartoma from congenital pseudarthrosis of the tibia associated with neurofibromatosis type 1*. *JBJS*, 2008. **90**(12): p. 2735-2744.
325. Zhou, Q., et al., *Generation of Fertile Cloned Rats by Regulating Oocyte Activation*. *Science*, 2003. **302**(5648): p. 1179-1179.
326. O'Sullivan, G.J., et al., *Potential and limitations of genetic manipulation in animals*. *Drug Discovery Today: Technologies*, 2006. **3**(2): p. 173-180.

327. Horvath, P. and R. Barrangou, *CRISPR/Cas, the immune system of bacteria and archaea*. Science, 2010. **327**(5962): p. 167-170.
328. Mashiko, D., et al., *Generation of mutant mice by pronuclear injection of circular plasmid expressing Cas9 and single guided RNA*. Scientific reports, 2013. **3**.
329. Wang, H., et al., *One-Step Generation of Mice Carrying Mutations in Multiple Genes by CRISPR/Cas-Mediated Genome Engineering*. Cell, 2013. **153**(4): p. 910-918.
330. Carroll, K.J., et al., *A mouse model for adult cardiac-specific gene deletion with CRISPR/Cas9*. Proceedings of the National Academy of Sciences, 2016. **113**(2): p. 338-343.
331. Yang, H., et al., *One-step generation of mice carrying reporter and conditional alleles by CRISPR/Cas-mediated genome engineering*. Cell, 2013. **154**(6): p. 1370-1379.
332. Fu, Y., et al., *High frequency off-target mutagenesis induced by CRISPR-Cas nucleases in human cells*. Nature biotechnology, 2013. **31**(9): p. 822-826.
333. Hsu, P.D., et al., *DNA targeting specificity of RNA-guided Cas9 nucleases*. Nature biotechnology, 2013. **31**(9): p. 827-832.
334. Tycko, J., V.E. Myer, and P.D. Hsu, *Methods for optimizing CRISPR-Cas9 genome editing specificity*. Molecular cell, 2016. **63**(3): p. 355-370.
335. Gori, J.L., et al., *Delivery and specificity of CRISPR/Cas9 genome editing technologies for human gene therapy*. Human gene therapy, 2015. **26**(7): p. 443-451.
336. Yin, H., et al., *Structure-guided chemical modification of guide RNA enables potent non-viral in vivo genome editing*. Nature biotechnology, 2017. **35**(12): p. 1179.
337. Song, Y., et al., *Efficient dual sgRNA-directed large gene deletion in rabbit with CRISPR/Cas9 system*. Cellular and molecular life sciences, 2016. **73**(15): p. 2959-2968.
338. Ni, W., et al., *Efficient gene knockout in goats using CRISPR/Cas9 system*. PloS one, 2014. **9**(9): p. e106718.
339. Crispo, M., et al., *Efficient generation of myostatin knock-out sheep using CRISPR/Cas9 technology and microinjection into zygotes*. Plos one, 2015. **10**(8): p. e0136690.
340. Oishi, I., et al., *Targeted mutagenesis in chicken using CRISPR/Cas9 system*. Scientific reports, 2016. **6**: p. 23980.
341. Jain, V.V., et al., *Growing Rods Are an Effective Fusionless Method of Controlling Early-Onset Scoliosis Associated With Neurofibromatosis Type 1 (NF1): A Multicenter Retrospective Case Series*. Journal of Pediatric Orthopaedics, 2017. **37**(8): p. e612-e618.
342. Zhu, W., et al., *An effective delivery vehicle of demineralized bone matrix incorporated with engineered collagen-binding human bone morphogenetic protein-2 to accelerate spinal fusion at low dose*. Journal of Materials Science: Materials in Medicine, 2018. **29**(1): p. 2.
343. Kim, B.J., et al., *Osteogenic Potential of Tauroursodeoxycholic Acid as an Alternative to rhBMP-2 in a Mouse Spinal Fusion Model*. Tissue Engineering Part A, 2017.
344. Zwolak, P., et al., *Local effect of zoledronic acid on new bone formation in posterolateral spinal fusion with demineralized bone matrix in a murine model*. Archives of orthopaedic and trauma surgery, 2017: p. 1-6.